

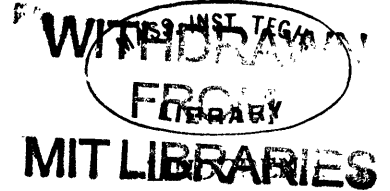
PHASE EQUILIBRIUM IN THE METAMORPHIC ROCKS OF ST. PAUL
ISLAND AND CAPE NORTH, NOVA SCOTIA

by

WILLIAM CHARLES PHINNEY

S.B., Massachusetts Institute of Technology
(1953)

M.S., Massachusetts Institute of Technology
(1956)



SUBMITTED IN PARTIAL FULFILLMENT OF THE REQUIREMENTS
FOR THE DEGREE OF DOCTOR OF PHILOSOPHY
at the
MASSACHUSETTS INSTITUTE OF TECHNOLOGY

September, 1959

Signature of Author.....
Department of Geology and Geophysics
August 14, 1959

Certified by.....
Thesis Supervisor

Accepted by.....
Chairman, Departmental Committee
on Graduate Students

Abstract

Phase Equilibrium in the Metamorphic Rocks of St. Paul Island and Cape North, Nova Scotia

by

William C. Phinney

Submitted to the Department of Geology and Geophysics on August 14, 1959 in partial fulfillment of the requirements for the degree of Doctor of Philosophy.

Metamorphic rocks of St. Paul Island and Cape North, Nova Scotia were mapped and studied both petrographically and chemically. Twenty-four schists--one from the garnet zone, 20 from the staurolite zone, two from the kyanite isograd, and one from the kyanite zone-- were separated into their constituent minerals. Chemical analyses of one chlorite and of 23 sets of coexisting biotites and garnets were carried out by photometric and titrimetric procedures. Precision of the analyses is generally within a relative error of 2%.

Plots of the garnet-biotite tie lines on the phase diagrams of Thompson (1957) result in intersecting tie lines which cannot be ascribed to experimental error. Grouping the assemblages on the basis of comparable MnO , CaO , and Fe_2O_3/FeO , factors not considered in Thompson's original diagrams, still results in intersecting tie lines. At a constant chemical potential of H_2O the number of phases and components in the samples indicate divariant assemblages, except the two from the kyanite isograd. Theoretical considerations argue that at equilibrium tie lines of divariant assemblages should not intersect.

Further examination of the data shows a relationship between the garnet/staurolite ratio and the $\frac{FeO}{FeO + MgO}$ ratio in biotites. An explanation of this by means of Thompson's diagrams requires that diffusion equilibrium of Fe and Mg be restricted to volumes smaller than that of a hand specimen. Emission spectrographic analyses of Fe/Mg ratios in biotites indicated that this ratio varied among biotites taken little more than a centimeter apart. The variation was greatest in samples where garnet and staurolite grains were separated a centimeter or more. Furthermore, the two samples which were highly homogeneous and contained a complete mineral assemblage within any radius of a few millimeters did not show variations in the Fe/Mg ratio.

The apparent disequilibrium indicated by the intersecting tie lines is most easily explained by assuming maximum diffusion radii for Fe and Mg which are too small to overcome the initial inhomogeneities in composition. The radius of diffusion is a function of temperature, pressure, composition, and time. In the St. Paul Island rocks it is estimated that the limit of diffusion for Fe and Mg is of the order of a few millimeters.

Thesis Supervisor: H. W. Fairbairn
Professor of Geology

TABLE OF CONTENTS

PART 1

I INTRODUCTION	2
II GEOLOGY.....	4
III SAMPLING AND MINERAL SEPARATION	10
IV CHEMICAL ANALYSES	
A. Problems and Techniques	13
B. Precision	14
C. Accuracy	15
V RESULTS	
A. Compositions of phases	42
B. Phase Diagrams	55
VI DISCUSSION OF RESULTS	
A. Theory	69
B. Comparison of Data and Theory.....	76
C. Future Work	87
VII SUMMARY	89
ACKNOWLEDGMENTS	91

PART 2

I INTRODUCTION	
A. Purpose of Investigation	93
B. Location of Area	95
C. Methods of Investigation	97
II GEOLOGY	
A. Introduction	97
B. Topography	100
C. Drainage	102

TABLE OF CONTENTS (Cont.)

D. Vegetation and Animal Life	103
E. Geomorphic Features	105
F. Erosion and Soils	108
G. Glacial Features	109
H. Stratigraphy and Petrography	111
I. Structural Geology	129
J. Summary	137
III SAMPLING AND MINERAL SEPARATION	
A. Theory	139
B. Choice of Final Samples	143
C. Separations	145
IV CHEMICAL ANALYSES	
A. Problems and Techniques	148
B. Precision	149
C. Accuracy	150
BIBLIOGRAPHY	154
BIOGRAPHICAL SKETCH	160

List of Illustrations and Tables

3	Figure 1. Index Map
5	Figure 2. Reference map relating St. Paul Island and Money Point
6	Figure 3. Geologic map of St. Paul Island
9	Figure 4. Geologic Map of Money Point
132	Figure 5. Deflection of foliation by pegmatite
132	Figure 6. Relative ages of pegmatite and faulting-
133	Figure 7. Ptygmatic fold
133	Figure 8. Faulted ptygmatic fold
135	Figure 9. Boudinaged epidote layer within a boudin
135	Figure 10. Crumulation on foliation
146	Figure 11 Flow chart for mineral separations
56	Figure 12. Method of projection
57	Figure 13. Result of projection
60-65	Figures 14-19. Phase diagrams
80	Figure 20. Possible explanation of garnet/staurolite ratios
19-26	Table 1. Pairs of analyses
27-30	Table 2. Duplicate analyses
31-32	Table 3. Precision of analyses
33	Table 4. Comparison of standards
34-37	Table 5. Biotite, garnet, and chlorite compositions and associated assemblages
38-40	Table 6. Molecular ratios of garnets to 12 oxygens
41	Table 7. Molecular ratios corrected for excess SiO ₂
44	Table 8. Plagioclase δ -indices and compositions
45	Table 9. Muscovite λ -indices

Table 10. Mineral analyses from other sources	46-54
Table 11. MnO and $\text{Fe}_2\text{O}_3/\text{FeO}$ groupings of biotites and garnets	59
Table 12. Relation of garnet/ staurolite ratio and $\frac{\text{FeO}}{\text{FeO MgO}}$ in biotites	79
Table 13. Spectrographically determined relative intensities of Fe/Mg in biotites	82

PART 1

I. INTRODUCTION

The degree to which chemical equilibrium is achieved in field occurrences of metamorphic mineral assemblages has always been a problem of paramount importance, and increasingly so in recent years since laboratory synthesis has opened up metamorphic processes to critical analysis. Investigation of synthetic assemblages now requires of the field petrologist much greater attention to detail, and shows particularly the need to know exact chemical compositions of minerals coexisting in very small volumes of rock. Only by these means can one discover whether reactions were completed, whether retrogressive reactions took place, how much diffusion took place, whether gradients are present in the composition of isomorphous phases, and many other details. The contribution to this problem presented here stems from detailed mapping of the metamorphic complex on St. Paul Island, N.S. (Figure 1). This area meets several necessary specifications for a study of this type. These specifications include: coarse-grained assemblages in which the minerals may be recognized in hand specimen, accessibility of fresh samples, and enough outcrop to allow good sample control. In addition, the mineral assemblages must contain enough phases to limit the degrees of freedom of the phase rule to two, or less.

In August of 1957 the writer and three assistants spent 16 days on St. Paul Island. During this time the island was

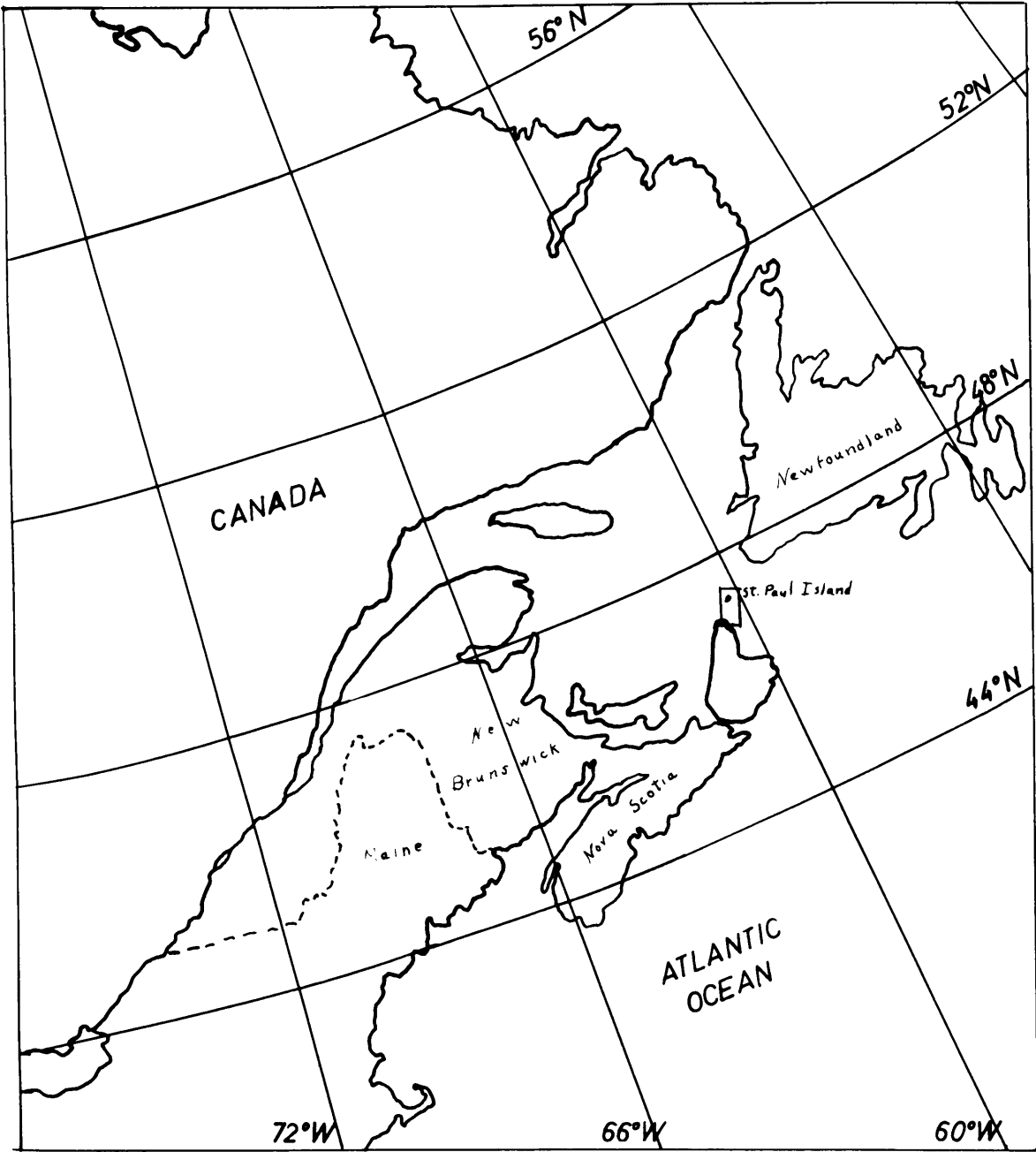


Figure 1. Index map for the area of study

mapped and approximately 120 samples were collected. Another week was spent studying the geology and collecting samples in the vicinity of Money Point on the northeast tip of Cape Breton Island, Nova Scotia. This area lies directly along strike with St. Paul Island and offers an interesting correlation problem (See Figure 2).

Laboratory work included microscopic examination of approximately 100 thin sections, separation by magnetic and heavy liquid techniques of 24 rocks into their constituent minerals, chemical analyses by means of photometric instrumental techniques of coexisting biotites, garnets, and chlorite, and synthesis of the data into the appropriate phase diagrams.

II GEOLOGY

Although a reconnaissance map of the island (Neale, 1956b) was available, this proved inadequate and a much more detailed map was made (Figure 3). Sea Cliffs border the entire island and allow excellent exposures for mapping and sampling. All of the rock units of St. Paul Island are metamorphic. The western 2/3 of the island is mapped as one unit, gneiss, schist, and pegmatite. In general the proportion of schist increases to the east and that of pegmatite to the west. However, the predominant rock type is gneiss. Several of the schists contain kyanite. A rather spectacular development of kyanite was discovered at Petrie Point where a schist contains a narrow band consisting of nearly 50% kyanite as bladed

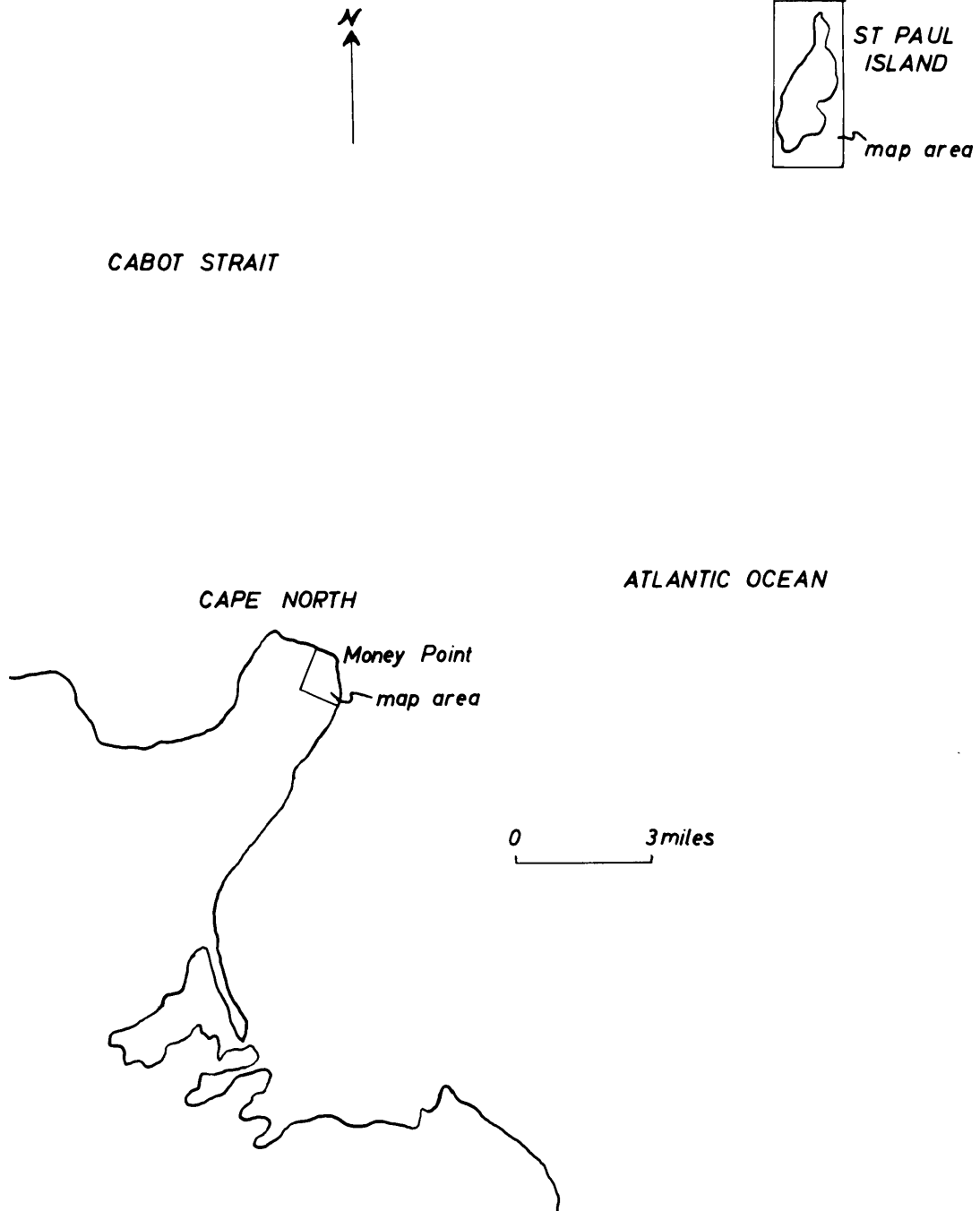
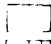
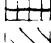
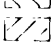
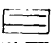

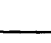



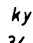
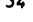


Figure 2. Reference map relating St. Paul Island and Money Point

GEOLOGY OF ST. PAUL ISLAND

LEGEND

- gneiss, schist, pegmatite 
- schist 
- amphibolite, quartzite 
- schist, amphibolite 
- epidote-amphibolite 
- stauralite schist 
- approximate contact 
- fault 
- kyanite isograd 
- kyanite schist samples 
- 34 

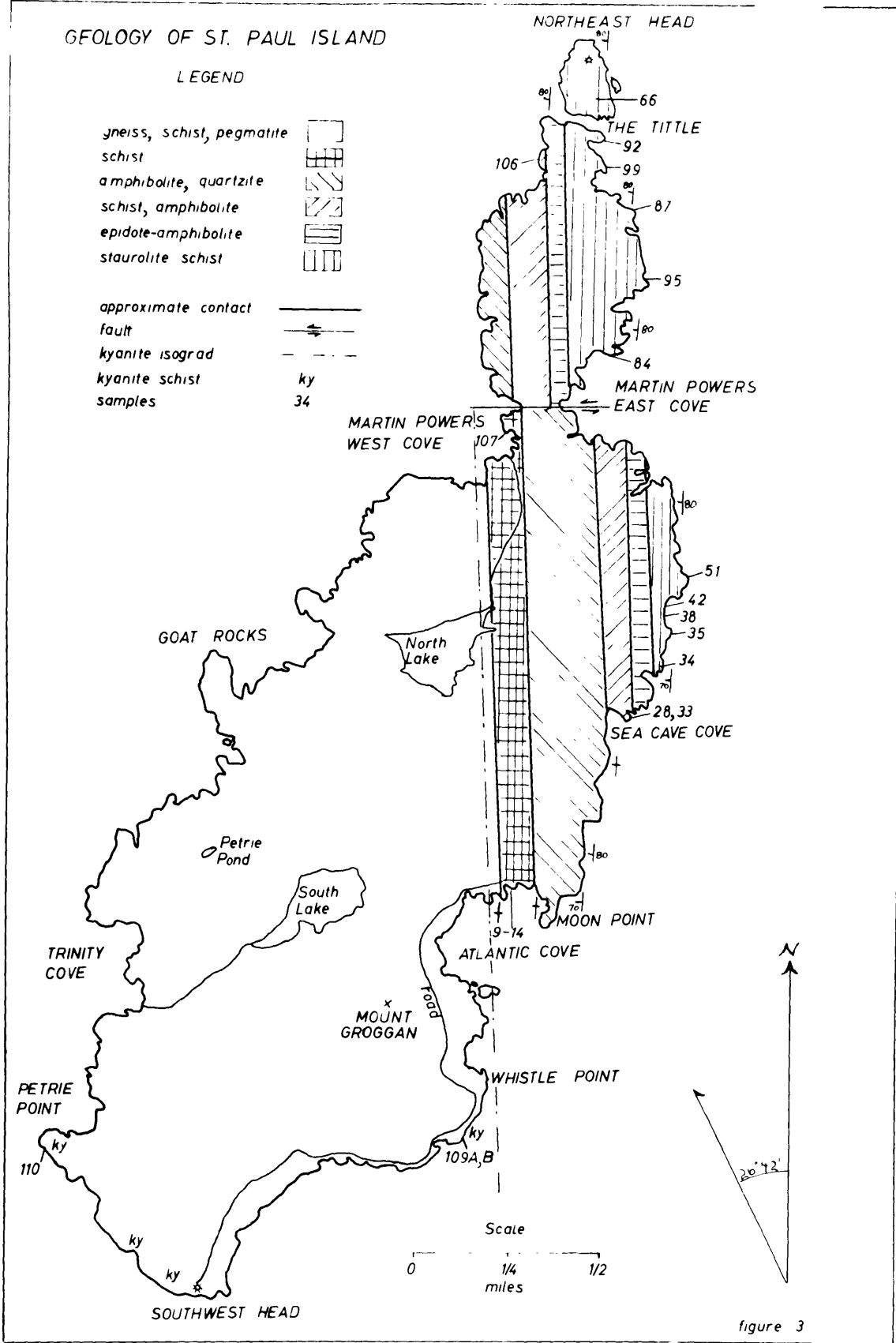


figure 3

crystals one inch long. At Lookout Point staurolite occurs with the kyanite. In the schists to the east of this point there is much staurolite but no kyanite. On the basis of the occurrences of kyanite and staurolite an approximate kyanite isograd has been drawn on the map. The gneisses and pegmatites are granitic in composition.

The northeastern portion of the island has been divided into the following units with areal distribution as shown on the accompanying map.

	Rock Type	Thick-ness	Mapped Unit
west	Interbedded schist and quartzite	525'	525'
	Amphibolite	880'	930'
	Interbedded amphibolite and quartzite	50'	
	Interbedded schist and quartzite	240'	510'
	Interbedded schist and amphibolite	270'	
	Epidote-rich amphibolite	275'	275'
east	Staurolite schist	900+'	900'

Mineral assemblages of the schists are included in Table 5. The amphibolites contain varying proportions of hornblende, oligoclase, clinozoisite, quartz, and sphene. In some instances the sphene surrounds small opaque cores. Apatite is always present as an accessory mineral.

On St. Paul Island the bedding and foliation are parallel, striking from N10°E to N20°E and dipping nearly vertical. Shear zones, ptygmatic folding, boudinage structures, and faults are common. A major left hand fault at Martin Powers Coves has a strike slip of nearly 700 feet.

The geology of the Money Point area on Cape Breton is shown in the geologic map of Figure 4. As on St. Paul Island the metamorphic grade increases to the west; but at Money Point the rocks are of a lower grade. Along the coast near Money Point the rocks consist of phyllites and volcanics. In many of the mafic volcanics tiny needles of hornblende occur in porphyroblastic bundles. In the schists along the coast and in the stream bed to the west of the Money Point Lighthouse porphyroblasts of biotite and garnet occur in a fine-grained matrix of chlorite, muscovite, and quartz. In the schists found in the stream to the west of the radio station there is no chlorite but much staurolite. Interbedded with the staurolite schists are amphibolites.

The lithology of both St. Paul Island and Money Point indicates an original sequence of interbedded volcanics and sediments. The strikes of the bedding and foliation coincide to within a few degrees. In both areas the metamorphic grade increases from east to west. It seems reasonable to assume that both areas have similar geologic histories.

A potassium-argon age determination was made on one of the biotites from a staurolite schist which outcrops on the Northeast

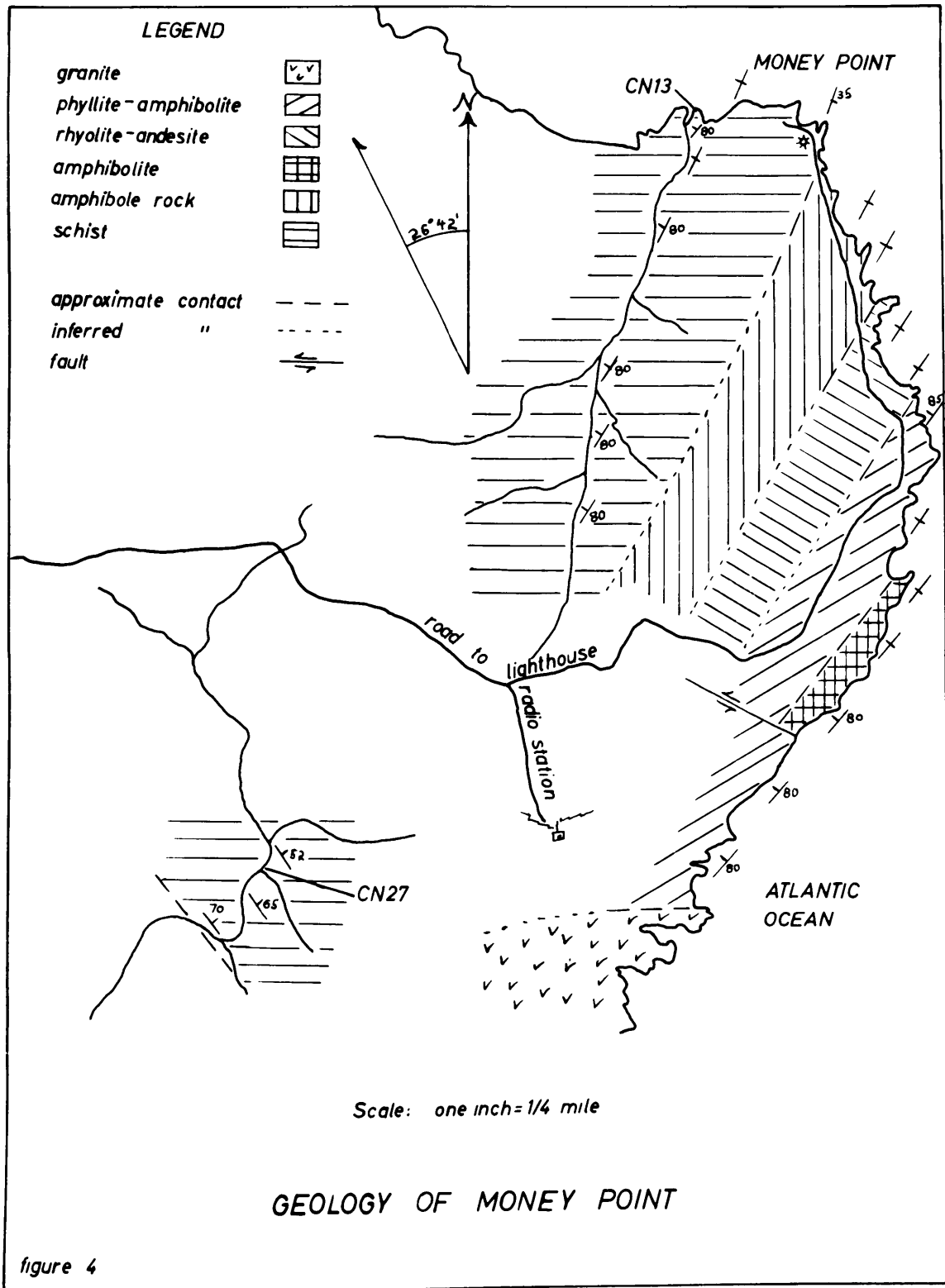


figure 4

Head of St. Paul Island. The A/K ratio corresponds with an age of 360 million years. Previous age work on Nova Scotia granites (Fairbairn et al., in press), show this to be the age of crystallization of micas in the granites which intrude Devonian sediments on the mainland. Therefore, the recrystallization of biotite on St. Paul Island appears to have accompanied the crystallization of granite on the mainland of Nova Scotia. This event is often referred to as the Acadian Revolution.

III SAMPLING AND MINERAL SEPARATION

From the phase rule it is apparent that the more phases in a rock of a given number of components, the fewer the degrees of freedom and, consequently, the more one can deduce about the conditions of formation of the rock.

For the problem under study--high grade metamorphism of pelitic sediments--the system was defined by SiO_2 , Al_2O_3 , K_2O , MgO , FeO , and H_2O . It was realized that other components such as Na_2O , MnO , and CaO would be present, but it was hoped that these would make up only a minor part of the total composition. If these components are present in only small quantities the phase relations will be little changed. In the six component system defined above it is reasonable to assume that H_2O might well be a mobile component. Therefore, a rock with five ($c-1$), or more, phases containing these components would be a suitable sample. For example, a typical staurolite zone specimen composed of quartz, muscovite, garnet, biotite, and staurolite would contain SiO_2 , K_2O , Al_2O_3 , FeO , MgO , and

H₂O (assuming the garnet to be a member of the almandine-pyrope series). Such a specimen would be adequate. More desirable would be a specimen from the kyanite isograd, composed of quartz, muscovite, biotite, garnet, staurolite, and kyanite. This has the same components but an extra phase has been added. A specimen containing only quartz, muscovite, biotite, and garnet would be discarded.

As far as possible correct identification must be made in the field. This is insufficient if a garnet contains a large amount of MnO or CaO, or if a biotite contains 5% TiO₂. These are problems which have their final solution only in the laboratory. By collecting several samples which, at least, appear suitable there is a good chance that a few will meet the requirements. Another problem which cannot always be avoided in the field is the collection of specimens which have undergone retrograde or replacement reactions. In many samples these features are obvious only under a microscope.

Another problem which has its solution in microscopic observation is that of inclusions. In order to analyze pure specimens the inclusions must be liberated and separated. All of the staurolite grains contain inclusions of quartz but these are usually larger than 50 microns and can be mechanically separated. All but a few of the garnet grains are literally filled with quartz inclusions. When a large percentage of these inclusions are smaller than 30 microns it becomes extremely difficult to separate the quartz and garnet.

After elimination of samples which showed alteration or excessive inclusions, 24 remained for separation into constituent phases. The minerals were separated by standard techniques using heavy liquids and the Frantz Isodynamic Separator. However, the inclusions in most staurolites and garnets required the following additional processing.

1. Grind in agate mortar
2. Screen, collecting -200 +325; -325 +400; and -400 fractions
3. Using liquid close to the index of refraction of the mineral being separated check each size fraction for liberation of inclusions.
4. If -400 fraction must be used place small portions of it in a 100ml beaker and with a wash bottle squirt acetone into the beaker until the sample is well-stirred. After five seconds decant the acetone. Continue this procedure until the acetone remains clear after five seconds. The remaining grains are coarse enough to pass through the Frantz.
5. Pass the coarsest fraction in which the inclusions are liberated through the Frantz. After several passes the samples are quite pure.

These procedures produce staurolite which is 98%+ pure. It is impossible to remove all of the quartz inclusions from most garnets. There are always a few inclusions in the 5-10 micron size range. These make up a very small percentage of the total sample and can be neglected. All of the separated mineral samples were checked under the petrographic microscope in a liquid having an index of refraction close to that of the mineral. Grain counts were made and samples which were not at least 98% pure were rerun through appropriate steps of the separation procedure until the desired purity was attained. Because of very fine quartz inclusions in the garnets

some of the garnets may contain more than 2% quartz.

IV CHEMICAL ANALYSES

A. Problems and Techniques

The analyses were made by instrumental, or so-called, "rapid silicate" techniques. In brief, the SiO_2 , TiO_2 , Al_2O_3 , total iron as Fe_2O_3 , and MnO are determined spectrophotometrically with the following indicators; molybdenum blue, tiron, alizarin red-S, orthophenanthroline, and permanganate, respectively. The CaO and MgO are titrated with versene using murexide and eriochrome black-T, respectively, as indicators. FeO is titrated with dichromate; and K_2O and Na_2O are determined with a Perkin-Elmer flame photometer using Li as an internal standard.

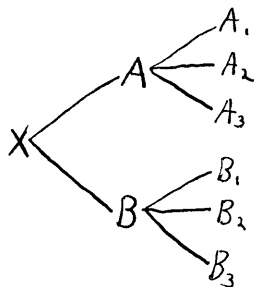
Although several of the procedures were modified, the outline of Shapiro and Brannock (1956) was used. The major departure from the original outline is in the CaO and MgO determinations. This change was adopted by Shapiro and Brannock in 1958 (personal communication). The change involves complexing the R_2O_3 group with a solution of triethanolamine and sodium cyanide before titrating with versene. This is considerably easier, and perhaps more accurate, than the previous method of precipitation and filtration of the R_2O_3 group at a carefully controlled pH. Other changes were minor, involving concentration changes which must be varied considerably more with mineral analyses than with rock analyses. The details of the procedures used are available

in the spectrophotometer laboratory of the Department of Geology and Geophysics at M.I.T.

B. Precision

Perhaps the greatest advantage offered by instrumental techniques is the ease with which replicate analyses can be made, with resultant high precision. The final value for an element from any single weighing can usually be shown to have a reasonably small standard error.

Nearly all of the minerals were analyzed in duplicate. In a few cases enough sample for duplicate weighings was not available. From each of the duplicate weighings a solution was made. From each solution pairs of aliquots were taken for determinations. Thus most of the final results are a combined average of pairs of solutions from each of duplicate weighings. The diagram below may better illustrate this procedure. The original sample, x, is weighed in duplicate and made into duplicate solutions, A and B. From each of solutions A and B pairs of aliquots are taken, A₁ and A₂ from A; and B₁ and B₂ from B.



In the determinations of CaO and MgO a third aliquot was frequently taken from solutions A and B. These are shown as A₃

and B₃ in the diagram. The results from pairs are shown in Table 1, and those of duplicates in Table 2.

In order to illustrate the reproducibility of the analyses the best and worst results of pairs, such as A₁ and A₂, and of duplicate weighings, such as A and B, are shown in Table 3. The standard deviations, standard errors, and relative errors for the worst pairs and the worst duplicates are also included in Table 3. Definitions of these terms are:

$$\text{standard deviation, } s = \sqrt{\frac{\sum d^2}{n-1}}$$

where d is the deviation from the arithmetic mean of a single measurement.

and n is the number of measurements.

$$\text{standard error (of the mean), } s_{\bar{x}} = \frac{s}{\sqrt{n}}$$

$$\text{relative error, } E = \frac{s_{\bar{x}}}{\bar{x}}$$

where \bar{x} is the arithmetic mean.

C. Accuracy

In order to test the accuracy of the procedures one can analyze standards which have compositions similar to that of the analyzed samples. Available standards which approximate the compositions of almandite garnet and the biotites of this study do not exist. The closest approximation is the diabase W-1 which has been analyzed by 35 laboratories (Fairbairn et al, 1953). In Table 4 a comparison of the values

obtained for W-1 in the present study and the average of 35 laboratories is made. Values obtained for G-1 and Haplogranite are also compared with the averages from other laboratories. G-1 and Haplogranite have compositions which are considerably different from the analyzed garnets and biotites and should not be considered in a rigorous comparison of accuracy.

Further tests of accuracy can be made with the garnet analyses. First, the totals of the analyses should be close to 100%; and second, the molecular ratios should balance according to the idealized formula $(RO)_3 \cdot (R_2O_3)_2 \cdot (SiO_2)_3$. It may be seen from Table 5 that all of the garnet analyses are close to 100% total. From Table 6 it may be seen that the molecular ratios are high for SiO_2 and low for RO and R_2O_3 . It was stated previously in the section on mineral separations that garnet could not be obtained free from tiny quartz inclusions. The excess SiO_2 is usually about 3% which is approximately the amount one would estimate from oil mounts of the garnet grains. A correction for the excess quartz can be made and the results after correction are shown in Table 7. It is seen that most of the analyses now show a small excess of R_2O_3 and a comparable deficit of RO .

There are four possible explanations of these small variations from the expected values. 1) Some of the iron might be oxidized during the FeO determination. 2) There may be a consistent error in the determination of total iron. 3) There may be a consistent error in the determination of some

combination of elements from both the R_2O_3 and RO groups.

4) Some of the ferric iron may be in the structural site of ferrous iron. In order to help resolve the problem Dr. Ito of the Harvard Mineralogy Department kindly offered to analyze one of the St. Paul garnets, using gravimetric procedures.

His results are given below.

	SP109B (Ito)	mole ratios	corrected for SiO_2	SP109B photometric
SiO_2	37.89	3.045	3.00	38.43
TiO_2	.36	.021		.15
Al_2O_3	20.45	1.936	2.02	20.14
Fe_2O_3	.61	.037		1.25
FeO	31.74	2.132		31.77
MnO	2.58	.176		2.64
MgO	2.99	.358	2.98	2.34
CaO	2.80	.241		2.69
total	99.42			

A comparison of Dr. Ito's results with the writer's in Table 5 indicates that explanation 1) above is not probable, but that explanations 2) and 3) are possibilities. Even after correction for excess SiO_2 the molecular ratios for Dr. Ito's analysis are slightly high for R_2O_3 and low for RO. TiO_2 was considered as in the structural site of SiO_2 . If it were considered as part of the R_2O_3 group the molecular ratios would be even further from the expected values. Although explanations 2) and 3) may partially answer the problem it would appear that explanation 4) is also a possibility. One of the best examples of a high R_2O_3 garnet is found in an infra red absorption study

(Clark, 1957) where intense lines, believed to be caused by ferric iron, were noted. The molecular ratios for this garnet are included in Table 7.

Although there is the possibility of a significant error in the accuracy of any of the components listed in Table 5 the error would be consistent in all of the determinations. Because each determination is compared with the same set of standards any error in the standards would be reflected in all of the samples. From the statistics presented previously the results for the major elements seem to be highly reproducible. Therefore, any comparison of compositions of various mineral assemblages would be little affected by any absolute errors which might exist. In any comparison the errors are relative; and in the present study the relative errors are small. In the phase diagrams of the next chapter one of the coordinates is the mole fraction $\frac{\text{MgO}}{\text{MgO} + \text{FeO}}$. A 1% change in this fraction corresponds with a 0.20 change in the MgO content. From the summary of precision shown in Table 3 it is seen that a 0.20% change is approximately the worst standard error to be expected from duplicate weighings. Thus any difference of more than 1% in the above mole fraction is probably real.

Table 1. Pairs-Biotites

	SP9		SP9		SP12		SP12		SP12		SP13		SP13	
	A ₁	A ₂	B ₁	B ₂	A ₁	A ₂	B ₁	B ₂	C ₁	C ₂	A ₁	A ₂	B ₁	B ₂
SiO ₂	35.26	35.32	35.38	35.50	35.87	35.87	36.34	36.40	36.15	36.08	36.45	36.45	36.45	36.51
TiO ₂	1.66	1.66	1.65	1.65	1.65	1.64	1.59	1.64			1.61	1.61	1.61	1.61
Al ₂ O ₃ *	18.12	18.15	18.54	18.51	18.34	18.29	18.28	18.19			18.18	18.18	18.38	18.11
	18.42	18.41	18.15	18.31	18.17	18.13					18.49	18.36	18.14	18.18
Total Fe as Fe ₂ O ₃	22.75	22.85	22.56	22.50	21.21	21.17	20.98	20.98			21.70	21.69	21.67	21.71
MgO	9.76	9.77	9.67	9.63	10.73	10.79	10.81	10.81			10.34	10.31	10.38	10.38
Na ₂ O	.27	.30	.26	.27	.29	.28	.33	.35			.24	.23	.23	.24
K ₂ O	7.62	7.62	7.47	7.53	8.40	8.41	8.60	8.46			8.36	8.41	8.35	8.34

	SP14		SP14		SP28		SP28		SP33		SP33		SP33	
	A ₁	A ₂	B ₁	B ₂	A ₁	A ₂	B ₁	B ₂	A ₁	A ₂	B ₁	B ₂	C ₁	C ₂
SiO ₂	36.43	36.55	36.39	36.45	36.64	36.76	36.82	36.95	35.78	35.78	35.81	35.87	35.78	35.84
TiO ₂	1.74	1.69	1.71	1.67					1.65	1.65	1.65	1.66		
Al ₂ O ₃ *	18.17	18.10			17.40	17.22	17.60	17.36	17.54	17.46	17.75	17.75		
	18.05	17.99	18.05	18.17					17.40	17.37	17.58	17.75		
Total Fe as Fe ₂ O ₃	21.10	20.97	20.92	20.71	21.35	21.54	21.81	21.55	24.87	24.90	24.58	24.62		
MnO											.042	.042		
MgO	10.71	10.73	10.71	10.70	10.42	10.55	10.43	10.48	8.59	8.69	8.63	8.56		
Na ₂ O	.27	.30	.27	.37	.28	.31	.28	.28	.32	.33	.32	.31		
K ₂ O	8.93	9.01	8.81	8.83	8.47	8.49	8.54	8.59	8.41	8.38	8.62	8.63		

*upper row from Ni crucible fusions, lower row from Ag crucible fusions

	SP34		SP34		SP35		SP35		SP38		SP38		SP42	
	A ₁	A ₂	B ₁	B ₂	A ₁	A ₂	B ₁	B ₂	A ₁	A ₂	B ₁	B ₂	A ₁	A ₂
SiO ₂	35.13	35.13	35.16	35.16	36.12	36.36	36.45	36.52	36.61	36.55	36.89	36.89	35.66	35.60
TiO ₂	1.81	1.81	1.81	1.80	1.59	1.63	1.62	1.62	1.56	1.56	1.55	1.55	1.72	1.69
Al ₂ O ₃	17.37	17.30	17.73	17.75	18.03	18.00	18.14	18.14	17.83	17.79	17.98		17.63	17.58
	17.41	17.41	17.43	17.46	17.87	18.11	17.81	17.82	18.07	17.95	17.79	17.62	17.56	17.53
Total Fe as Fe ₂ O ₃	24.36	24.35	24.21	24.13	20.33	20.35	20.22	20.21	19.42	19.39	19.17	19.11	22.81	22.74
MnO													.071	.072
MgO	9.88	10.00	9.80	9.73	11.50	11.45	11.58	11.54	12.17	12.17	12.07	12.02	10.25	10.28
Na ₂ O	.32	.32	.24	.25	.30	.30	.38	.42	.32	.31	.30	.30	.33	.40
K ₂ O	7.87	7.98	7.76	7.73	8.68	8.68	8.73	8.73	8.73	8.83	8.66	8.61	9.09	8.98

	SP42		SP51		SP51		SP66		SP66		SP84		SP84	
	B ₁	B ₂	A ₁	A ₂	B ₁	B ₂	A ₁	A ₂	B ₁	B ₂	A ₁	A ₂	B ₁	B ₂
SiO ₂	35.94	35.81	36.70	36.70	36.40	36.33	36.08	36.02	35.96	36.02	36.31	36.24	36.73	36.73
TiO ₂	1.67	1.71	1.60	1.61	1.56	1.55	1.65	1.65	1.62	1.62	1.62	1.63	1.63	1.63
Al ₂ O ₃	17.90	17.84	18.06	18.02	17.80	17.58	18.14	18.13	18.02	17.95	18.00	17.99	17.92	17.94
			17.88	17.90	17.64	17.92	17.98	17.93	17.97	17.83	18.08	18.03	18.00	18.03
Total Fe as Fe ₂ O ₃	22.53	22.52	22.70	22.51	22.20	22.19	22.73	22.73	22.47	22.51	20.48	20.57	20.61	20.56
MnO									.072	.069				
MgO	10.10	10.12	10.26	10.31	10.21	10.16	10.01	10.04	9.85	9.79	11.01	11.00	10.99	10.95
Na ₂ O	.33	.33	.34	.35	.36	.34	.56	.55	.36	.35	.37	.37	.29	.31
K ₂ O	9.02	8.96	8.42	8.53	8.38	8.36	7.86	7.86	7.77	7.70	8.82	8.88	8.79	8.81

Table 1. Pairs-Biotites (cont)

	SP87		SP87		SP92		SP92		SP95		SP95		SP95	
	A ₁	A ₂	B ₁	B ₂	A ₁	A ₂	B ₁	B ₂	A ₁	A ₂	B ₁	B ₂	C ₁	C ₂
SiO ₂	35.50	35.56	35.59	35.59	35.59	35.65	35.90	35.84	35.87	35.75	36.08	36.15	35.78	35.66
TiO ₂	1.59	1.59	1.63	1.62	1.67	1.68	1.61	1.68	1.67	1.91	1.68	1.68		
Al ₂ O ₃	18.23	18.18	18.05	17.93	17.94	17.86	18.45	18.33	18.00	17.97	18.00	17.92		
	17.96	17.95	17.93	17.87	18.33	18.27	17.92	17.94	17.79	17.72	18.11	18.09		
Total Fe as Fe ₂ O ₃	21.50	21.43	21.61	21.57	22.99	22.95	23.06	22.95	21.17	21.09	20.97	20.89		
MnO			.105	.103	.059	.058								
MgO	11.46	11.35	11.35	11.39	9.86	9.88	9.86	9.88	11.05	11.05	11.05	10.97		
Na ₂ O	.29	.31	.25	.25	.32	.27	.27	.29	.33	.35	.30	.29		
K ₂ O	8.03	8.11	8.00	7.98	8.43	8.43	8.12	8.12	8.57	8.70	8.35	8.30		

	SP99		SP99		SP99		SP106		SP106		SP107		SP107	
	A ₁	A ₂	B ₁	B ₂	C ₁	C ₂	A ₁	A ₂	B ₁	B ₂	A ₁	A ₂	B ₁	B ₂
SiO ₂	35.97	35.91	36.00	36.06			36.76	36.70	36.67	36.67	35.57	35.50	35.47	35.54
TiO ₂	1.65	1.64	1.61	1.62			1.98	1.99	1.94	1.96	1.63	1.68	1.66	1.66
Al ₂ O ₃	18.13	18.02	18.14	18.09	18.13	18.02	18.04	18.12	17.98	17.83	17.64	17.75	17.59	17.73
	18.02	18.04	18.11	18.08			17.82	17.88	17.71	17.69	17.60	17.54	17.79	17.81
Total Fe as Fe ₂ O ₃	22.44	22.53	22.49	22.52			19.49	19.49	19.59	19.62	22.37	22.40	22.51	22.43
MnO														
MgO	9.86	9.85	9.90	9.81			11.25	11.33	11.25	11.18	9.90	9.94	9.94	9.85
Na ₂ O	.37	.47	.30	.30			.44	.39	.34	.35	.25	.30	.20	.21
K ₂ O	8.67	8.76	8.55	8.52			8.67	8.77	8.51	8.55	8.35	8.37	8.18	8.16

Table 1. Pairs-Biotites (cont)

Table 1. Pairs-Biotite(cont)

	SP109A		SP109A		SP109B		SP109B		SP110		SP110		SP110	
	A ₁	A ₂	B ₁	B ₂	A ₁	A ₂	B ₁	B ₂	A ₁	A ₂	B ₁	B ₂	C ₁	C ₂
SiO ₂	36.21	36.15	35.87	35.93	35.60	35.66	35.75	35.81	35.87	35.94	36.34	36.34	36.28	36.34
TiO ₂	2.03	2.03	2.01	2.02	1.67	1.73	1.72	1.72	2.18	2.17	2.17	2.17		
Al ₂ O ₃	17.57	17.56	17.31	17.26	18.28	18.31	18.46	18.49	17.32	17.32	17.17	17.21		
	17.62	17.47			18.39	18.38			17.46	17.20	17.48	17.58		
Total Fe as Fe ₂ O ₃	22.44	22.41	22.52	22.61	22.28	22.12	22.10	22.18	22.26	22.17	22.40	22.37		
MgO	9.67	9.62	9.57	9.46	10.27	10.38	10.27	10.18	9.20	9.21	9.18	9.21		
Na ₂ O	.32	.34	.32	.32	.27	.30	.22	.22	.28	.30	.23	.29		
K ₂ O	8.92	8.93	8.93	9.00	8.38	8.44	8.13	8.18	9.36	9.36	9.18	9.22		

	CN13		CN13		CN27		CN27		CN27		chlorite CN13		chlorite CN13	
	A ₁	A ₂	B ₁	B ₂	A ₁	A ₂	B ₁	B ₂	C ₁	C ₂	A ₁	A ₂	B ₁	B ₂
SiO ₂	36.73	36.80	36.15	36.33	35.32	35.38	35.54	35.35	35.47	35.60	27.46	27.22	27.35	27.23
TiO ₂					1.60	1.62	1.62	1.60						
Al ₂ O ₃	16.90	16.91	16.93		18.09	18.18	18.33	18.22			21.18	21.05	21.19	21.23
					17.87	17.81	17.90	17.89						
Total Fe as Fe ₂ O ₃	21.29	21.48			22.51	22.37	22.50	22.35			24.44	24.63		
MnO											.321	.320		
MgO	10.65	10.44			10.59	10.68	10.85	10.78			14.48	14.60		
CaO	.25	.23												
K ₂ O	7.56	7.52			7.53	7.56	7.63	7.61			.54	.49		
Na ₂ O	.31	.34			.30	.30	.29	.30			.54	.49		

Table 1. Pairs-garnet (cont)

	SP9		SP9		SP12		SP12		SP13		SP13		SP14	
	A1 A3	A2 A4	B1 B3	B2 B4	A1 A3	A2 A4	B1 B3	B2 B4	A1 A3	A2 A4	B1 B3	B2 B4	A1 A3	A2 A4
SiO ₂	38.44	38.57	38.10	37.97	38.47	38.35	37.97	38.03	38.16	38.16	38.28	38.28	38.55	38.23
	38.59	38.65	38.22	38.10	38.40	38.40	38.14	38.08						
Al ₂ O ₃	20.27	20.21	20.28	20.27	20.14	20.16	20.00	19.97	20.22	20.15	20.18	20.08	20.50	20.47
							20.01	20.00						
Total Fe as Fe ₂ O ₃	35.57	35.57	35.61	35.23	35.70	35.57	35.53	35.53	35.31	35.44	35.74	35.48	34.84	34.71
MgO	2.66	2.59	2.62	2.48	2.65	2.42	2.65	2.58	2.08	2.17	2.04	2.11	2.26	2.21
	2.57		2.56		2.74				2.06		1.94			
CaO	3.41	3.41	3.55	3.43	3.10	3.09	3.01	3.00	3.70	3.52	3.72	3.64	4.80	
			3.48		3.02						3.75			
	SP14		SP28		SP28		SP33		SP33		SP34		SP34	
	B1 B3	B2 B4	A1 A3	A2 A4	B1 B3	B2 B4	A1 A3	A2 A4	B1 B3	B2 B4	A1 A3	A2 A4	B1 B3	B2 B4
SiO ₂	38.26	38.14	38.44	38.57	38.16	38.03	37.71	37.77	37.69	37.81	38.10	37.98	38.16	38.03
			38.46	38.40	38.10	38.10								
Al ₂ O ₃	20.22	20.17	20.33	20.29	20.18	20.05	19.93	20.00	19.82	19.77	20.17	20.21	19.97	20.01
Total Fe as Fe ₂ O ₃	34.61	34.74	36.77	36.77	36.45	36.58	37.41	37.54			36.74	36.48	36.45	36.71
							37.55	37.16						
MnO			3.17	3.18										
MgO	2.14	2.17	3.09	3.08	3.09	2.97	2.38	2.31			2.10	1.97	2.08	2.02
					2.93									
CaO	4.80	4.78	1.94	1.89	1.92	2.05	2.98	3.02			3.25	3.40	3.45	3.41

Table 1. Pairs-garnet (cont)

	SP35		Sp35		SP38		SP42		SP42		SP51		SP51	
	A1 A3	A2 A4	B1 B3	B2 B4	A1 A3	A2 A4	B1 B3	B2 B4	A1 A3	A2 A4	B1 B3	B2 B4	A1 A3	A2 A4
SiO ₂	37.85	38.01	37.75	37.93	38.38	38.38	37.74	37.80	37.66	37.60	37.95	37.89	37.48	37.36
											37.91	37.91	37.48	37.48
Al ₂ O ₃	20.08	20.08	19.84	19.85	20.28	20.32	20.49	20.49	20.61	20.58	20.37	20.42	20.58	20.42
Total Fe as Fe ₂ O ₃	32.96	32.96	32.90	32.77	30.32	30.32	33.81	33.68	33.95	34.21	36.48	36.48	36.45	36.71
					30.19	30.00								
MnO					7.34	7.33								
MgO	1.99	1.77	1.82	1.91	1.95	2.11	2.11	2.03	2.29	2.19	2.05	2.12	2.08	2.14
CaO	4.73	4.79	4.66	4.80	4.49	4.17	3.74	3.83	3.70	3.78	3.47	3.41	3.42	3.34
					4.34									
	SP66		SP66		SP84		SP84		SP87		SP92		SP92	
	A1 A3	A2 A4	B1 B3	B2 B4	A1 A3	A2 A4	B1 B3	B2 B4	A1 A3	A2 A4	A1 A3	A2 A4	B1 B3	B2 B4
SiO ₂	39.02	38.90	38.84	38.96	37.55	37.67	37.89	38.01	37.60	37.48	37.74	37.50	37.32	37.38
Al ₂ O ₃	20.17	20.17	20.04	20.01	20.11	20.19	20.37	20.53	20.80	20.66	20.19	20.07		
	20.39	20.43	20.06	20.02							20.32	20.29		
Total Fe as Fe ₂ O ₃	35.83	35.83	36.00	35.61	33.62	33.36	33.27	33.14	34.66	34.53	37.15	37.41		
											37.42	37.16		
MnO					4.81	4.84			3.93	3.97				
MgO	2.48	2.50	2.47	2.58	1.97	2.00	2.12	1.98	2.47	2.56	2.72	2.77		
			2.34											
CaO	2.86	2.79	2.90	2.77	4.26	4.28	4.25	4.14	3.55	3.48	2.72	2.69		

Table 1. Pairs-garnet (cont)

	SP99		SP99		SP106		SP106		SP107		SP107		SP109A	
	A ₁ A ₃	A ₂ A ₄	B ₁ B ₃	B ₂ B ₄	A ₁ A ₃	A ₂ A ₄	B ₁ B ₃	B ₂ B ₄	A ₁ A ₃	A ₂ A ₄	B ₁ B ₃	B ₂ B ₄	A ₁ A ₃	A ₂ A ₄
SiO ₂	37.83	37.83	37.44	37.62	37.74	37.86	37.83	37.77	37.98	37.98	37.89	38.06	37.74	37.80
Al ₂ O ₃	20.22	20.25	20.06	20.00	20.39	20.35	20.18	20.22	20.14	20.08	19.88	19.92	20.47	20.48
	20.44	20.36							20.30	20.30	19.88	19.72	20.59	20.69
Total Fe as Fe ₂ O ₃	37.92	37.65	37.63	37.63	34.82	34.95	35.00	35.00	36.74	36.61	36.97	37.24	37.39	37.26
					34.84	34.84	34.69	34.95						
MgO	2.64	2.63	2.65	2.66	3.13	3.18	3.00	3.06	2.93	2.81	2.90	2.74	3.53	3.53
					2.97		3.09							
CaO	2.57	2.63	2.59	2.65	2.58	2.45	2.51	2.65	2.63	2.44	2.76	2.58	2.21	2.30
					2.54				2.57		2.59			

	SP109A		SP109B		SP109B		SP110		SP110		ON13		ON13	
	B ₁ B ₃	B ₂ B ₄	A ₁ A ₃	A ₂ A ₄	B ₁ B ₃	B ₂ B ₄	A ₁ A ₃	A ₂ A ₄	B ₁ B ₃	B ₂ B ₄	A ₁ A ₃	A ₂ A ₄	B ₁ B ₃	B ₂ B ₄
SiO ₂	37.71	37.71	38.41	38.41	38.47	38.41	37.11	37.05	37.38	37.38	39.15	39.15	39.16	39.35
Al ₂ O ₃	20.04	20.03	20.25	20.26	19.99	19.98	20.26	20.40	20.23	20.22	19.43	19.35	19.31	19.31
	20.21	20.05							20.13	20.02				
Total Fe as Fe ₂ O ₃	37.28	37.41	36.52	36.52	36.71	36.45	36.38	36.25	36.38	36.38	27.53	27.39	27.76	27.76
							36.61	36.22					27.65	27.40
MgO	3.43	3.63	2.34	2.34	2.33	2.34	2.26	2.18	2.33	2.39	.20		.18	.25
	3.41						2.30		2.32					
CaO	2.44	2.40	2.77	2.72	2.64	2.63	1.11	1.17	1.16		5.78		5.80	

Table 1. Pairs-garnet (cont)

	CN27		CN27	
	A ₁	A ₂	B ₁	B ₂
SiO ₂	38.23	38.04	38.20	38.44
Al ₂ O ₃	20.06	20.09	20.01	19.97
Total Fe as Fe ₂ O ₃	36.87	36.87	36.45	36.71
MgO	2.88	2.84	2.79	2.92
			2.69	
CaO	2.89	2.97	2.95	3.09

Table 2. Duplicate Weighings

	Biotites														
	SP9		SP12			SP13		SP14		SP28		SP33			
	A	B	A	B	C	A	B	A	B	A	B	A	B	C	
SiO ₂	35.29	35.44	35.87	36.37	36.12	36.45	36.48	36.49	36.42	36.70	36.89	35.78	35.81	35.84	
TiO ₂	1.66	1.65	1.65	1.62		1.61	1.61	1.72	1.69	1.55	1.58	1.65	1.66		
Al ₂ O ₃ *	18.52	18.14	18.32	18.24		18.18	18.25	18.20	18.22	17.31	17.48	17.50	17.75		
	18.23	18.42	18.16			18.43	18.16	18.14				17.39	17.67		
Total Fe as Fe ₂ O ₃	22.80	22.53	21.19	20.98		21.70	21.69	21.04	20.82	21.44	21.68	24.89	24.60		
FeO	18.18	18.29	16.95	17.07	16.90	17.56	17.68	16.60	16.53	16.64	16.63	19.20	19.22	19.20	
MnO	.115	.117	.071	.065		.057	.049	.065	.066			.042	.035		
MgO	9.77	9.65	10.76	10.81		10.33	10.38	10.72	10.71	10.49	10.45	8.64	8.60		
Na ₂ O	.29	.27	.29	.34		.24	.24	.29	.30	.30	.28	.33	.32		
K ₂ O	7.62	7.50	8.41	8.53		8.39	8.35	8.97	8.82	8.48	8.56	8.40	8.63		

	Garnets													
	SP9		SP12		SP13		SP14		SP28		SP33		SP34	
	A	B	A	B	A	B	A	B	A	B	A	B	A	B
SiO ₂	38.56	38.10	38.40	38.06	38.16	38.28	38.29	38.20	38.46	38.10	37.74	37.75	38.04	38.09
TiO ₂	.20	.20	.34	.34	.19	.21	.15	.14	.12	.15	.33		.23	.22
Al ₂ O ₃	20.24	20.28	20.15	20.00	20.19	20.13	20.48	20.20	20.31	20.12	19.96	19.80	20.19	19.99
Total Fe as Fe ₂ O ₃	35.57	35.42	35.64	35.53	35.38	35.61	34.78	34.68	36.77	36.52	37.42		36.61	36.58
FeO	30.88	30.94	30.80	30.89	31.19	30.81	(30.11, 30.17, 30.08)	31.77	31.88	32.54	32.49		32.04	31.96
MnO	2.47	2.45	3.11	3.11	3.31	3.31	2.76	2.74	3.18	3.16	2.34		2.66	2.70
MgO	2.60	2.56	2.60	2.62	2.10	2.03	2.24	2.16	3.09	3.00	2.34		2.04	2.05
CaO	3.41	3.48	3.07	3.01	3.61	3.70	4.80	4.79	1.92	1.98	3.00		3.33	3.43

* upper row from Ni crucible fusions, lower row from Ag crucible fusions

Table 2 (cont)

	SP34		SP35		SP38		Biotites SP42		SP51		SP66		SP84	
	A	B	A	B	A	B	A	B	A	B	A	B	A	B
SiO ₂	35.13	35.16	36.24	36.49	36.58	36.86	35.63	35.88	36.70	36.37	36.05	35.99	36.28	36.73
TiO ₂	1.81	1.81	1.61	1.62	1.56	1.55	1.71	1.69	1.61	1.56	1.65	1.56	1.63	1.62
Al ₂ O ₃	17.34 17.41	17.74 17.45	18.02 17.99	18.14 17.82	17.81 18.01	17.98 17.71	17.61 17.55	17.87	18.04 17.89	17.69 17.78	18.14 17.96	17.99 17.90	18.00 18.06	17.93 18.02
Total Fe as Fe ₂ O ₃	24.36	24.17	20.34	20.22	19.41	19.14	22.78	22.53	22.61	22.20	22.73	22.49	20.52	20.59
FeO	18.70	18.60	15.20	15.25	14.43	14.35	17.55	17.37	16.89	16.73	17.34	17.28	15.23	15.32
MnO	.039	.041	.071	.071	.104	.111	.072	.072	.042	.042	.065	.071	.084	.086
MgO	9.94	9.77	11.48	11.56	12.17	12.04	10.27	10.11	10.29	10.19	10.03	9.82	11.01	10.97
Na ₂ O	.32	.25	.30	.40	.32	.30	.37	.33	.35	.35	.56*	.36	.36	.37
K ₂ O	7.93	7.75	8.68	8.73	8.78	8.64	9.04	8.99	8.48	8.37	7.86	7.74	8.85	8.80

*probably contamination

	SP35		SP38		SP42		SP51		SP66		SP84		SP87		SP92	
	A	B	A	B	A	B	A	B	A	B	A	B	A	B	A	B
SiO ₂	37.92	37.84	38.38	37.63	37.77	37.45	37.91	38.96	38.90	37.61	37.95	37.54	37.63	37.35		
TiO ₂	.39	.39	.23	.18	.18	.25	.26	.19	.19	.39	.41	.17	.28			
Al ₂ O ₃	20.08	19.85	20.30	20.60	20.49	20.50	20.40	20.29	20.04	20.15	20.35	20.73	20.22			
Total Fe as Fe ₂ O ₃	32.96	32.84	30.21	34.08	33.75	36.58	36.48	35.83	35.81	33.49	33.21	34.60	37.29			
FeO	28.21	28.09	25.93	29.09	29.01	31.16	31.14	30.94	31.22	28.60	28.70	29.62	32.60	32.61		
MnO	5.00	4.94	7.34	5.04	4.94	2.91	2.91	2.84	2.86	4.82	4.80	3.95	1.96			
MgO	1.88	1.87	2.03	2.24	2.07	2.11	2.09	2.49	2.47	1.99	2.04	2.52	2.74			
CaO	4.76	4.73	4.33	3.74	3.78	3.38	3.44	2.82	2.84	4.27	4.20	3.52	2.70			

Table 2 (cont)

	SP87		SP92		SP95			Biotites SP99			SP106		SP107		SP109A	
	A	B	A	B	A	B	C	A	B		A	B	A	B	A	B
SiO ₂	35.53	35.59	35.62	35.87	35.82	36.11	35.72	35.94	36.03	36.73	36.67	35.54	35.51	36.18	35.90	
TiO ₂	1.59	1.63	1.68	1.63	1.69	1.68		1.65	1.61	1.99	1.95	1.66	1.66	2.03	2.02	
Al ₂ O ₃	18.21	17.99	17.90	18.39	17.99	17.96		18.08	18.12	18.08	17.91	17.70	17.66	17.51	17.29	
	17.96	17.90	18.30	17.93	17.76	18.10		18.03	18.10	17.85	17.70	17.57	17.80	17.56		
Total Fe as Fe ₂ O ₃	21.47	21.59	22.97	23.01	21.13	20.93		22.49	22.51	19.49	19.61	22.39	22.47	22.43	22.57	
FeO	16.22	16.10	17.70	17.75	15.80	15.75		17.43	17.55	15.90	15.85	18.25	18.45	16.95	17.00	
MnO	.096	.104	.059	.059	.084	.089		.045	.040	.092	.097	.094	.089	.029	.029	
MgO	11.41	11.37	9.87	9.88	11.05	11.01		9.86	9.86	11.29	11.22	9.92	9.90	9.65	9.52	
Na ₂ O	.30	.25	.30	.28	.34	.30		.42	.30	.42	.35	.28	.21	.33	.32	
K ₂ O	8.07	7.99	8.43	8.12	8.64	8.33		8.72	8.54	8.72	8.53	8.36	8.17	8.93	8.97	

	SP99		SP106		SP107			Garnets SP109A			SP109B		SP110		CW13	
	A	B	A	B	A	B	A	B	C	A	B	A	B	A	B	
SiO ₂	37.83	37.53	37.80	37.80	37.98	37.97	37.77	37.71		38.41	38.44	37.08	37.38	39.15	39.25	
TiO ₂	.36	.37	.10	.12	.34	.33	.20	.20		.14	.15	.04	.05	.37	.37	
Al ₂ O ₃	20.32	20.03	20.37	20.20	20.21	19.84	20.55	20.10		20.26	19.99	20.33	20.15	19.39	19.31	
Total Fe as Fe ₂ O ₃	37.78	37.53	34.86	34.91	36.68	37.10	37.33	37.35		36.52	36.58	36.37	36.38	27.46	27.64	
FeO	33.00	33.03	30.43	30.51	32.79	32.81	32.89	32.57	32.63	31.82	31.72	30.71	30.72	23.45	23.37	
MnO	1.78	1.75	4.14	4.12	2.05	2.07	1.83	1.79		2.64	2.64	5.58	5.64	9.95	10.01	
MgO	2.64	2.61	3.09	3.05	2.87	2.82	3.53	3.50		2.34	2.34	2.25	2.34	.20	.21	
CaO	2.60	2.62	2.53	2.55	2.55	2.64	2.26	2.42		2.74	2.64	1.14	1.16	5.70	5.80	

Table 2 (cont)

	SP109B		SP110		Biotite			Chlorite			Carnet			
	A	B	A	B	C	CN13		CN27		CN13		CN27		
						A	B	A	B	C	A	B	A	B
SiO ₂	35.63	35.78	35.91	36.34	36.31	36.77	36.24	35.35	35.45	35.54	27.34	27.29	38.14	38.32
TiO ₂	1.71	1.72	2.18	2.17		1.49		1.61	1.61		.30		.39	.40
Al ₂ O ₃	18.30 16.39	18.48	17.32 17.34	17.19 17.53		16.91	16.93	18.14 17.84	18.28 17.90		21.12	21.21	20.08	19.99
Total Fe as Fe ₂ O ₃	22.20	22.14	22.22	22.39		21.38		22.44	22.43		24.54		36.87	36.58
FeO	16.35	16.27	17.20	17.15		16.12		17.69	17.71		19.43		31.87	31.90
MnO	.065	.061	.163	.159		.24		.073	.072		.32		1.81	1.82
MgO	10.33	10.23	9.21	9.20		10.55		10.64	10.82		14.54		2.86	2.80
CaO						.24							2.93	3.02
Na ₂ O	.29	.22	.29	.26		.32		.30	.30		.16			
K ₂ O	8.41	8.16	9.36	9.20		7.54		7.55	7.62		.52			

Table 3. Precision of Analyses

A, A₂ A B
weighing

Component	Pairs	Duplicates	Worst Pair	Worst Duplicate
SiO ₂	best: 23 of 96 pairs are identical worst: gar CN27 B ₁ 38.20 B ₂ 38.44	best: gar SP106 is identical bio SP13, 34, and 107 have differences of 0.03 worst: gar SP9 A 38.56 B 38.10 all but 4 within 0.30 bio CN13 A 38.56 B 38.10 all but 4 within 0.30	s 0.17 s _x 0.12 E 0.3%	s 0.37 s _x 0.26 E 0.7%
Al ₂ O ₃	best: 10 of 143 pairs are identical worst: bio SP51 B ₁ 17.64 B ₂ 17.92 difference of more than 0.10 is unusual	best: gar SP9 A 20.24 B 20.28 bio SP14 s 0.02 worst: gar SP109A A 20.55 B 20.10 all but 5 within 0.25 bio SP92 s 0.12	s 0.20 s _x 0.14 E 0.8%	s 0.32 s _x 0.23 E 1.1%
Total Fe as Fe ₂ O ₃	best: 13 of 100 are identical worst: gar SP66 B ₁ 36.00 B ₂ 35.61 most are within 0.30 bio SP28 B ₁ 21.81 B ₂ 21.55 most are within 0.15	best: gar SP110 A 36.37 B 36.38 bio CN27 A 22.44 SP13 A 21.70 B 22.43 B 21.69 worst: gar SP107 A 36.68 B 37.10 all but 2 within 0.30 bio SP51 A 22.61 B 22.20 all but 4 within 0.25	s 0.18 s _x 0.13 E 0.6%	s 0.29 s _x 0.20 E 0.9%
MnO garnets only		best: 4 of 20 duplicates identical worst: gar SP42 A 4.94 B 5.04 over half are within 0.02		s 0.07 s _x 0.05 E 1.0%
TiO ₂	best: 18 of 40 pairs are identical worst: bio SP92 B ₁ 1.61 B ₂ 1.68 all but 6 within 0.02	best: 4 biotites and 7 garnets identical worst: bio SP51 A 1.61 B 1.56 all but 6 within 0.02	s 0.05 s _x 0.03 E 1.8%	s 0.04 s _x 0.03 E 1.8%

Remarks

For SiO₂, Al₂O₃, and total Fe as Fe₂O₃ each of the aliquots A₁, A₂, etc. contains enough solution to make four separate readings on the spectrophotometer. Therefore, each A₁, A₂, etc. is the average of four readings.

In order to further check the reproducibility of SiO₂ eight garnets were run as a second set of pairs which might be called A₃ and A₄ or B₃ and B₄. The results are shown in table 1 as garnets SP9 A and B, SP12 A and B, SP28 A and B, and SP51 A and B.

The Al₂O₃ results for biotites were determined by both Ni and Ag crucible fusions. In tables 1 and 2 the upper row of Al₂O₃ values are from Ni crucibles, the lower row from Ag crucibles. Only the biotites were done in this manner. All of the Al₂O₃ values for garnets are from Ni crucible fusions.

Because the permanganate method for MnO is highly sensitive it was found that pairs of MnO determinations were unnecessary. The few pairs which were run are included in table 1. The variation between biotite pairs is in the third decimal place. Even in the higher concentration range of garnets the variation between pairs is too small to be significant.

TiO₂ determinations on biotites were done in pairs but for similar reasons as discussed for MnO it was deemed unnecessary to run the garnets in pairs.

Determinations of CaO and MgO are based on a titration for CaO and a second titration for total CaO and MgO. The MgO is calculated by subtracting CaO from total CaO and MgO. Because errors in the CaO determination will be reflected in the MgO calculation it is necessary to obtain high precision for CaO. In several instances the titration for CaO was repeated three times. All but one biotite had no detectable CaO. The lower detection limit for CaO was 0.05%. Several of the garnets were titrated in triplicate for total CaO and MgO.

Table 3 (cont.)

TiO ₂ cont.		gar SP28 A 0.12 B 0.15 all but 3 within 0.01		
CaO garnets only	best: one identical pair worst: SP13 A ₁ 3.70 A ₂ 3.52 28 pairs within 0.10	best: SP14 A 4.80 B 4.79 worst: SP109 A 2.26 B 2.42 all but one within 0.10	s 0.13 s _x 0.09 E 2.6%	s 0.11 s _x 0.08 E 3.3%
MgO	best: 3 of 46 biotite pairs are identical 2 garnet pairs identical 4 garnet pairs within 0.01 worst: bio CN13 A ₁ 10.65 A ₂ 10.44 all but one within 0.11 gar SP35 A ₁ 1.99 A ₂ 1.77 most garnets within 0.15	best: one garnet and one biotite identical worst: bio SP66 A 10.03 B 9.82 all but 4 of the 23 are within 0.15 gar SP42 A 2.07 B 2.24 all but one of 19 are within 0.10	biotite s 0.15 s _x 0.10 E 1.0% garnet s 0.16 s _x 0.11 E 5.8%	biotite s 0.15 s _x 0.10 E 1.0% garnet s 0.12 s _x 0.08 E 3.7%
FeO		best: bio SP28 A 16.64 B 16.63 gar SP92 A 32.60 SP110 A 30.71 B 32.61 B 30.72 worst: bio SF107 A 18.25 B 18.45 all but 4 within 0.15 gar SP13 A 31.19 B 30.81 all but 3 within 0.15		biotite s 0.18 s _x 0.13 E 0.7% garnet s 0.27 s _x 0.19 E 0.6%
K ₂ O biotite only	best: 6 of 47 pairs are identical worst: SP12 B ₁ 8.60 B ₂ 8.46 all but 2 within 0.11	best: SP109A A 8.93 SP13 A 8.39 B 8.97 B 8.35 worst: SP95 A 8.64 B 8.33 all but 4 within 0.20	s 0.10 s _x 0.07 E 0.8%	s 0.22 s _x 0.16 E 1.9%
Na ₂ O biotites only	best: 12 of 47 pairs are identical worst: SP14 B ₁ 0.22 B ₂ 0.37	best: 3 of 23 are identical worst: SP66 A 0.56 B 0.36		

Remarks (cont)

Because each FeO determination requires a separate weighing it is not possible to run pairs from each weighing. Because Fe₂O₃ is determined by subtraction of FeO from total Fe high precision is desirable for the FeO analyses. Biotites SP12 and 33, and garnets SP14 and 109A were done in triplicate to test further the reproducibility of the method. The results are shown in Table 2.

K₂O and Na₂O were determined only for the biotites and the one chlorite. Because garnets contain such a small amount of the components (usually less than 0.20% total) it was not believed that flame photometry would produce significant results. Interference and contamination at these concentrations becomes severe.

H₂O determinations were not attempted. The necessary equipment for proper H₂O determinations was not available.

Table 4. Accuracy by comparison with standards

	W-1 this study	W-1 35 lab ave.	Q-1 this study	Q-1 35 lab ave.	Haplo this study	Haplo others	Haplo known
SiO ₂	52.56	52.34*	72.55	72.36**	72.56	72.23	72.64
TiO ₂	1.09	1.10	.24	.25			
Al ₂ O ₃	14.64	15.07*	14.35	14.44**	16.22	16.19	15.78
Fe ₂ O ₃	1.67	1.50	1.03	.93			
FeO	8.61	8.71	.88	.99			
MnO	.144	.165	.02	.027			
MgO	6.57	6.63	.35	.39	.81	.85	.80
CaO	10.75	10.96	1.31	1.41	1.76	1.94	1.82
Na ₂ O	2.20	2.00	3.05	3.25	3.27	3.24	3.19
K ₂ O	.53	.63	5.62	5.42	5.76	5.69	5.76
H ₂ O	.54	.56	.34	.365			
P ₂ O ₅	.140	.126	.11	.09			
total	99.44	99.80	99.85	99.92	100.38	100.14	99.99

*preferred estimates SiO₂ 52.69

Al₂O₃ 14.72

**preferred estimates SiO₂ 72.86

Al₂O₃ 13.94

Table 3. Biotite, chlorite, and garnet compositions and associated assemblages

	Biotites											
	SP9	SP12	SP13	SP14	SP28	SP33	SP34	SP35	SP38	SP42	SP51	SP66
SiO ₂	35.37	36.12	36.47	36.46	36.80	35.81	35.15	36.37	36.72	35.75	36.54	36.02
TiO ₂	1.66	1.64	1.61	1.71	1.57	1.66	1.81	1.62	1.56	1.70	1.59	1.64
Al ₂ O ₃	18.33	18.24	18.25	18.19	17.40	17.58	17.49	18.00	17.88	17.68	17.85	18.00
Fe ₂ O ₃	2.61	2.42	2.32	2.71	3.25	3.62	3.75	3.53	3.45	3.45	3.92	3.57
FeO	18.24	16.97	17.62	16.57	16.64	19.21	18.65	15.23	14.39	17.46	16.81	17.31
MnO	.116	.068	.053	.066		.039	.040	.071	.108	.072	.042	.068
MgO	9.71	10.79	10.36	10.72	10.47	8.62	9.86	11.52	12.11	10.19	10.24	9.73
CaO	nil	nil	nil	nil	nil	nil	nil	nil	nil	nil	nil	nil
Na ₂ O	.28	.32	.24	.30	.29	.33	.28	.35	.31	.35	.35	.35
K ₂ O	7.56	8.47	8.37	8.90	8.52	8.52	7.84	8.71	8.71	9.02	8.43	7.80
P ₂ O ₅	.126	nd	.058	nd	nd	nd	nd	nd	nd	nd	.060	.072
total no H ₂ O	94.01	95.02	95.41	95.58		95.43	94.87	95.40	95.17	95.73	95.75	94.81
assemblage	quartz muscovite garnet staurolite biotite oligocl. magnetite ilmenite apatite tourmaline	same	same	same	same	same	same	same	same	same	same	same
γ-index	1.630	1.626	1.630	1.629	1.625	1.633	1.636	1.620	1.625	1.629	1.634	1.631

Table 5 (cont)

	Biotites											
	SP84	SP87	SP92	SP95	SP99	SP106	SP107	SP109A	SP109B	SP110	CN13	CN27
SiO ₂	36.50	35.56	35.75	35.88	35.98	36.70	35.53	36.04	35.71	36.19	36.50	35.45
TiO ₂	1.65	1.61	1.66	1.69	1.63	1.97	1.66	2.03	1.72	2.18	1.49	1.61
Al ₂ O ₃	18.00	18.02	18.13	17.95	18.09	17.89	17.68	17.47	18.39	17.38	16.92	18.04
Fe ₂ O ₃	3.75	3.76	3.49	3.67	3.26	2.08	2.24	3.82	2.03	3.51	3.65	2.97
FeO	15.28	16.16	17.73	15.78	17.49	15.88	18.35	16.98	18.31	17.18	16.12	17.70
MnO	.085	.100	.059	.087	.043	.095	.092	.029	.063	.161	.24	.073
MgO	10.99	11.30	9.88	11.03	9.86	11.26	9.91	9.59	10.28	9.21	10.55	10.73
CaO	nil	nil	nil	nil	nil	nil	nil	nil	nil	nil	.124	nil
Na ₂ O	.37	.28	.29	.32	.36	.39	.25	.33	.26	.28	.32	.30
K ₂ O	8.83	8.03	8.28	8.49	8.63	8.63	8.27	8.95	8.29	9.28	7.54	7.59
P ₂ O ₅	nd	.040	.040	nd	nd	nd	nd	.040	.042	nd	nd	nd
total	95.44	94.95	95.28	94.93	95.34	94.90	94.01	95.28	95.08	95.24	93.46	94.46
assem- blage	same as SP9	same	same	same	same	same plus kyanite	same as SP9	same plus kyanite	same as SP9	quartz musc. bio. gar. kyanite oligocl. magnetite ilmenite apatite tourm.	quartz musc. bio. gar. chlorite oligocl. magnetite ilmenite apatite tourm.	same as SP9
γ-index	1.624	1.624	1.631	1.623	1.629	1.630	1.636	1.637	1.633	1.638	1.637	1.629

Table 5 (cont)

	Chlorite CN13	Garnets										
		SP9	SP12	SP13	SP14	SP28	SP33	SP34	SP35	SP38	SP42	SP51
SiO ₂	27.32	38.33	38.23	38.22	38.25	38.28	37.75	38.07	37.84	38.38	37.70	37.68
TiO ₂	.30	.20	.34	.20	.15	.14	.33	.23	.39	.23	.18	.26
Al ₂ O ₃	21.17	20.26	20.08	20.16	20.34	20.22	19.88	20.09	19.97	20.31	20.55	20.45
Fe ₂ O ₃	3.13	1.16	1.21	1.05	1.28	1.28	1.29	1.04	1.63	1.40	1.64	1.92
FeO	19.43	30.91	30.85	31.00	30.12	31.83	32.52	32.00	28.15	25.93	29.05	31.15
MnO	.32	2.46	3.11	3.31	2.75	3.17	2.34	2.68	4.97	7.34	4.99	2.91
MgO	14.54	2.58	2.61	2.07	2.20	3.05	2.34	2.05	1.88	2.03	2.16	2.10
CaO	nil	3.44	3.04	3.66	4.80	1.95	3.00	3.38	4.75	4.33	3.76	3.41
Na ₂ O	.16											
K ₂ O	.52											
total	86.89	99.34	99.47	99.67	99.89	99.92	99.45	99.54	99.58	99.95	100.03	99.88

assem- same as listed under biotites
blage

γ-index 1.623

Table 5 (cont)

	Garnets											
	SP66	SP84	SP87	SP92	SP99	SP106	SP107	SP109A	SP109B	SP110	CN13	CN27
SiO ₂	38.93	37.78	37.54	37.49	37.68	37.80	37.98	37.74	38.43	37.23	39.20	38.23
TiO ₂	.19	.40	.17	.28	.37	.11	.34	.20	.15	.05	.37	.40
Al ₂ O ₃	20.17	20.25	20.73	20.22	20.18	20.29	20.03	20.33	20.14	20.24	19.35	20.04
Fe ₂ O ₃	1.29	1.48	1.69	1.06	0.96	1.03	0.45	0.98	1.25	2.24	1.52	1.29
FeO	31.08	28.65	29.62	32.61	33.02	30.47	32.80	32.73	31.77	30.72	23.43	31.89
MnO	2.85	4.81	3.95	1.96	1.77	4.13	2.06	1.81	2.64	5.61	9.98	1.82
MgO	2.48	2.02	2.52	2.74	2.63	3.07	2.85	3.52	2.34	2.30	.21	2.83
CaO	2.83	4.24	3.52	2.70	2.61	2.56	2.60	2.34	2.69	1.15	5.79	2.98
total	99.82	99.63	99.74	99.06	99.22	99.46	99.11	99.65	99.41	99.54	99.84	99.48

assemblages same as listed under corresponding biotite number

Table 6. Molecular fractions to 12 oxygens

Garnets

	SP9	SP12	SP13	SP14	SP28	SP33	SP34	SP35
SiO ₂	3.064	3.070	3.073	3.059	3.064	3.051	3.069	3.046
TiO ₂	.012	.021	.012	.009	.009	.020	.013	.024
Al ₂ O ₃	1.908	1.900	1.910	1.916	1.907	1.893	1.908	1.894
Fe ₂ O ₃	.070	.073	.064	.077	.076	.078	.062	.098
FeO	2.066	2.070	2.084	2.014	2.131	2.198	2.156	1.894
MnO	.210	.211	.226	.186	.215	.160	.183	.339
MgO	.307	.312	.248	.262	.363	.282	.246	.225
CaO	.294	.261	.315	.411	.167	.260	.292	.410

Table 6. (cont)

Garnets

	SP38	SP42	SP51	SP66	SP84	SP87	SP92	SP99
SiO ₂	3.067	3.023	3.027	3.106	3.039	3.045	3.034	3.045
TiO ₂	.014	.011	.016	.011	.024	.010	.017	.022
Al ₂ O ₃	1.912	1.942	1.936	1.896	1.919	1.982	1.929	1.922
Fe ₂ O ₃	.084	.099	.115	.077	.088	.103	.064	.058
FeO	1.732	1.948	2.092	2.073	1.927	2.009	2.207	2.231
MnO	.497	.339	.198	.193	.328	.271	.134	.121
MgO	.241	.258	.251	.295	.242	.305	.331	.316
CaO	.371	.323	.293	.242	.365	.175	.234	.226

Table 6. (cont)

Garnets

	SP106	SP107	SP109A	SP109B	SP110	GM13	GM27
SiO ₂	3.041	3.081	3.038	3.089	3.019	3.159	3.067
TiO ₂	.007	.021	.012	.018	.006	.022	.024
Al ₂ O ₃	1.923	1.897	1.928	1.908	1.936	1.837	1.894
Fe ₂ O ₃	.062	.027	.058	.080	.136	.092	.078
FeO	2.050	2.204	2.203	2.135	2.083	1.578	2.139
MnO	.281	.140	.123	.180	.385	.681	.124
MgO	.368	.341	.389	.280	.278	.025	.338
CaO	.220	.224	.202	.232	.100	.456	.256

Table 7. Molecular ratios corrected for excess SiO₂*

SiO ₂ TiO ₂	SP9	SP12	SP13	SP14	SP28	SP33	SP34	SP35	SP38	SP42	SP51	SP66	SP84	SP87	SP92	SP99
	3.00	3.00	3.00	3.00	3.00	3.00	3.00	3.00	3.00	3.00	3.00	3.00	3.00	3.00	3.00	3.00
Al ₂ O ₃ Fe ₂ O ₃	2.02	2.02	2.02	2.03	2.03	2.01	2.03	2.03	2.03	2.06	2.07	2.04	2.04	2.11	2.02	2.02
FeO MnO MgO CaO	2.95	2.93	2.95	2.93	2.94	2.97	2.97	2.94	2.92	2.90	2.87	2.92	2.92	2.81	2.95	2.95

SiO ₂ TiO ₂	SP106	SP107	SP109A	SP109B	SP110	CN13	CN27
	3.00	3.00	3.00	3.00	3.00	3.00	3.00
Al ₂ O ₃ Fe ₂ O ₃	2.01	1.98	2.01	2.06	2.08	2.06	2.03
FeO MnO MgO CaO	2.96	3.01	2.96	2.93	2.87	2.91	2.94

* Detailed correction worked out for one garnet, SP12. On the basis of the resulting corrections other garnets were changed proportionally. Similarities in garnet compositions make this procedure nearly correct.

V RESULTS

A. Compositions of Phases

All of the rocks which were separated and analyzed for phase equilibrium studies were schists. There were four mineral assemblages investigated: 1) quartz, muscovite, biotite, garnet, chlorite, oligoclase, magnetite, and ilmenite; 2) quartz, muscovite, biotite, garnet, staurolite, oligoclase, magnetite, ilmenite; 3) quartz, muscovite, biotite, garnet, staurolite, kyanite, oligoclase, magnetite, and ilmenite; 4) quartz, muscovite, biotite, garnet, kyanite, oligoclase, magnetite, and ilmenite.

There is no need to analyze quartz and kyanite. Biotite, garnet, chlorite, and staurolite, however, show extensive solid solution. Although the relationships of physical and chemical properties are well known (Ford, 1915; Fleischer, 1937; Juurinen, 1956; Winchell, 1927; Hall, 1941a,b) chemical analysis of these minerals appears to be the only certain way of determining their compositions. With the exception of staurolite, which is not immediately adaptable to the analytical techniques used, the other isomorphous minerals were analyzed and the results are shown in Table 5. A scheme of analysis for staurolite must await a future study.

The relationship of index of refraction to chemical composition of the plagioclase feldspars has been shown to be essentially independent of thermal history (Geophysical

Laboratory Annual Rpt, 1956-57). β index determinations were considered sufficient for the present study. The indices were measured on grains having centered optic axis figures. Measurements were taken with sodium light and the liquids were frequently checked against a calibrated refractometer. The β indices and their associated compositions are shown in Table 8. Several of the mounts were checked in liquid having a refractive index of 1.530. All of the grains were considerably higher in index than the liquid, and it was concluded that no potash-rich feldspar was present.

The muscovites are assumed to have nearly constant compositions. As a control on any significant changes in compositions, indices and cell sizes were checked. The indices are listed in Table 9. The cell sizes were measured with an X-ray diffractometer using $\text{Cu}_{K\alpha}$ radiation with a Ni filter. The 003 reflection was scanned at a speed of $1/4^\circ$ per minute. Because no internal standard was used only the relative changes in cell size could be determined. Twenty-three of the samples have a total variation in their basal spacing of 0.018 \AA . The one remaining muscovite, SP28, differed from the mean of the other 23 by 0.041 \AA . Although the correlation of optical and X-ray data with composition is not accurately known it would appear that the compositional variations of these samples is small.

Table 10 contains analyses of garnets, biotites, staurolites, and muscovites from other sources. Where possible,

Table 8. Plagioclase Indices and Compositions

β -index	SP9 1.544	SP12 1.544	SP13 1.543	SP14 1.543	SP28 1.543	SP33 1.543	SP34 1.544	SP35 1.549	SP38 1.543	SP42 1.543	SP51 1.543	SP66 1.543	SP84 1.544	SP87 1.544
composition	An ₂₁	An ₂₁	An ₁₉	An ₁₉	An ₁₉	An ₁₉	An ₂₁	An ₃₂	An ₁₉	An ₁₉	An ₁₉	An ₁₉	An ₂₁	An ₂₁

β -index	SP92 1.544	SP95 1.543	SP99 1.543	SP106 1.542	SP107 1.542	SP109A 1.544	SP109B 1.540	SP110 1.536	GN13 1.546	GN27 1.545
composition	An ₂₁	An ₁₉	An ₁₉	An ₁₇	An ₁₇	An ₂₁	An ₁₂	An ₆	An ₂₆	An ₂₃

Table 9. Muscovite δ -indices

SP9	1.599
SP12	1.599
SP13	1.599
SP14	1.599
SP28	1.600
SP33	1.599
SP34	1.599
SP35	1.599
SP38	1.599
SP42	1.599
SP51	1.599
SP66	1.600
SP84	1.601
SP87	1.600
SP92	1.599
SP95	1.599
SP99	1.600
SP106	1.599
SP107	1.599
SP109A	1.602
SP109B	1.599
SP110	1.600
ON13	1.603
ON21	1.600

Table 10. Mineral Analyses from other sources.

	1	2	3	4	5	Staurolites		8	9	10	11
						6	7				
SiO ₂	28.08	27.68	27.73	27.84	27.81	27.70	27.23	28.82	27.12	28.15	28.19
TiO ₂	.73	.77					.50	.84			
Al ₂ O ₃	51.90	53.37	53.29	54.46	54.09	53.22	50.72	49.21	45.92	52.17	52.15
Fe ₂ O ₃	1.80	2.33	2.83	2.83	2.76	4.82	4.96	9.51	8.64	1.70	1.59
FeO	13.39	12.69	11.21	10.60	12.48	9.72	3.42	nd	6.90	13.84	14.12
MnO		tr	.53	.59		.34	.08	.15	.53		
MgO	2.08	1.78	1.81	1.85	1.92	2.66	2.56	3.22	4.41	2.54	2.42
CaO									3.67		
Na ₂ O											
K ₂ O											
H ₂ O- H ₂ O/	1.62	1.46	2.19	2.24	1.70	1.97	1.19	1.47	2.88	1.63	1.59
location	St Gotthard, Switz.	Aschaffenburg	St Gotthard	Windham Maine	Lisbon N. H.	Burnsville, N.C.	North Rhodesia	Cherokee County N. C.	Glen Urquhart Scotland	St Gotthard Switz.	Basen Switz
assemblage	mica schist	same	same	same	same	same	qtz kyanite magnetite	mica schist	edenite bio wollas anthophy garnet	mica schist	mica schist
ref.	Juurinen 1956	same	same	same	same	same	same	same	same	same	same
remarks							8.48% CoO	7.13% ZnO			

Table 10 (cont)

		Staurolites										
		12	13	14	15	16	17	18	19	20	21	22
S ₁₀		30.10	28.89	29.55	30.12	29.44	30.56	30.08	27.83	27.68	27.24	27.32
TiO ₂			.81	.21		.11		.90	.88	.81	.74	.82
Al ₂ O ₃		50.10	52.61	49.89	50.44	48.46	50.91	49.94	54.76	53.66	52.20	51.94
Fe ₂ O ₃		2.08	2.95	1.61	1.73	2.89	.81	1.56				
FeO		11.22	10.78	14.11	12.90	14.75	12.76	12.98	13.43*	13.69*	14.72*	13.74*
MnO		.64	.09		.07	tr	.14	.42	.12	.10	.09	.12
MgO		3.12	2.09	1.72	2.72	1.64	2.85	1.54	2.80	2.45	2.61	2.83
CaO		.07	0.00	.39	.05			.38				
Na ₂ O			1.78					.14	.35	.41	.20	.64
K ₂ O								.06	.04	.11	.18	.13
H ₂ O-												
H ₂ O/		2.33		2.26	2.20	2.65	2.17	1.92		1.21	2.19	2.61
locat- tion	Pizzo Forno	Scotch Highlands	Peters- dorf	West Australia	Bretagne	Rosa Alp	West Australia	Alpe Sponda Switz	same	same	same	
assem- blage	schist	<u>schist</u> qtz musc 13 bic 13 garnet staur oligocl magnetite ilmenite tourm					qtz bic musc endalu sillim					
ref.	Juurinen 1956	Chinner 1958	Juurinen 1956	same	same	same	same	same	same	same	same	same

re-
marks

*total Fe as FeO

Table 10 (cont)

						Staurolites					Biotite
	23	24	25	26	27	28	29	30	31	32	1
SiO ₂	27.75	27.33	28.68	27.45	27.46	27.22	28.30	26.93	28.64	27.50	35.88
TiO ₂	.55	.61	.68	1.10	.58	.56	.54	.55	.56	.90	.35
Al ₂ O ₃	53.87	52.64	41.30	53.57	53.94	54.16	53.06	53.35	50.14	49.89	18.52
Fe ₂ O ₃			11.44	1.11	1.16	1.47	1.20	.90	.84	6.16	8.85
FeO	12.43*	10.22*	6.51	11.38	12.22	12.31	13.02	13.90	7.18	11.14	13.67
MnO	.09	.09	.04	.20	.18	.23	.05	.42	.16	.29	.42
MgO	2.57	2.90	2.30	3.17	2.24	2.34	2.45	2.11	3.44	2.13	9.06
CaO			5.20	.00	.00	.00	.00	.00	.00	.10	.09
Na ₂ O	.91	3.19									.82
K ₂ O	.16	.24									6.24
H ₂ O-											.72
H ₂ O _f	1.69	2.85	4.11	2.44	2.37	1.98	1.75	2.11	1.92	1.95	5.72
location	Monte Campione Switz	same	?	Glen Urquhart Scotland	Pizzo Forno Switz	Windham Maine	Korve Tunturi Finland	Saari- koski Finland	Cherokee County N. C.	Carpa- thians Hungary	Eritono mura Japan
assem- blage					schist	schist			schist		schist qtz bio plag garnet l sericite chlorite clinozo opaque
ref.	Juurinen 1956	same	same	same	same	same	same	same	same	same	Miyashiro 1953

re-
marks7.44%
ZnO

*total Fe as FeO

Table 10 (cont)

	Biotites											
	2	3	4	5	6	7	8	9	10	11	12	
SiO ₂	36.01	34.87	36.82	37.39	33.09	76.71	45.65	34.79	34.74	34.70	33.37	
TiO ₂	2.74	5.12	4.82	2.48	1.30	14.68	1.42	2.19	3.03	2.00	4.18	
Al ₂ O ₃	18.65	19.79	16.34	20.17	17.65	15.60	13.49	19.99	20.30	20.47	21.25	
Fe ₂ O ₃	3.46	1.72	1.85	2.08	2.42		1.71	1.42	.73	1.17	.50	
FeO	16.36	17.79	18.02	14.32	29.22	8.56	16.39	18.96	18.69	19.43	20.09	
MnO	.05	.02	.50		.04		.16	.04	.08	.09	.07	
MgO	8.31	7.42	8.62	9.80	2.83	12.01	11.85	9.34	8.89	9.20	7.24	
CaO	.11	.54	1.01	.51	.10	1.60	.93	.00	.00	.00	.00	
Na ₂ O	.97	.67	.47	.87	.13	1.23	.52	.39	.46	.57	.82	
K ₂ O	8.57	8.18	8.82	8.56	9.04	6.81	5.56	8.19	8.61	8.30	9.20	
H ₂ O-	1.89	.21			.04	.10		.30	.20	.00	.00	
H ₂ O ⁺	2.21	2.89	2.73*	3.03	2.92	2.36	2.07*	4.00	3.80	3.90	3.02	
location	Samagawa mura Japan	Aberdeen- shire Scotland	Dutchess County N. Y.	same	Lemhi County Idaho	Kailas- garh India	Uganda	Scottish Highlands	same	same	same	
assemblage	qtz bio garnet 2 plagAn ₃₀ apatite graphite	garnet 3 cordier bio plagAn ₅₀ spinel	qtz sericite bio plag apatite sphene pyrite magnetite	qtz musc bio	bio garnet musc qtz sphene tour zircon	plagAn ₃₀ antiperth hypersth bio microcl garnet qtz opaque	qtz garnet hypersth	garnet bio musc sillim kyanite qtz oligocl magnetite ilmenite	misc 10	same	spinel cordierite corundum bio orthoocl oligoocl	
Ref.	Miyashiro 1953	Stewart 1942	Barth 1936	Barth 1936	Lee 1958	Naidu 1955	Groves 1935	Chinner 1958	same	same	same	
re- marks		.42% F		1.67% F	1.11% Cl .23% F		.11% F ₂	.00% F	.03% F	.00% F		

*H₂O by difference

Table 10 (cont)

	Biotites										muscovite
	13	14	15	16	17	18	19	78	79	80	1
SiO ₂	35.22	35.44	38.0	39.0	38.2	36.7	34.47	36.69	34.76	33.28	45.49
TiO ₂	1.26	1.48	1.4	3.5	1.5	2.4	3.22	1.09	2.19	4.08	.89
Al ₂ O ₃	21.80	21.85	19.7	19.4	20.0	21.4	13.56	21.49	20.53	19.37	37.51
Fe ₂ O ₃	1.86	.79	1.2	.15	.59	1.1	4.70	2.66	.78	.48	
FeO	15.14	17.78	13.6	17.1	11.5	18.9	17.09	11.92	18.50	24.78	
MnO	.02	.04	.17	.10	.28	.25		.24	.02	.13	
MgO	10.22	10.66	13.5	7.3	13.0	7.6	10.00	12.58	9.40	5.76	.20
CaO	.24	.00	.55	.55	.55	.76	.78	.00	.09	.00	.50
Na ₂ O	.59	.38	.35	.35	.50	.45	1.72	.53	.48	.23	1.72
K ₂ O	8.85	8.62	8.6	6.16	9.4	5.6	9.72	8.20	8.35	8.19	8.86
H ₂ O-	.26	.00					1.26	.10	.36	.00	
H ₂ O f	4.26	3.70	4.5	5.8	4.7	6.7	3.43	4.00	4.18	3.50	4.92
location	Scottish Highlands	same	Donegal	same	same	same	Tirol	Scottish Highlands	same	same	Dutchess County N. Y.
assemblage	staur 13 gar bio musc 13 qtz oligocl magneti ilmen tourm	kyan garnet bio musc qtz oligocl magneti ilmen tourm	qtz feldsp bio musc andalu chlorite	qtz feldsp bio andalu musc	qtz feldsp bio musc andalu chlorite	qtz feldsp bio musc andalu chlorite	2-mica gneiss musc 19	gar 78 bio musc 78 sillim kyan qtz oligocl magneti hematite	gar 79 same	gar 80 bio cordier spinel orthocl oligocl pyrrhotite	schist
Ref.	Chinner 1958	same	Pitcher and Sinha 1958	same	same	same	Seidel 1923	Chinner 1958	same	same	Barth 1936
re-marks	tr-F	tr-F		discolored		discolored		.00 F	.00 F	.00 F	

Table 10 (cont)

Garnets

	7	8	9	10	11	12	13	14	15	16	17
SiO ₂	37.53	36.60	35.58	39.75	37.82	38.40	37.00	36.21	38.47	37.21	36.59
TiO ₂	.03	.54	tr	.25					.00	.14	1.68
Al ₂ O ₃	22.42	20.47	21.94	19.94	22.00	21.68	20.36	21.32	21.47	20.90	22.42
Fe ₂ O ₃	.74	5.06	.00	3.76	.23	6.07	2.09	3.80	2.38	.04	.04
FeO	32.53	30.57	38.54	4.54	6.09	21.34	30.80	31.20	28.76	32.65	32.11
MnO	.66	.92	.70	24.25	30.62	2.84	7.57	5.12	3.59	2.02	1.42
MgO	5.74	4.18	.68	1.51	.53	3.75	1.52	2.41	3.51	2.74	5.41
CaO	.16	1.72	1.68	5.53	3.44	6.30	.98	.36	1.54	3.67	.54
Na ₂ O										.14	
K ₂ O										tr	
H ₂ O-			.12	.01						.10	
H ₂ O ⁺	.10	.66		.54						.15	
location	Great Slave Lake	Bohemian Massiv Austria	Botallack Cornwall	Gold Coast	Pohjanmaa Finland	Perthshire Scot.	O. Pfalz Germany	Balknap Mtns. N. H.	Austria	Muru-hatten Sweden	Aberdeen-shire Scot.
assemblage	gar qtz cordier sillim bio spinel graphite microcl andesine tourm	gar bio cordier apatite zircon qtz magneti ilmen	contact aureole bio gar qtz grunerite	gar qtz Mn oxide	rhodonite hornbl gar plag	mica schist	qtz bio sillim gar sericite	qtz misc bio plag gar Kspar apatite sphene hematite pyrite	qtz bio chlorite plag hornbl tour zoisite rutile sulfides	gar bio sillim qtz oligocl orthoel misc magneti apatite zircon	
Ref.	Folinsbee 1941	Preelik 1924	Alderman 1935	Junner 1927	Hietanen 1936	Phillips 1930	Gosner 1931	Modell 1936	Schumann 1930	DuRietz 1935	Stewart 1950

Table 10. (cont)

		Garnets										
		18	19	22	26	28	30	31	34	37	38	43
SiO ₂		37.35	37.39	40.30	38.73	38.44	37.94	37.22	38.26	38.35	37.65	38.54
TiO ₂		.79		tr	.34		1.04	.15	.00	.08	.04	.04
Al ₂ O ₃		20.36	20.46	21.86	19.76	20.62	22.87	15.38	19.93	21.10	20.87	22.13
Fe ₂ O ₃		2.27	2.89	2.16	5.45	7.39	nd	8.52	4.87	1.50	1.87	.39
FeO		31.36	31.87	19.08	19.31	17.09	32.45	2.35	20.40	28.48	27.65	25.71
MnO		1.18	3.47	.69	nd	4.22	1.77	1.47	.04	.71	1.10	1.10
MgO		2.22	2.46	11.28	8.92	2.51	1.83	.52	3.94	7.93	3.74	8.29
CaO		2.55	.92	5.22	7.87	10.08	2.04	34.07	12.02	2.04	7.16	3.68
Na ₂ O	} 1.69									.01	.09	.01
K ₂ O										.04	.02	.13
H ₂ O-		.04							.48	.02	.02	.04
H ₂ O _f		.16						.44	.12			.13
location	Wilmot N. H.	same	Silden Norway	Tirol	Scottish Highlands	Bald Mtn. N. Y.	Tennberg Mtn. Sweden	Russian River Calif.	Madras India	same	Adiron- dacks N. Y.	
assemblage	qtz bio sillim gar magneti fspar chlorite zircon rutile	same	eclogite	eclogite	gar bio clinozo albite hornbl	qtz musc gar bio staur plag apatite magneti	pegmatite limestone contact. monomin- eralic garnet layer	glaucoph actinol gar musc sphene rutile	granulite qtz kspar plag gar bio opaque apatite zircon	granulite plag orthopyr clinopyr gar hornbl opaque	plag ₅₄ hypersth hornbl gar bio ilmene apatite	
Ref.	Conant 1935	same	Eskola 1921	Alderman 1936	Wiseman 1934	Barth 1936	vonEcker- mann 1923	Pabst 1931	Howie and Subra- maniam 1957	same	Buddington 1952	

Table 10. (cont)

	45	54	57	68	72	Garnets 76	78	79	80	81
SiO ₂	39.29	36.70	39.50	37.76	41.10	40.71	37.76	37.32	35.96	37.6
TiO ₂	.05	.00	.29	.10	nd	.08	.12	.16	.05	.3
Al ₂ O ₃	22.12	16.58	21.00	21.06	22.40	22.31	20.04	21.62	21.90	21.8
Fe ₂ O ₃	.78	12.72	4.30	1.78	nil	1.31	.90	.07	.60	.7
FeO	19.63	20.70	22.15	nil	23.40	16.49	23.98	34.30	35.05	30.7
MnO	.38	3.00	.80	39.94	.44	.33	11.53	1.14	1.67	.6
MgO	11.48	2.73	9.74	1.46	11.12	12.03	3.56	2.74	3.27	1.4
CaO	6.16	7.00	2.96	1.23	1.92	6.77	1.63	2.79	1.32	7.2
Na ₂ O		.03								
K ₂ O		.11								
H ₂ O-	.03	.00				.09				
H ₂ O _f		.68				.23				
Loca- tion	Barton Mine Adiron- dacks	Varberg Sweden	Setajoki Lapland	Madagas- car	same	Madras India	Scottish Highlands	same	same	Argyll- shire
assem- blage	PlagAn ₅₀ hypersth hornbl gar bio sphene apatite augite	orthocl plagAn ₂₅ diopside hypersth apatite zircon	qtz plag gar hypersth	in a pegma- tite	manjakite eclogite	gar bio 78 musc 78 sillim kyan qtz oligocl magneti hematite	gar bio 79 musc sillim kyan qtz oligocl magneti ilmn	gar bio 80 cordier spinel orthocl oligocl pyrrhotite	schist of Dalradian Series	
Ref.	Budding- ton 1952	Quensel 1951	Eskola 1952	Duparc, et al. 1914	Lacroix 1914	Sabraman- iam 1956	Chinner 1958	same	same	Guppy 1956

the mineral assemblages are listed. Analyses of coexisting minerals are cross-referenced by the same number. From the available mineral assemblages it can be seen that there is little variation among the garnets and biotites from geologic environments similar to that of the present study. Garnets from a similar environment are 13, 14, 15, 16, 17, 18, 19, 30, 78, 79, and 81; biotites would be 1, 2, 5, 6, 9, 10, 13, 14, 15, 16, 17, 18, 78, 79. Heinrich (1946), in a study of biotites from various geologic environments, plots the composition of biotites from schists and gneisses in a very restricted range. The FeO varies between 15 and 20%, the MgO between 10-15%, and the Fe_2O_3 plus TiO_2 between 5-10%.

B. Phase Diagrams

In order to present graphically the analytical results from the coexisting minerals the phase diagrams of Thompson (1957) are used. These diagrams result from a projection through muscovite in the tetrahedron of Figure 12. The occurrence of FeO and MgO as separate components make this tetrahedron more desirable than AKF diagrams which treat FeO and MgO as one component. In the discussion of the results it will become apparent that these components must be treated separately. Furthermore, the AKF diagrams, although useful for representing mineral assemblages, cannot be used quantitatively as phase diagrams. The diagrams developed by Thompson can be used quantitatively as isothermal-isobaric

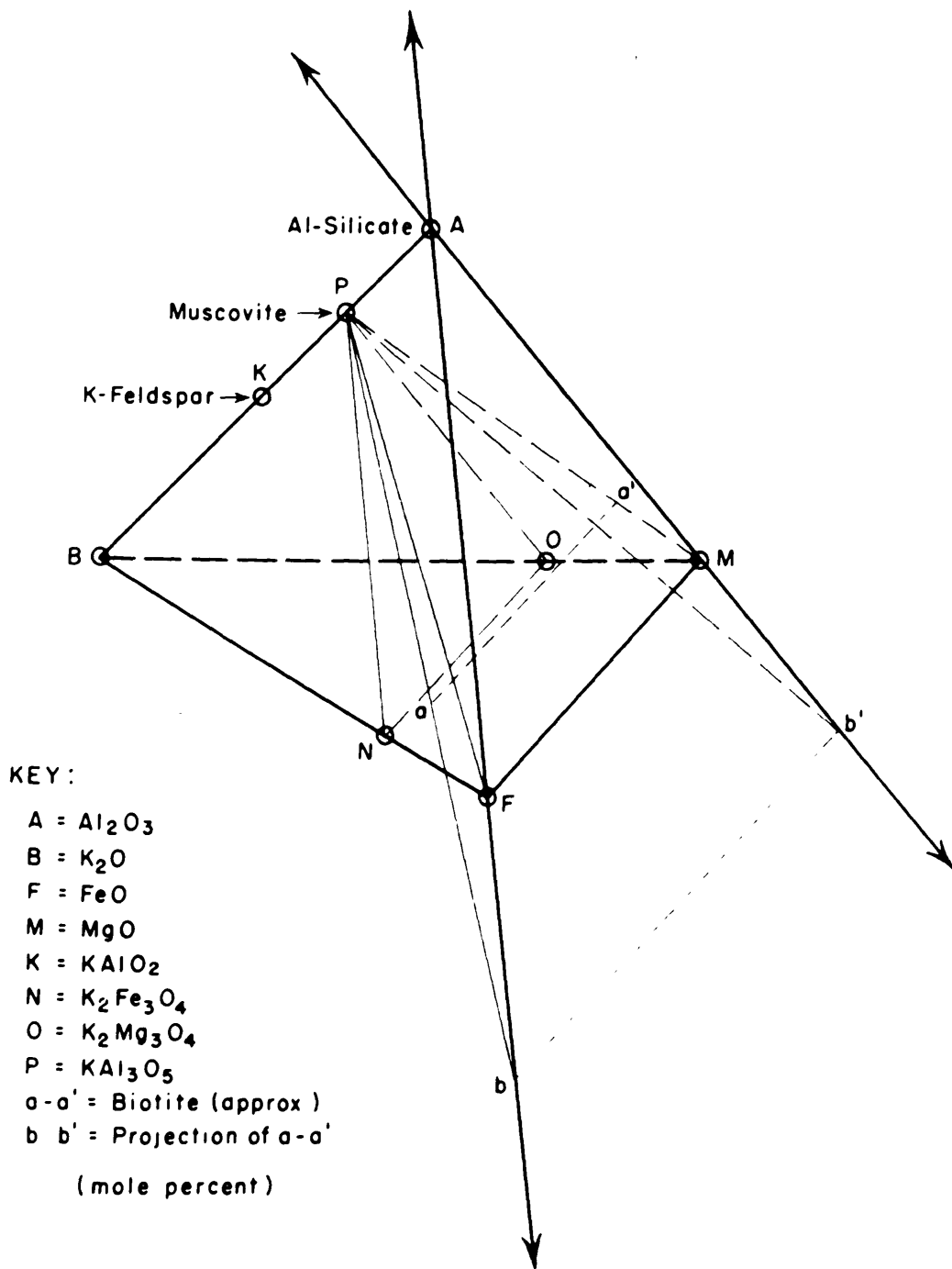


Figure 12. Method of Projection

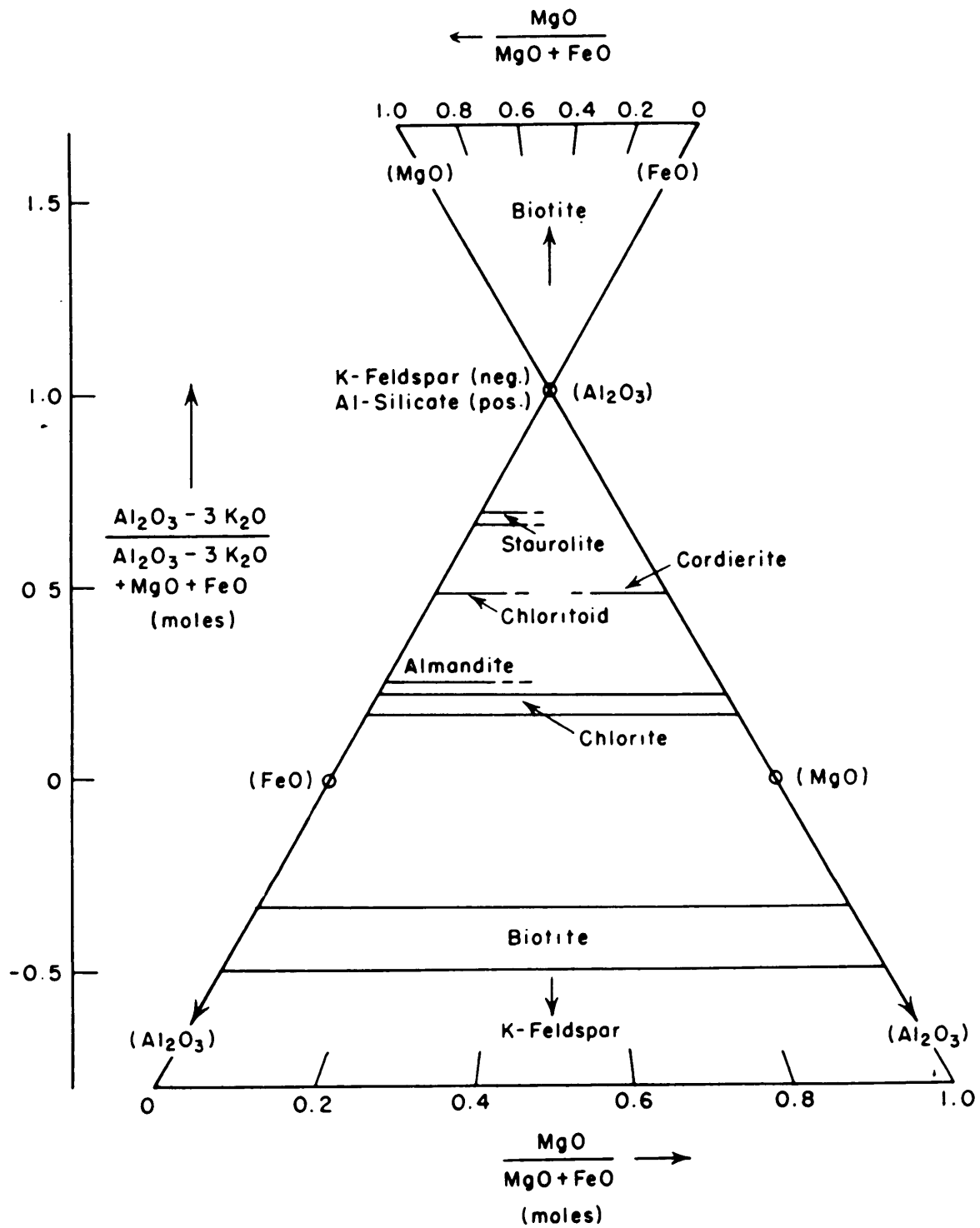


Figure 13. Result of Projection

sections. The two rectilinear coordinates of the diagram are different from ordinary triangular diagrams. Figure 13 shows the detailed relationships of phases and coordinates in the completed projection.

As stated in Thompson's paper there are several difficulties inherent in the use of the diagrams. They are valid only for the system SiO_2 , Al_2O_3 , MgO , FeO , K_2O , and H_2O ; furthermore, the chemical potential of H_2O must be constant if the diagrams are to be compared. From the analyses given in Table 5 it is clear that Fe_2O_3 in the biotites and MnO and CaO in the garnets must be considered as components. These are often in excess of 3%. A garnet with 4 or 5% MnO is well out of the projection; and comparison with an assemblage containing a Mn-free garnet would not be correct. Thus it is necessary to divide the garnets into groups which contain similar mole fractions of MnO . It is known that the stabilities of biotites are affected by the partial pressure of oxygen in the system (Wones, 1958). Therefore, a constant partial pressure of oxygen would be necessary for valid comparison of the phase diagrams. The $\text{Fe}_2\text{O}_3/\text{FeO}$ ratio should reflect any large variations in this partial pressure. Therefore, the biotites have been divided into groups having similar $\text{Fe}_2\text{O}_3/\text{FeO}$ ratios. The biotite-garnet pairs have been further divided into groups having similar MnO content and Fe_2O_3 ratios as shown in Table 11. The groups having more than one pair are plotted in Figures 14 through 18. In

Table 11. MnO and Fe₂O₃/FeO groupings of garnets and biotites

Garnet	MnO moles	Biotite	Fe ₂ O ₃ /FeO	Garnet-Biotite pairs
SP99	.121	SP109B	.111	SP110 MnO: .338-.384 SP42 Fe ₂ O ₃ /FeO: .198
SP109A	.123	SP107	.122	
CN27	.124	SP106	.131	SP35 MnO: .271-.338 SP84 Fe ₂ O ₃ /FeO: .232-.245 SP87
SP92	.134	SP13	.132	
SP107	.140	SP9	.143	SP9 SP12 MnO: .181-.225 SP13 Fe ₂ O ₃ /FeO: .143-.163 SP14
SP33	.160	SP12	.143	
SP109B	.179	SP14	.163	SP33 SP34 MnO: .160-.214 SP66 Fe ₂ O ₃ /FeO: .188-.206 SP28
SP14	.181	CN27	.168	
SP34	.182	SP99	.186	
SP66	.192	SP33	.188	SP92 MnO: .121-.134 SP99 Fe ₂ O ₃ /FeO: .186-.197
SP51	.197	SP28	.195	
SP9	.210	SP92	.197	
SP12	.211	SP110	.198	None of the remaining pairs can be grouped on the basis of sim- ilar MnO or Fe ₂ O ₃ /FeO content.
SP28	.214	SP42	.198	
SP15	.225	SP34	.201	
SP87	.271	SP66	.206	
SP106	.281	SP109A	.225	
SP84	.327	CN13	.226	
SP35	.338	SP35	.232	
SP42	.338	SP51	.233	
SP110	.384	SP87	.233	
SP38	.496	SP95	.233	
CN13	.680	SP38	.240	
		SP84	.245	

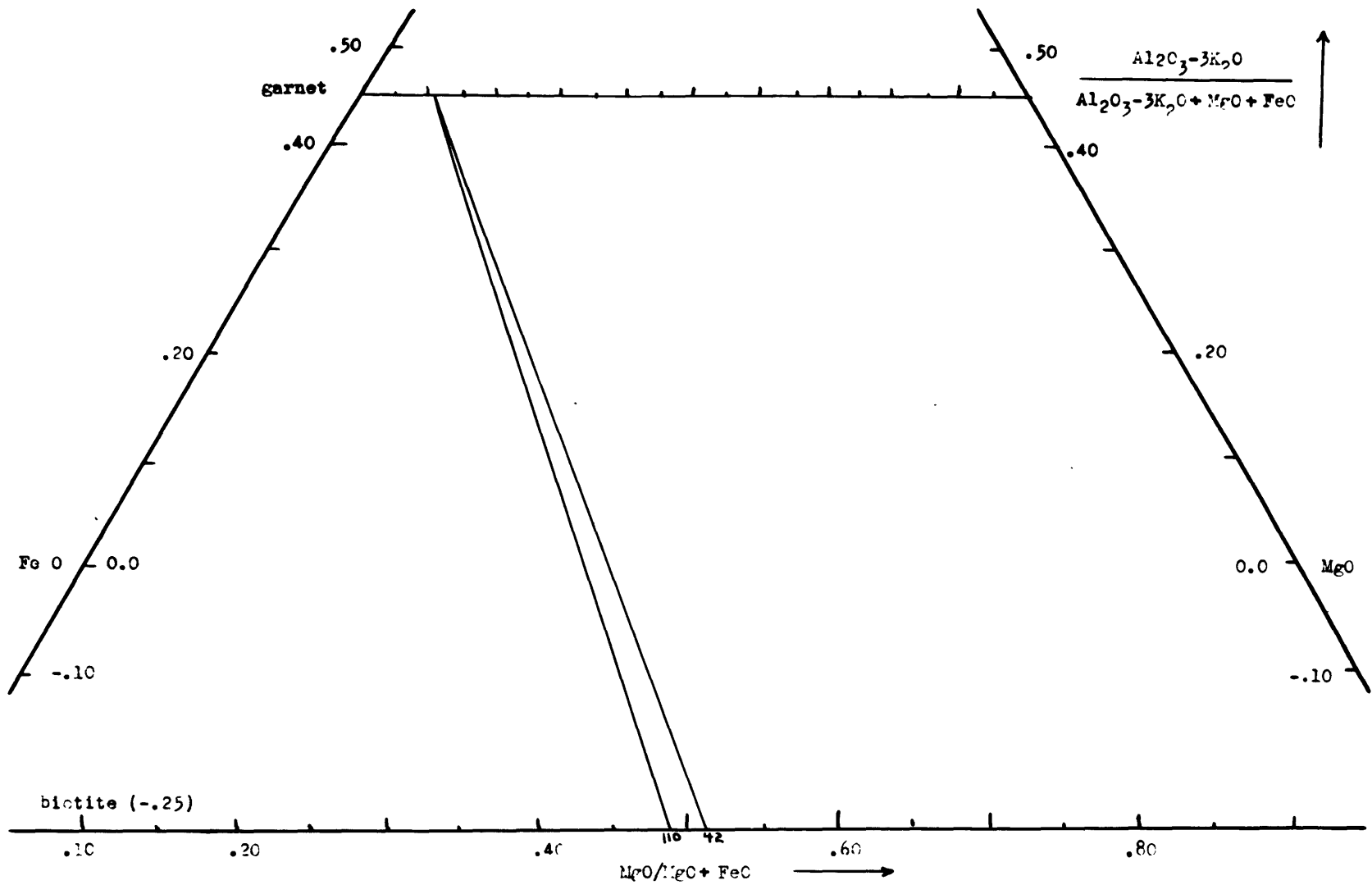


Figure 14. Garnet-biotite tie-lines for MnO between 0.338 and 0.384 moles and Fe_2O_3/FeO at 0.198

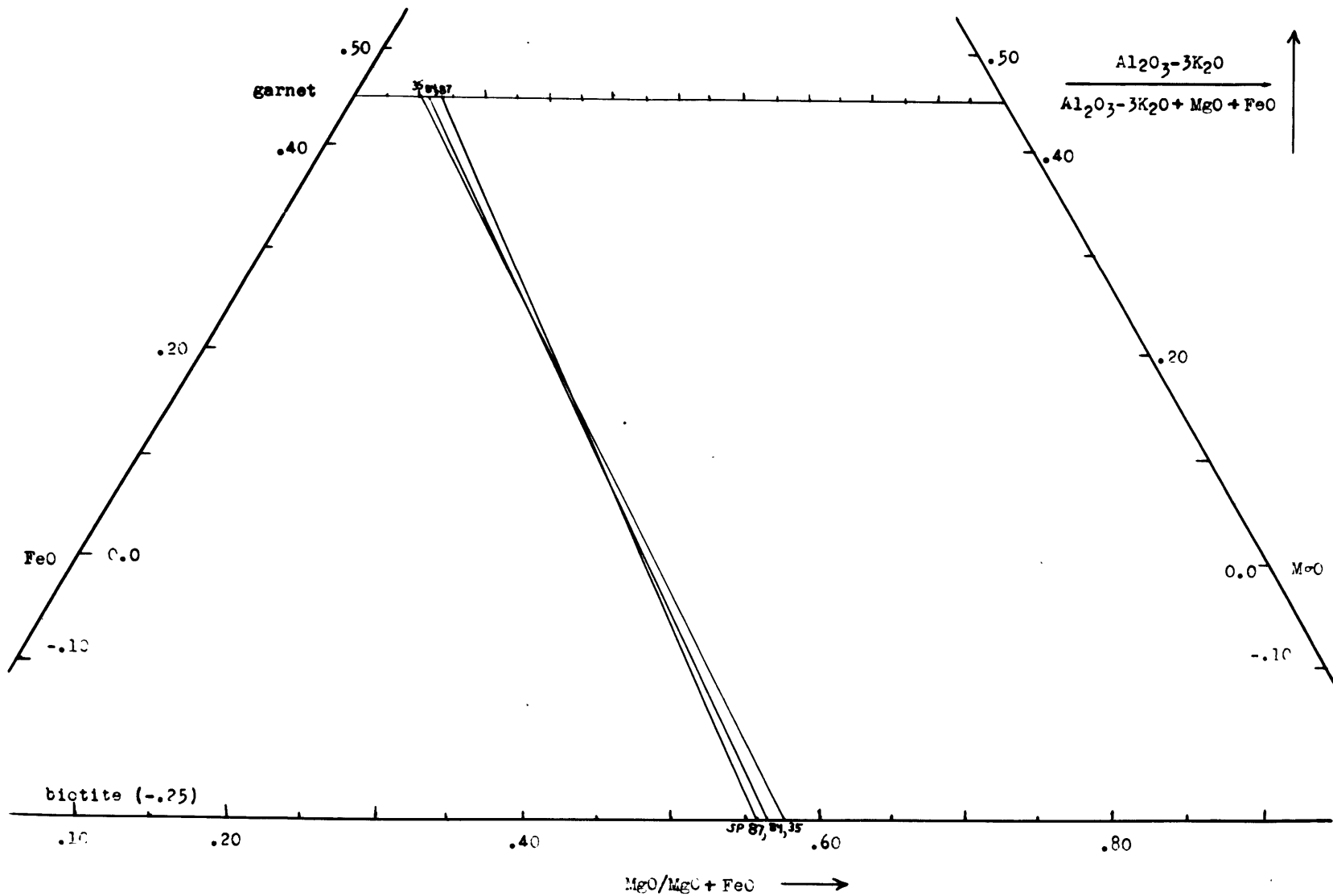


Figure 15. Garnet-biotite tie-lines for MnO between 0.271 and 0.338 moles end $\text{Fe}_2\text{O}_3/\text{FeO}$ between 0.232 and 0.245

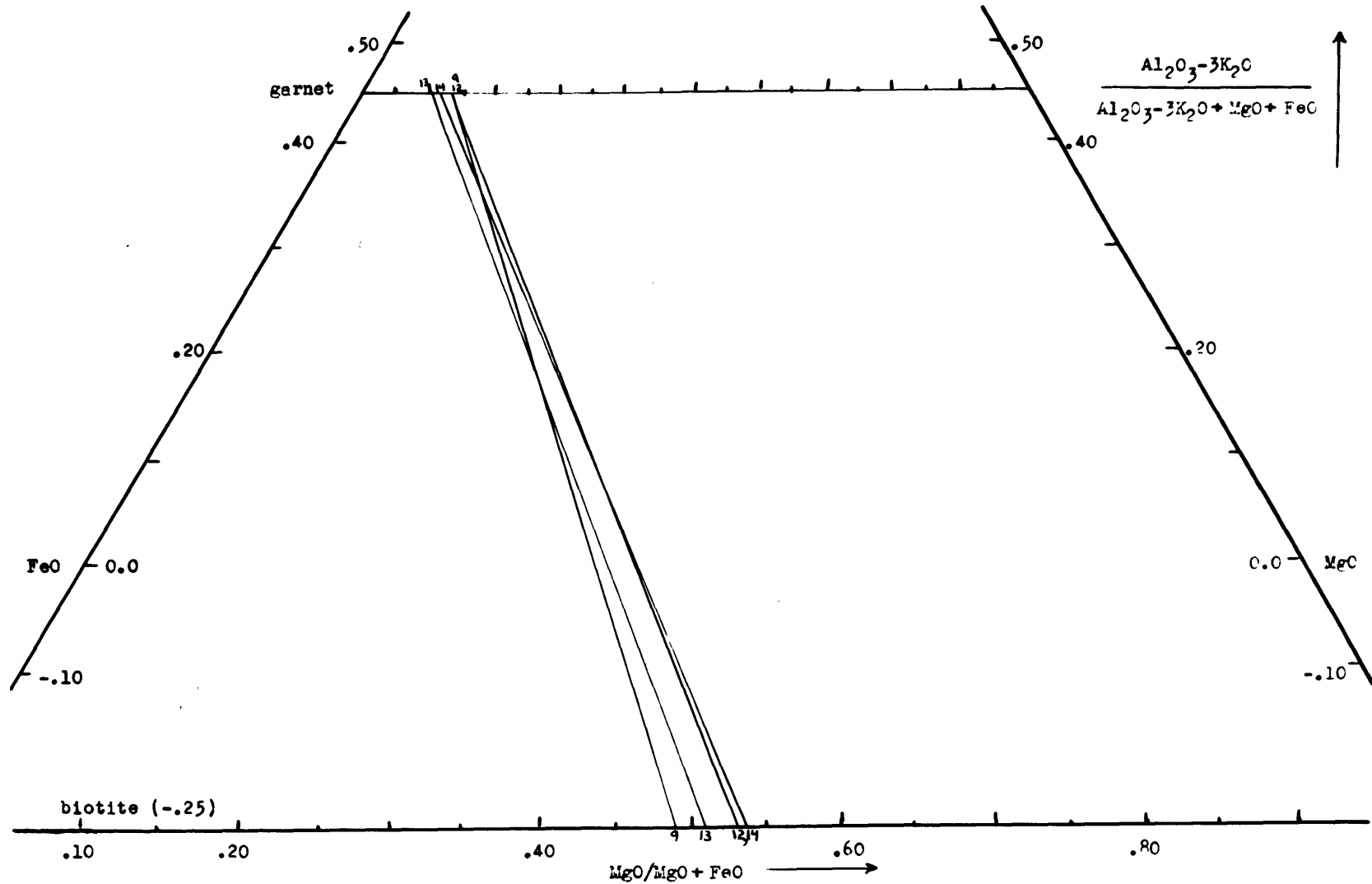


Figure 16. Garnet-biotite tie-lines for MnO between 0.181 and 0.225 moles and Fe₂O₃/FeO between 0.143 and 0.163

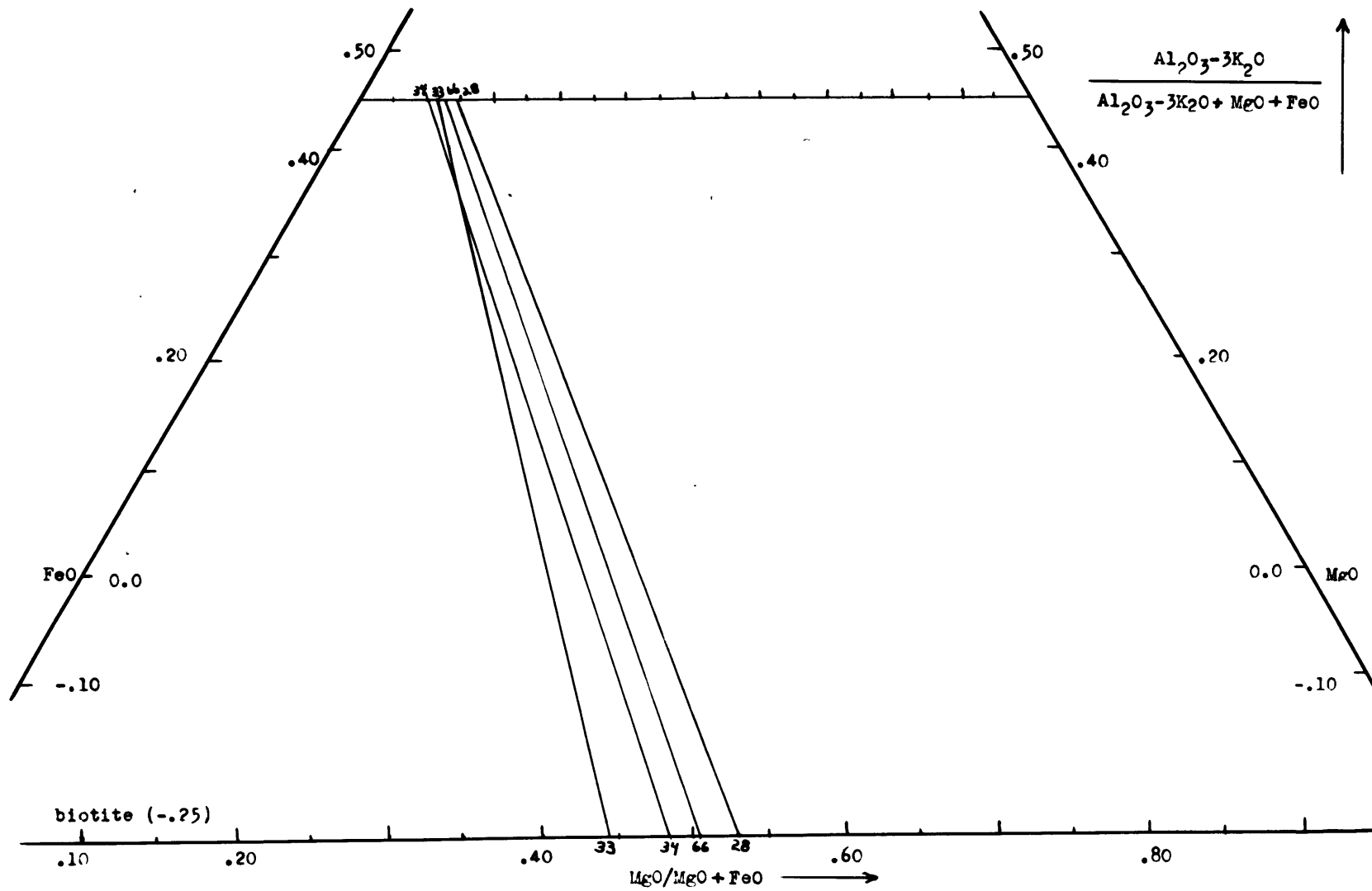


Figure 17. Garnet-biotite tie-lines for MnO between 0.160 and 0.214 moles and $\text{Fe}_2\text{O}_3/\text{FeO}$ between 0.188 and 0.206.

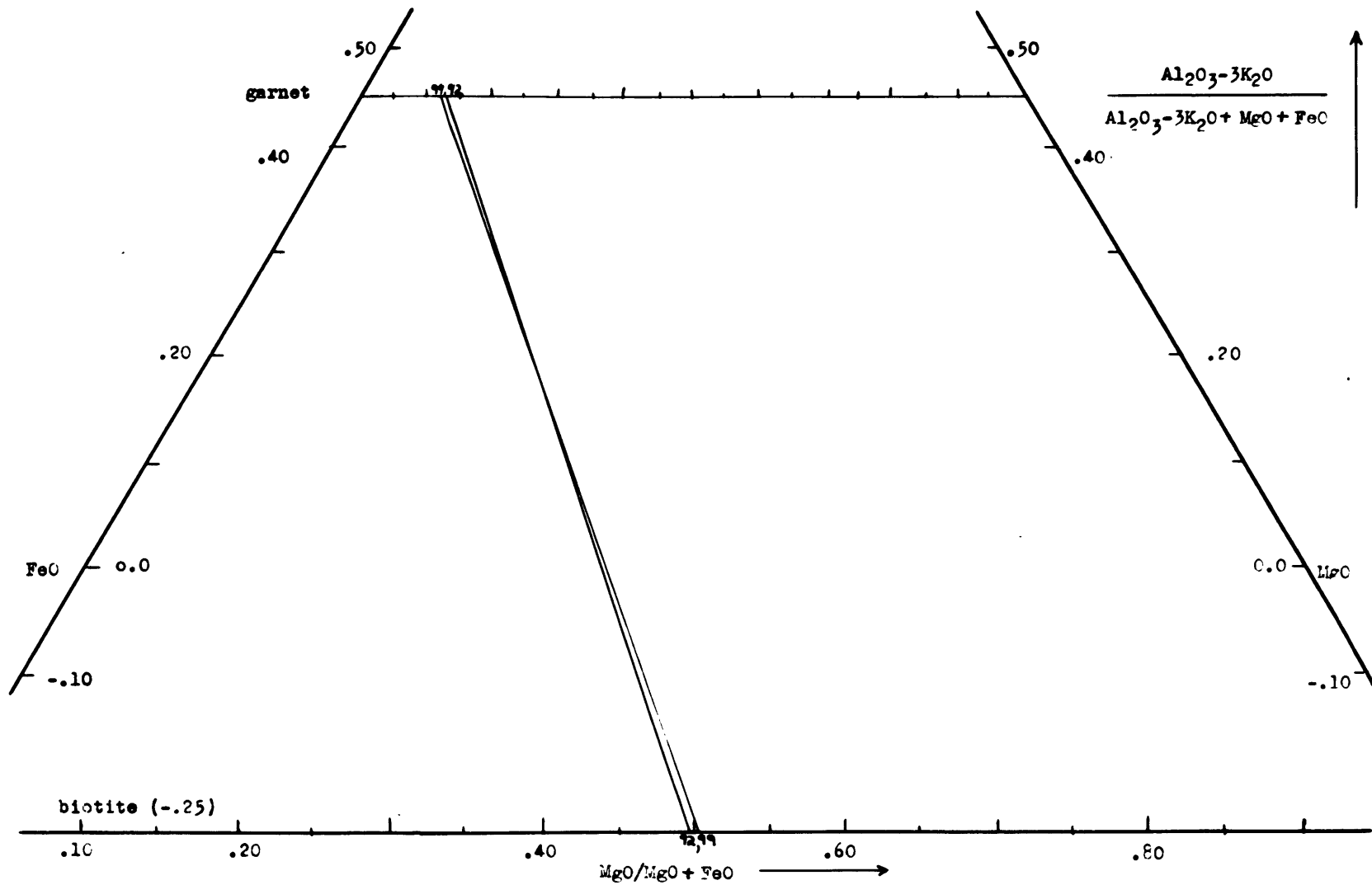


Figure 18. Garnet-biotite tie-lines for MnO between 0.121 and 0.134 moles and $\text{Fe}_2\text{O}_3/\text{FeO}$ between 0.168 and 0.197.

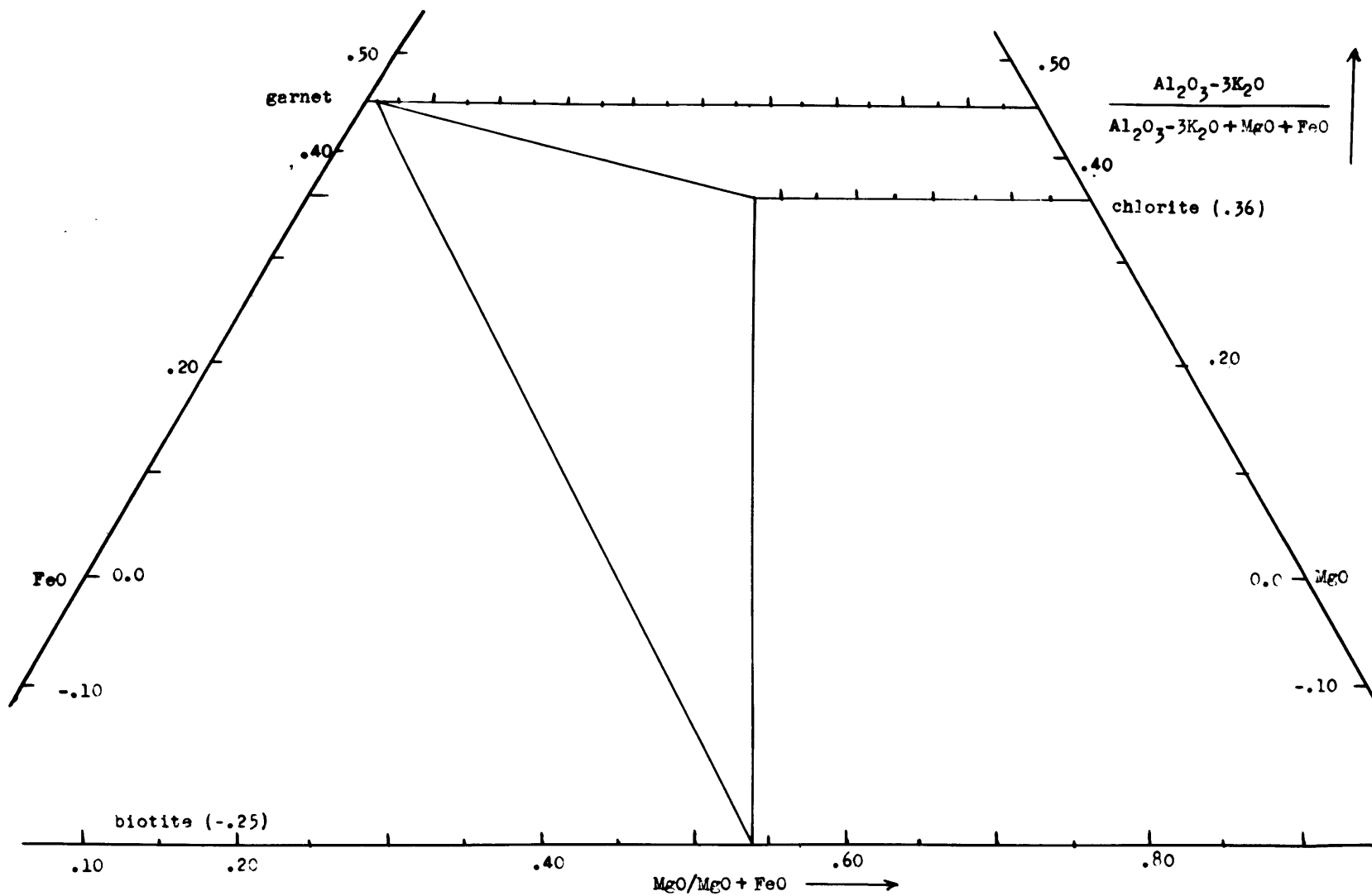


Figure 19. Garnet-biotite-chlorite tie-lines for sample CN13.

Figure 19 is plotted the assemblage garnet, biotite, and chlorite. Quartz and muscovite are present in all of the assemblages, as they must be for the diagrams to be valid. It should be pointed out that the garnet of diagram 19 is highly enriched in manganese.

Although no further subdivisions have been attempted based on CaO content, this component will certainly have some effect. Further discussion on the meaning of the diagrams is deferred to the following chapter.

Synthetic phase equilibrium studies have been conducted on several of the minerals which occur in the assemblages of this investigation. Most of the studies have involved single minerals or pairs, such as biotite and quartz. Perhaps the most useful information is offered by the stability relationships of the aluminum silicate polymorphs, andalusite, sillimanite, and kyanite. Because they constitute a one-component system there would be no change in the equilibrium curves on a pressure-temperature plot, as a result of additional components being in the system. Clarke, Robertson, and Birch (1957) conducted high temperature and pressure experiments in this system, and used thermochemical data to determine the polymorphic transitions as a function of temperature and pressure. Their results indicate that kyanite is not stable below $12,000 \pm 1000$ bars at 500°C . Even at 25°C the lower pressure limit is approximately 5000 bars.

Yoder (1954) has determined a P vs T curve for the

breakdown of pure almandite. The upper temperature limits of stability are 800°C at 1000 bars and 1050°C at 10,000 bars. Tilley (1926) observed that MnO in garnets seemed to enlarge their stability fields. He found that almandite garnets of regionally metamorphosed schists break down to cordierite and magnetite in contact aureoles. However, the garnets which are rich in MnO remain stable in the aureoles. In oxidizing hydrothermal studies at 1000 bars Shairer and Yagi (1952a,b) found that almandite garnet seemed to break down at temperatures above 500°C. Halferdahl (1956) has produced almandite, staurolite, and hercynite from the breakdown of chloritoid above 700°C and 10,000 bars. It would appear that Mn, as well as other components, and partial oxygen pressure will significantly affect the stability limits of almandite-rich garnet. In a study just commenced at the Geophysical Laboratory, Chinner is investigating the effect of partial oxygen pressure on the stability of the almandite-pyrope series.

Because of the unreacting nature of staurolite little is known of its stability limits. As mentioned above it has been produced by the breakdown of chloritoid at high temperatures and pressures.

The upper and lower stability limits of biotite along the annite-phlogopite join have been determined as a function of temperature, pressure, and partial oxygen pressure by Wones (1957, 1958). The lower temperature limit for the

formation of biotites having compositions similar to those of the present study varies from 500 to 700°C at 2000 bars total pressure, depending upon the partial pressure of oxygen. Chlorite is presently being investigated in the same manner by Turnock at the Geophysical Laboratory (personal communication).

Studies of muscovite and muscovite-paragonite stability relationships indicate that the upper temperature limit for muscovite at 4000 bars is approximately 800°C (Yoder and Eugster, 1954,1955). At higher pressures this temperature will be somewhat higher.

Although additional components will change the stability relationships of all of these minerals except kyanite, it is reasonable to assume that the rocks of this study formed at pressures above 10,000 bars and temperatures between 600 and 800°C. Because the isograd on St. Paul Island represents the breakdown of staurolite, any data on the P-T relations of the breakdown curve would greatly restrict the above limits.

VI DISCUSSION OF RESULTS

A. Theory

In a system containing phases with solid solution there should be a relationship between the intensive variables and the ratio of the substituting components in any phase. Because such a relationship is not contained in standard thermodynamics texts the writer has derived one by the method shown on the next few pages.

Definition of Terms

P	hydrostatic, or mean, pressure
T	absolute temperature
$\mu_{i\alpha}$	chemical potential of component i in phase α
v_{α}	specific volume of phase α
$\bar{v}_{i\alpha}$	partial molar volume of component i in phase α
$\Delta \bar{v}_i$	$\bar{v}_{i\alpha} - \bar{v}_{i\beta}$
s_{α}	specific entropy of phase α
$\bar{s}_{i\alpha}$	partial molar entropy of component i in phase α
$\Delta \bar{s}_i$	$\bar{s}_{i\alpha} - \bar{s}_{i\beta}$
G_{α}	Gibbs free energy of phase α
g_{α}	specific Gibbs free energy of phase α
$n_{i\alpha}$	number of moles of component i in phase α
$N_{i\alpha}$	mole fraction of component i in phase α
ΔN_i	$N_{i\alpha} - N_{i\beta}$

Consider two phases, α and β , in a system of two components, i and j. Both phases form solid solutions of both components. At equilibrium,

$$\mu_{i\alpha} = \mu_{i\beta} \quad (1)$$

and $\mu_{j\alpha} = \mu_{j\beta}$,

where

$$\mu_{i\alpha} = \left(\frac{\partial G_{\alpha}}{\partial n_{i\alpha}} \right)_{P, T, n_{j\alpha}}$$

From the first two relationships it must follow that

$$d\mu_{i\alpha} = d\mu_{i\beta} \quad (2)$$

and

$$d\mu_{j\alpha} = d\mu_{j\beta}$$

The chemical potential is a function of temperature, pressure, and the number of moles of each component, that is,

$$\mu_{i\alpha} = f(T, P, n_{i\alpha}, n_{j\alpha})$$

But rather than use $n_{i\alpha}$ and $n_{j\alpha}$ it is more convenient to use the mole fraction, $N_{i\alpha} = \frac{n_{i\alpha}}{n_{i\alpha} + n_{j\alpha}}$ and specific properties of the phases. Because $d\mu$ is a perfect differential an expression such as the one below can be written for each of the components in each of the phases.

$$\mu_{i\alpha} = f(T, P, N_{i\alpha})$$

$$d\mu_{i\alpha} = \left(\frac{\partial \mu_{i\alpha}}{\partial T} \right)_{P, N_{i\alpha}} dT + \left(\frac{\partial \mu_{i\alpha}}{\partial P} \right)_{T, N_{i\alpha}} dP + \left(\frac{\partial \mu_{i\alpha}}{\partial N_{i\alpha}} \right)_{P, T} dN_{i\alpha}$$

But from the relationship

$$dg_{\alpha} = v_{\alpha} dP - s_{\alpha} dT - \mu_{i\alpha} dN_{i\alpha} + \mu_{j\alpha} dN_{j\alpha}$$

the first two partial differentials take the forms

$$\left(\frac{\partial \mu_{i\alpha}}{\partial T} \right)_{P, N_{i\alpha}} = \frac{\partial^2 g_{\alpha}}{\partial N_{i\alpha} \partial T} = - \frac{\partial s_{\alpha}}{\partial N_{i\alpha}} = - \bar{s}_{i\alpha}$$

$$\left(\frac{\partial \mu_{i\alpha}}{\partial P} \right)_{T, N_{i\alpha}} = \frac{\partial^2 g_{\alpha}}{\partial N_{i\alpha} \partial P} = \frac{\partial v_{\alpha}}{\partial N_{i\alpha}} = \bar{v}_{i\alpha}$$

Substituting these back into the equation for $d\mu_{i\alpha}$ one obtains

$$d\mu_{i\alpha} = \bar{v}_{i\alpha} dP - \bar{s}_{i\alpha} dT + \left(\frac{\partial \mu_{i\alpha}}{\partial N_{j\alpha}} \right)_{P,T} dN_{j\alpha}$$

and similarly,

$$d\mu_{i\beta} = \bar{v}_{i\beta} dP - \bar{s}_{i\beta} dT + \left(\frac{\partial \mu_{i\beta}}{\partial N_{j\beta}} \right)_{P,T} dN_{j\beta}$$

$$d\mu_{j\alpha} = \bar{v}_{j\alpha} dP - \bar{s}_{j\alpha} dT + \left(\frac{\partial \mu_{j\alpha}}{\partial N_{i\alpha}} \right)_{P,T} dN_{i\alpha} \tag{3}$$

$$d\mu_{j\beta} = \bar{v}_{j\beta} dP - \bar{s}_{j\beta} dT + \left(\frac{\partial \mu_{j\beta}}{\partial N_{i\beta}} \right)_{P,T} dN_{i\beta}$$

Substituting these relations in equations (2),

$$\bar{v}_{i\alpha} dP - \bar{v}_{i\beta} dP + \bar{s}_{i\beta} dT - \bar{s}_{i\alpha} dT = \left(\frac{\partial \mu_{i\beta}}{\partial N_{j\beta}} \right)_{P,T} dN_{j\beta} - \left(\frac{\partial \mu_{i\alpha}}{\partial N_{j\alpha}} \right)_{P,T} dN_{j\alpha}$$

$$\bar{v}_{j\alpha} dP - \bar{v}_{j\beta} dP + \bar{s}_{j\beta} dT - \bar{s}_{j\alpha} dT = \left(\frac{\partial \mu_{j\beta}}{\partial N_{i\beta}} \right)_{P,T} dN_{i\beta} - \left(\frac{\partial \mu_{j\alpha}}{\partial N_{i\alpha}} \right)_{P,T} dN_{i\alpha}$$

or, in a more compact form,

$$\Delta \bar{v}_i dP - \Delta \bar{s}_i dT = \left(\frac{\partial \mu_{i\beta}}{\partial N_{j\beta}} \right)_{P,T} dN_{j\beta} - \left(\frac{\partial \mu_{i\alpha}}{\partial N_{j\alpha}} \right)_{P,T} dN_{j\alpha} \tag{4}$$

$$\Delta \bar{v}_j dP - \Delta \bar{s}_j dT = \left(\frac{\partial \mu_{j\beta}}{\partial N_{i\beta}} \right)_{P,T} dN_{i\beta} - \left(\frac{\partial \mu_{j\alpha}}{\partial N_{i\alpha}} \right)_{P,T} dN_{i\alpha} \tag{5}$$

Solving equation (4) for $dN_{j\beta}$

$$dN_{j\beta} = \frac{\Delta \bar{v}_i dP - \Delta \bar{s}_i dT + \left(\frac{\partial \mu_{i\alpha}}{\partial N_{j\alpha}} \right)_{P,T} dN_{j\alpha}}{\left(\frac{\partial \mu_{i\beta}}{\partial N_{j\beta}} \right)_{P,T}}$$

and substituting this in equation (5) results in:

$$\begin{aligned} \Delta \bar{v}_j dP - \Delta \bar{s}_j dT &= \left(\frac{\partial \mu_{j\beta}}{\partial N_{j\beta}} \right)_{P,T} \left[\frac{\Delta \bar{v}_i dP - \Delta \bar{s}_i dT + \left(\frac{\partial \mu_{i\alpha}}{\partial N_{j\alpha}} \right)_{P,T} dN_{j\alpha}}{\left(\frac{\partial \mu_{i\beta}}{\partial N_{j\beta}} \right)_{P,T}} \right] - \left(\frac{\partial \mu_{j\alpha}}{\partial N_{j\alpha}} \right)_{P,T} dN_{j\alpha} \\ &= \frac{\left(\frac{\partial \mu_{j\beta}}{\partial N_{j\beta}} \right)_{P,T}}{\left(\frac{\partial \mu_{i\beta}}{\partial N_{j\beta}} \right)_{P,T}} \left[\Delta \bar{v}_i dP - \Delta \bar{s}_i dT + \left(\frac{\partial \mu_{i\alpha}}{\partial N_{j\alpha}} \right)_{P,T} dN_{j\alpha} \right] - \left(\frac{\partial \mu_{j\alpha}}{\partial N_{j\alpha}} \right)_{P,T} dN_{j\alpha} \end{aligned} \quad (6)$$

But at constant temperature and pressure

$$N_{i\alpha} d\mu_{i\alpha} + N_{j\alpha} d\mu_{j\alpha} = 0$$

or

$$\frac{\left(\frac{\partial \mu_{j\alpha}}{\partial N_{j\alpha}} \right)_{P,T}}{\left(\frac{\partial \mu_{i\alpha}}{\partial N_{j\alpha}} \right)_{P,T}} = - \frac{N_{i\alpha}}{N_{j\alpha}} \quad (7)$$

Substituting this into equation (6)

$$\Delta \bar{v}_j dP - \Delta \bar{s}_j dT = - \frac{N_{i\beta}}{N_{j\beta}} \left[\Delta \bar{v}_i dP - \Delta \bar{s}_i dT + \left(\frac{\partial \mu_{i\alpha}}{\partial N_{j\alpha}} \right)_{P,T} dN_{j\alpha} \right] - \left(\frac{\partial \mu_{j\alpha}}{\partial N_{j\alpha}} \right)_{P,T} dN_{j\alpha}$$

Multiplying through by $N_{j\beta}$

$$N_{j\beta} \Delta \bar{v}_j dP - N_{j\beta} \Delta \bar{s}_j dT = - N_{i\beta} \Delta \bar{v}_i dP + N_{i\beta} \Delta \bar{s}_i dT - \left[N_{i\beta} \left(\frac{\partial \mu_{i\alpha}}{\partial N_{j\alpha}} \right)_{P,T} + N_{j\beta} \left(\frac{\partial \mu_{j\alpha}}{\partial N_{j\alpha}} \right)_{P,T} \right] dN_{j\alpha}$$

or,

$$\begin{aligned} (N_{j\beta} \Delta \bar{v}_j + N_{i\beta} \Delta \bar{v}_i) dP - (N_{j\beta} \Delta \bar{s}_j + N_{i\beta} \Delta \bar{s}_i) dT &= - \left[(1 - N_{j\beta}) \left(\frac{\partial \mu_{i\alpha}}{\partial N_{j\alpha}} \right)_{P,T} + N_{j\beta} \left(\frac{\partial \mu_{j\alpha}}{\partial N_{j\alpha}} \right)_{P,T} \right] dN_{j\alpha} \\ &= - \left\{ \left(\frac{\partial \mu_{i\alpha}}{\partial N_{j\alpha}} \right)_{P,T} + N_{j\beta} \left[\left(\frac{\partial \mu_{j\alpha}}{\partial N_{j\alpha}} \right)_{P,T} - \left(\frac{\partial \mu_{i\alpha}}{\partial N_{j\alpha}} \right)_{P,T} \right] \right\} dN_{j\alpha} \quad (8) \end{aligned}$$

But from equation (7) it is seen that

$$\left(\frac{\partial \mu_{j\alpha}}{\partial N_{j\alpha}} \right)_{P,T} = - \frac{N_{i\alpha}}{N_{j\alpha}} \left(\frac{\partial \mu_{i\alpha}}{\partial N_{j\alpha}} \right)_{P,T}$$

Substituting this in (8) gives

$$\begin{aligned} (N_{j\beta} \Delta \bar{v}_j + N_{i\beta} \Delta \bar{v}_i) dP - (N_{j\beta} \Delta \bar{s}_j + N_{i\beta} \Delta \bar{s}_i) dT &= - \left[\left(\frac{\partial \mu_{i\alpha}}{\partial N_{j\alpha}} \right)_{P,T} - N_{j\beta} \left[\frac{N_{i\alpha}}{N_{j\alpha}} + 1 \right] \left(\frac{\partial \mu_{i\alpha}}{\partial N_{j\alpha}} \right)_{P,T} \right] dN_{j\alpha} \\ &= - \left[\left(\frac{\partial \mu_{i\alpha}}{\partial N_{j\alpha}} \right)_{P,T} - \frac{N_{j\beta}}{N_{j\alpha}} \left(\frac{\partial \mu_{i\alpha}}{\partial N_{j\alpha}} \right)_{P,T} \right] dN_{j\alpha} \\ &= \left[\left(\frac{\partial \mu_{i\alpha}}{\partial N_{i\alpha}} \right)_{P,T} - \frac{N_{j\beta}}{N_{j\alpha}} \left(\frac{\partial \mu_{i\alpha}}{\partial N_{i\alpha}} \right)_{P,T} \right] dN_{j\alpha} \\ &= \frac{1}{N_{j\alpha}} (N_{i\alpha} - N_{j\beta}) \left(\frac{\partial \mu_{i\alpha}}{\partial N_{i\alpha}} \right)_{P,T} dN_{j\alpha} \\ &= \frac{\Delta N_j}{N_{j\alpha}} \left(\frac{\partial \mu_{i\alpha}}{\partial N_{i\alpha}} \right)_{P,T} dN_{j\alpha} \end{aligned}$$

And finally,

$$dN_{j\alpha} = \frac{N_{j\alpha} [(N_{j\beta} \Delta \bar{v}_j + N_{i\beta} \Delta \bar{v}_i) dP - (N_{j\beta} \Delta \bar{s}_j + N_{i\beta} \Delta \bar{s}_i) dT]}{\Delta N_j \left(\frac{\partial \mu_{i\alpha}}{\partial N_{i\alpha}} \right)_{P,T}}$$

Similarly,

$$dN_{j\beta} = \frac{N_{j\beta} (N_{j\alpha} \Delta \bar{v}_j + N_{i\alpha} \Delta \bar{v}_i) dP - (N_{j\alpha} \Delta \bar{s}_j + N_{i\alpha} \Delta \bar{s}_i) dT}{\Delta N_j \left(\frac{\partial \mu_{i\beta}}{\partial N_{i\beta}} \right)_{P,T}}$$

From these results it is seen that the mole fraction of j in phase α or β is a continuous function of temperature and pressure, except at phase changes, where there are

discontinuities in the v and s terms; or at the special cases of maxima, minima, or pure end members. In the cases of maxima or minima the ΔN_j term becomes 0 in both expressions simultaneously. At pure end members terms such as $\left(\frac{\partial \mu_i}{\partial N_i}\right)_{T,P}$, $\Delta \bar{v}_j$, $\Delta \bar{s}_j$, etc. become either infinite or zero, thus making the equations indeterminate. Projections of $\frac{dT}{dN}$ onto planes of constant pressure illustrate these special cases in familiar temperature vs. composition diagrams. However, in the more general case the mole fractions should be continuous functions of pressure and temperature. This relationship also holds for a system of several components and several phases, some of which contain solid solution. A set of simultaneous equations for the change of the chemical potential would be set up and the solution would involve matrix algebra.

Another relationship which might be of use is the distribution of minor elements between two phases. McIntire has combined the work on this problem into a concise and rigorous treatment (McIntire, 1958, pp. 8-20). He first expands the internal energy and volume in powers of the molecular ratios of each solute to solvent. The assumption is then made that the solution be sufficiently dilute that all terms beyond the first order may be neglected. By substituting the resulting equations into the expression

$$dS = \frac{1}{T} (dU + PdV)$$

and making use of the fact that dS is a perfect differential

he obtains an expression for S. The evaluation of the integration constant for S requires only that the process take place in such a way as to leave unchanged the number of moles of the solvent and each solute.

By substituting the values for U, V, and S into the expression for the chemical potential, and requiring the chemical potential of any solute to be the same in any two phases it is possible to obtain a distribution coefficient of the form

$$K_1 (P,T) = \frac{N_{1\beta}}{N_{1\alpha}}$$

This coefficient is a function only of pressure and temperature, and does not depend upon the number of moles of the various solutes. However, the solvent must have a fixed composition. Therefore, in phases having solid solution the distribution coefficient can be compared only between identical members of the solid solution series. As an illustration of this one might consider the distribution of Mn between quartz and biotite. If in one assemblage the Fe/Mg ratio of the biotite is 2/1 and in another assemblage 1/2, then a comparison of the two distribution coefficients is not valid. Both biotites should have the same Fe/Mg ratio.

A second difficulty is the determination of a concentration above which the given expression of the distribution law no longer holds. That is, at what concentration of a solute do the second and higher order terms in the expansion

of internal energy and volume become significant. There is nothing in the thermodynamic theory which predicts the concentration below which the higher order terms may be neglected. These concentrations must be determined experimentally.

B. Comparison of Data and Theory

The expression for dN , derived above, was for a two component-two phase system, or in other words, for a divariant system. In a first approximation we can apply this relationship to the assemblages being studied. However, the chemical potentials of H_2O and oxygen must remain constant and minor components such as MnO and CaO must be ignored, or compensated for in some manner. We can now treat the system being studied as one of eight components; SiO_2 , Al_2O_3 , TiO_2 , FeO , Fe_2O_3 , MgO , K_2O , and Na_2O , and eight phases; quartz, muscovite, biotite, garnet, staurolite, plagioclase, ilmenite, and magnetite. This would be divariant. In fact, where kyanite is added to the above assemblage the system becomes univariant and the relationship no longer holds. It must be emphasized that in order to be divariant we must assume a projection at constant chemical potentials of water and oxygen, and neglect the minor components CaO and MnO .

Because the temperature and pressure are assumed to be continuous functions there should be gradients of FeO/MgO in the isomorphous phases of divariant regions. The presence of crossing tie lines in the phase diagrams indicates that this is not so in the rocks which were analyzed. If such a

gradient existed in the coexisting biotites and garnets it would be impossible for the tie lines to cross. Ignoring SP33 in Figure 17 the three assemblages SP 28, 34, and 66 do exhibit a smooth gradient of the type expected. These three samples however are taken nearly parallel to the isograd. It would be expected that the temperature and pressure gradient would be perpendicular to the isograd and, therefore, the FeO/MgO gradient should be perpendicular to the isograd.

In order to explain the discrepancies one first turns to extra components or variations in the chemical potentials of water and oxygen. The variations in MnO content and chemical potential of oxygen have been accounted for in the manner described under the section on phase diagrams in the previous chapter. This is a rather crude method of handling these variations, but it should make the comparisons more valid. Little can be assumed about the variation of the chemical potential of water. It is hoped that the mobility of water is great enough to equalize the chemical potential over the entire area. The CaO content can be examined for various garnets which are compared in the same phase diagrams. A glance at the CaO contents of garnets SP9, 12, 13, and 14 (Table 5), all plotted on diagram 16, shows a variation from 3.04 to 4.80%. The CaO content of SP9 and SP13 are quite similar, 3.44 and 3.66, respectively. Yet the tie lines for these two assemblages differ greatly in slope; and cross with a rather large angle. Similarly the CaO content of SP33 and 66

of diagram 17 are nearly the same. Yet the tie lines have radically different slopes. Therefore, variations in composition and chemical potential of oxygen do not appear to explain completely the apparent disequilibrium.

While separating garnets from staurolites it was noticed that the garnet/staurolite ratio (by volume) was related to the FeO/MgO ratio of the biotites, which had been analyzed previously. It will be noticed in Table 12 that the lowest FeO contents are associated with the lowest garnet/staurolite ratios. Similarly, the highest FeO contents are associated with the high garnet/staurolite ratios. An explanation of this association appears to be available in Thompson's diagrams. (Thompson, 1957)

If a hand specimen is imagined to be composed of numerous small increments of volume, each having its own bulk composition, then the bulk compositions of the volumes might cover the range encircled in the schematic phase diagram of Figure 20a. If each increment of volume contained the mineral assemblage characteristic of its bulk composition there would be many garnet biotite tie lines on the FeO-rich side of the limiting tie line for the garnet-biotite-staurolite field. The rock would also have a high ratio of garnet to staurolite. Similarly, a rock with increments of volume having the range of bulk compositions encircled in Figure 20b would have a lower FeO content and a low garnet to staurolite ratio.

Table 12. Relation of garnet/staurolite and $\frac{\text{FeO}}{\text{FeO}+\text{MgO}}$ in biotites

	garnet/staurolite	$\frac{\text{FeO}}{\text{FeO} + \text{MgO}}$	mole %
SP87	10/90	44.3	
SP95	10/90	44.5	
SP84	15/85	43.8	
SP38	30/70	40.0	
CN27	30/70	48.1	
SP55	35/65	42.6	
SP9	50/50	51.3	
SP12	50/50	46.9	
SP13	50/50	48.8	
SP51	50/50	48.0	
SP66	50/50	49.5	
SP92	50/50	50.2	
SP106	50/50	44.2	
SP99	55/45	49.9	
SP109B	60/40	50.0	
SP42	80/20	49.0	
SP107	80/20	51.0	
SP28	90/10	47.1	
SP33	95/5	55.6	
SP34	95/5	51.5	
SP109A	95/5	49.9	

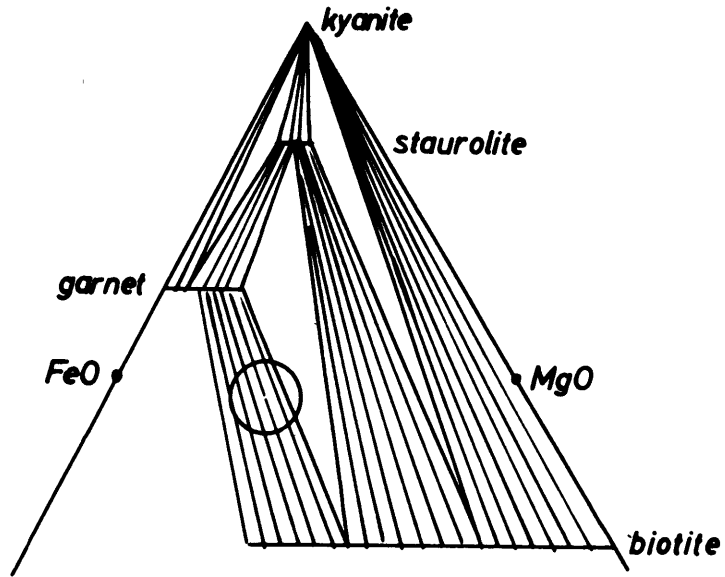


Figure 20a

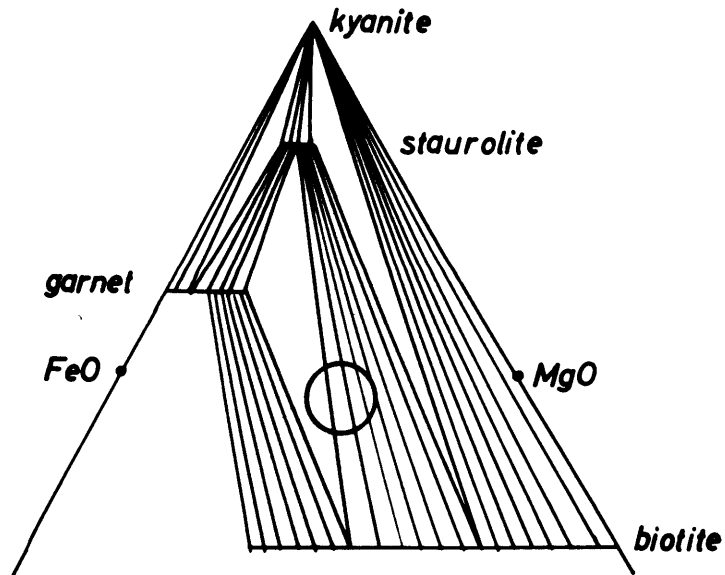


Figure 20b

Figure 20. Possible explanation of garnet/staurolite ratios.

This reasoning would indicate that the diffusion of Fe and Mg during metamorphism takes place over a very limited range. In order to check on this possibility one would have to separate and analyze minerals from volumes of a cubic millimeter or less. It was found that the optical spectrograph could be used to determine relative intensities of Fe/Mg in samples of biotite weighing as little as 2 milligrams. To test this a thin slice was cut from each of five hand specimens and a few flakes of biotite from various points on the slice were hand picked under a binocular microscope. When picking the biotite grains the distances between each biotite sample and to the nearest staurolite and garnet grains were recorded. Because of the lack of knowledge of the third dimension these distances can be considered only as approximations. The samples were finely ground, diluted carbon/sample in a ratio of 2/1, and run with quartz optics and a five step sector. The results are shown in Table 13.

In order to estimate the precision of the method two samples, SP95-1 and SP34-2 were run in triplicate, and one sample, SP34-1, in duplicate. Enough material for duplicate runs was not available in the other samples. On the basis of the three samples run in replicate a difference of 12% or more between samples is considered to be real. Using this criteria the biotites from different points in slices from SP33, 34, and 38 have different Fe/Mg ratios. SP95 has differences which are on the borderline of being real; but SP66 and 87 appear to have the same Fe/Mg ratios, no matter where the biotite is taken.

Table 13. Spectrographically determined relative intensities of Fe/Mg in biotites

	Fe/Mg
SP33-1	2.15
33-2	.91
SP34-1a	.96
1b	.96
34-2a	1.03
2b	1.08
2c	1.15
34-3	.85
SP38-1	.71
38-2	.42
SP66-1	.80
66-2	.78
66-3	.82
SP87-1	.89
87-2	.94
87-3	.97
SP95-1a	.87
1b	.88
1c	.98
95-2	1.08

Admittedly these data are not completely convincing and should contain many more analyses, but there is an indication that certain slices show similar Fe/Mg ratios for all samples of biotite, and other slices show significantly different ratios depending upon where the biotite is sampled. A study of the slices from which the biotites were taken, and the measurements of distance between various minerals, reveals that the slices from SP66 and 87 have very homogeneous textures. In fact, a complete mineral assemblage of quartz, muscovite, biotite, garnet and staurolite can usually be found within a radius of 6 to 8 millimeters. Slices of samples SP33, 34, and 38 often show distances of 2cm., or more, between garnet and staurolite grains. It would appear then, that the radius over which Fe and Mg have diffused is of the order of a few millimeters in these rocks.

It is interesting to note that Harker reached similar conclusions in 1893 on the basis of textural studies (Harker, 1893). He cites the case of calcite amygdules in lavas which have been thermally metamorphosed in aureoles. Quite often the outer layers of the amygdules are calc-silicates but the core remains calcite. Similar occurrences are found at the contacts of quartz and calcite in thermally metamorphosed impure limestones. In many cases as little as 1/20 of an inch of calc-silicate material has formed. Harker amplified these remarks later to include further studies of textures (Harker, 1932). He mentions that bands of differing composition, and

only a few millimeters thick, are preserved as distinct bands even into high grades of metamorphism. The arenaceous material of grits is preserved even in the highest grades of thermal metamorphism. The mineralogy may have changed but the outlines of the original grains are preserved.

It should now be clear that the use of Thompson's diagrams and chemical analyses of the coexisting phases has produced much information. On an AKF diagram of Turner's *Staurolite-Quartz Subfacies of Almandine-Amphibolite Facies* (Fyfe, Turner, and Verhoogen; 1958, p. 230) the details of the chemical analyses could not have been plotted. The important isomorphous substitutions, which would indicate the conditions of equilibrium (or disequilibrium), in coexisting biotite, garnet, and staurolite cannot be shown on AKF diagrams. Therefore, the detailed chemical analyses necessary for equilibrium studies must be used with another type of diagram. In the present study the crossing tie lines and the relationship between the garnet/staurolite and biotite FeO/MgO ratios were made apparent by the diagrams developed by Thompson. Although these features indicate disequilibrium, and possibly the nature of the disequilibrium, they could not have been discovered with AKF diagrams.

The application of dilute solution theory to the present study is rather unsuccessful. Perhaps the use of trace elements would yield more satisfactory results. Miyashiro (1953) showed that the distribution coefficient for MnO between garnet

and biotite followed a smooth curve when plotted against increasing metamorphic grade. The ratio of MnO in garnets to that in biotites shows a continuous decrease. Any attempt to do this with the present study meets with complete failure. There are two reasons which probably explain why this does not succeed. First, the MnO content of the garnets may be too high for dilute solution theory to hold true, and second, the change in the FeO/MgO ratio of the biotites would invalidate many of the comparisons.

Similar unsuccessful results are met with in the distribution of CaO between garnet and plagioclase. There is a rough correlation between the garnets with the highest CaO content, SP35 and CN13, and the plagioclases with the highest CaO content. Also SP110 has the lowest CaO content of both garnet and plagioclase. However, there is no quantitative change between these two extremes. The reasons for this failure are probably the same as those for MnO.

Because of the possible interference of Cr with the TiO₂ determination in the garnets a study of the distribution of TiO₂ between garnets and biotite is doomed to failure before even attempting it. However, there is a regular increase of TiO₂ in the biotites as the grade increases. The weight per cent TiO₂ increases from a low of 1.49 in the garnet-chlorite assemblage through 1.60-1.70 in the staurolite zone, to 2.00 in the two biotites from the kyanite isograd, and finally to 2.18 in the kyanite zone.

100

It is interesting to note the large variation in the $\text{Fe}_2\text{O}_3/\text{FeO}$ ratio of the biotites. In general this ratio in the garnets changes in the same manner as in the biotites. Changes in this ratio should represent changes in the partial pressure of oxygen. Samples SP9, 12, 13, and 14 were taken within a radius of 25 feet and have almost identical $\text{Fe}_2\text{O}_3/\text{FeO}$ ratios. However, samples SP109A and B were taken only five feet apart and have radically different ratios.

A comparison of the number of phases, eight, with the number of components, nine including water, shows that there can be three intensive variables; pressure, temperature, and the chemical potential of a mobile component. If water is considered as the mobile component, then the system is not open to oxygen. The partial pressure of oxygen at any location would be a function of the original composition, in addition to temperature and pressure. Certain zones such as the one including samples SP9-14 might have similar partial pressures of oxygen, but other zones such as the one including samples SP109A and B might have sudden variations within a few feet.

An alternative interpretation of the number of phases and components would have water present as a separate and immobile phase during the formation of the assemblages. In such a case the number of phases, nine, would equal the number of components, nine, and the system would be completely closed. The only intensive variables would be temperature and pressure.

C. Future Work

Further work on the radii of diffusion of the various elements during metamorphism is necessary. In order to study this from the natural mineral assemblages one must remember several points during sampling. Most of these points were discussed in the chapter on sampling but further restrictions are caused by the apparent limits of diffusion. If one requires samples for phase equilibrium studies then there should be a complete mineral assemblage within a radius of a few millimeters at every point in the rock. If one is to study diffusion radii the samples must include some of the above-mentioned type and some with a few centimeters or less between certain of the minerals.

Analyses of the small samples necessary for radius of diffusion studies should be greatly aided by the development of electron probes in X-ray fluorescence. These probes are gradually becoming more accurate and will eventually be able to analyze volumes down to 1 cubic micron. With a technique of this nature all of the elements can be easily analyzed; and many different rock types could be checked in a relatively short time. From studies of this type the amount of diffusion of many elements in rocks representing many geologic environments can eventually be determined. This would not solve the problem of a mechanism for diffusion. Such a problem would require laboratory studies which would utilize high pressure

and radioactive tracers.

Future geologic work in the thesis area should be aimed at establishing the extent and time of metamorphism of the interbedded sediments and volcanics found on northern Cape Breton and St. Paul Island.

VII SUMMARY

The important observations and conclusions may be summarized as follows:

- 1.) Two weeks on St. Paul Island permitted compilation of a more detailed geologic map than the one previously published by the Geological Survey of Canada.
- 2.) Twenty-four rocks were separated into their constituent minerals. Of the separated minerals twenty-four biotites, one chlorite, and twenty-three garnets were analyzed for major constituents. The precision of the analyses is generally within a relative error of 2%. The accuracy appears to be of the same order.
- 3.) On the phase diagrams plotted from the mineral analyses many of the garnet-biotite tie lines intersect.
- 4.) The equation for dN derived in Chapter VI shows that within a divariant region, such as might be represented by the staurolite zone, there should be a continuous gradient in the FeO/MgO ratio in the phases containing solid solution of these two components. Such a continuous gradient is not compatible with the intersecting tie lines of the phase diagrams.
- 5.) The components MnO and CaO, and differences in the partial pressure of oxygen, although not accounted for in Thompson's original projections, were considered as possible causes of the crossing tie lines. Comparison of assemblages having similar values for these still shows tie line intersections.

6.) It was found that the relationship of the garnet/staurolite ratio and the $\frac{\text{FeO}}{\text{FeO} + \text{MgO}}$ ratio in biotites could be explained using Thompson's phase diagrams. However, the explanation requires that diffusion equilibrium of Fe and Mg be restricted to volumes much smaller than that of a hand specimen.

7.) Emission spectrographic analyses of Fe/Mg intensity ratios in biotites indicated that this ratio varied among biotites taken little more than a centimeter apart. The variation was greatest in samples where garnet and staurolite grains were separated a centimeter or more. Furthermore, the two samples which were highly homogeneous and contained a complete mineral assemblage within any radius of a few millimeters did not show variations in the Fe/Mg ratio.

8.) The apparent disequilibrium indicated by the intersecting tie lines is most easily explained by assuming maximum diffusion radii for Fe and Mg which are too small to overcome the initial inhomogeneities in composition. The radius of diffusion is a function of temperature, pressure, composition, and time. In the St. Paul Island rocks it is estimated that the limit of diffusion for Fe and Mg is of the order of a few millimeters.

ACKNOWLEDGMENTS

The author wishes to acknowledge the valuable discussions and suggestions of Prof. H. W. Fairbairn of the Massachusetts Institute of Technology Department of Geology and Geophysics, Prof. J. B. Thompson of the Harvard Mineralogy Department, and Prof. G. J. F. MacDonald of the Institute of Geophysics at U.C.L.A. The M.I.T. Geology Summer Camp furnished assistants and supplies for the field work. Dr. J. Ito of the Harvard Mineralogy Department performed a gravimetric analysis and offered many useful suggestions concerning analytical techniques. A Grant-in-Aid from the Nova Scotia Research Foundation helped defray the cost of field expenses. The laboratory research was financed by the National Research Foundation under contract NSF G-2938.

PART 2

I INTRODUCTION

A. Purpose of Investigation

In order to understand more completely the environment in which certain rock types form, most of the common rock-forming minerals have been synthesized under controlled conditions. In attacking the problem from this point of view, investigators have been limited thus far to relatively simple systems. "Simple" in the sense that the mineral assemblages produced have contained very few phases, i.e. simple; but the problems of reaction rates, instrumentation, interpretation, etc. have been far from simple. While the laboratory "rock-makers" gradually approach the complex systems which are the actual rocks, it remains the task of a geologist to obtain as much information as possible from these complex systems.

With few exceptions all of the geologically important phase equilibrium studies through the mid-1940's had been with igneous minerals at atmospheric, or relatively low, pressures and liquidus temperatures. However, during recent years the development of high pressure techniques has provided a means of studying the conditions of formation of metamorphic rocks, and also, igneous rocks at more realistic pressures. At present this type of study of metamorphic rocks is confined primarily to an understanding of the individual metamorphic minerals. Studies are

underway on biotites, garnets, cordierites, chlorites, spinels, and amphiboles. Much work has already been completed on the white micas, feldspars, and Al_2SiO_5 polymorphs. Preliminary data for staurolite and chloritoid have been obtained. Because of the large amount of solid solution in most of these minerals, the slow reaction rates, and the effect of partial O_2 pressure on the iron-bearing minerals, it has been a major problem to discover the stability relationships of each separate mineral as its composition changes from one end member to another. But eventually systems will become more complex; and mineral assemblages similar to those of actual metamorphic rocks will be produced. When this end is achieved it is reasonable to assume that there will be a need for good chemical analyses of coexisting metamorphic minerals. Such data is practically non-existent in geologic literature.

One of the purposes of this investigation is to provide analyses of the coexisting minerals from several metamorphic rocks. However, one should not be misled into believing that a study of the mineral assemblages in rocks should be relegated to a position of secondary importance, useful only for comparison with the laboratory produced assemblages. Rather it should be realized that first-hand knowledge of the field relationships, careful sampling, detailed investigations of microscopic textures, good analyses of coexisting phases, and knowledge of the chemistry and

physics involved in the formation of the rocks, are all necessary for the complete understanding of the processes which produced the rocks. Only by these means can one discover whether reactions were completed, whether retrogressive reactions took place, how much diffusion took place, whether gradients are present in the composition of isomorphous phases, and many other facts. Or stated more generally - to what extent was equilibrium attained?

The second, and major, purpose of this investigation is to study in some detail the mineral assemblages from a small area where the geology can be relatively well studied; and to glean from the data as much as possible concerning the extent to which equilibrium was achieved. It should be noted that this study is primarily of a physical chemical nature and does not attempt to investigate the details of mechanical deformation. The latter type of investigation would produce as much data as the present study; and ideally the two should be combined.

B. Location of Area

If one is to sample adequately and map an area which will yield the detailed information desired, there are several necessary specifications which the area must meet. These include: coarse-grained assemblages in which the minerals may be recognized while in the field, accessibility of fresh samples, enough outcrop to allow good sample

control, and from the given bulk composition of the rocks there must be the correct mineral assemblages which allow a minimization of the degrees of freedom in the application of the phase rule.

Because of the facilities offered by the M.I.T. Summer Geology Camp near Antigonish, Nova Scotia, it was desired to find an area of this nature in Nova Scotia. While studying a series of Geological Survey of Canada Preliminary Reports on northern Nova Scotia the occurrence of high-grade, coarse-grained metamorphic rocks was noticed on St. Paul Island, which lies about 15 miles northeast of the northern tip of Nova Scotia as shown on the index map (GSC Paper 55-23). Communication with E.R.W. Neale, the G.S.C. party chief who had mapped the island, provided confirmation that all of the specifications were met.

In August of 1957 the writer and three assistants from the M.I.T. Summer Camp sailed from Dingwall, Nova Scotia with a swordfishing crew which landed us on the island and picked us up 16 days later. During this time the island was mapped and approximately 120 samples were collected. Another week was spent studying the geology and collecting samples in the vicinity of Money Point on the northeast tip of Cape Breton Island, Nova Scotia. This area lies directly along strike with St. Paul Island; and offered an interesting correlation problem.

C. Methods of Investigation

Laboratory work with the rocks included microscopic examination of approximately 100 thin sections, separation by magnetic and heavy liquid techniques of 24 rocks into their constituent minerals, chemical analyses by means of rapid instrumental techniques of coexisting biotites, garnets, and chlorite, and synthesis of the data into the appropriate phase diagrams.

II GEOLOGY

A. Introduction

St. Paul Island is located in the Cabot Strait approximately 15 miles northeast of Cape North, Cape Breton, Nova Scotia, and about 40 miles south of Newfoundland. It lies between latitudes $47^{\circ}11'$ and $47^{\circ}14'$ north and longitudes $60^{\circ}8'$ and $60^{\circ}10'$ west. The Island is $3\frac{1}{2}$ miles from northeast to southwest and $1\frac{1}{4}$ miles at its greatest width. Also investigated was an area about 1 mile square at Money Point on the northeast tip of Cape Breton Island, Nova Scotia. This area lies between latitudes $47^{\circ}1'$ and $47^{\circ}2'$ north and longitudes $60^{\circ}23'$ and $60^{\circ}24'$ west.

St. Pauls, as it is called locally, is accessible only by boat. During the summer months a mailboat makes the trip to the island about once a month. Also, one may persuade some of the swordfishermen at Dingwall to make the

trip. However, no one is particularly anxious to land passengers or supplies at St. Pauls, which has no docking facilities. Landings must be made by a dory which has to be launched from a larger vessel hovering a few hundred feet from shore. Landings are usually made in Atlantic Cove where the shore is partially protected from the swells of the open ocean.

The Island is strategically placed to be of great danger to shipping entering the St. Lawrence, and its history is by no means devoid of numerous shipwrecks. Warm eddies from the Gulf Stream System, the tail of the Labrador Current, current from the St. Lawrence River, and the open Atlantic Ocean meet in the area, thus making weather conditions extremely variable. Fog, winds, and currents are always uncertain. For over a century the Canadian Government has maintained two lighthouses on the island, one at the Southwest Head and another at the Northeast Head. In addition to the lighthouses a rescue station was established on the north side of Atlantic Cove. During the pre-radio years of this and the previous century the men from this station kept open many trails and patrolled the island. A cannon, which was used as a fog horn before the advent of steam whistles, still remains at the site of the old rescue station. The rusted remains of an old steam whistle station may yet be found at Whistle Point.

In more recent years a Canadian Navy radar station has been located on St. Paul Island. Also located there is a LORAN low frequency radio beacon. The abandoned radar tower may still be seen at the top of Groggan Mountain, altitude 475'. During the years which the navy spent on the island a few roads were cleared for their jeeps; but today these roads are nothing but alder swamps. Until the summer of 1956 the LORAN station was located at Atlantic Cove. In that summer it was moved to the lighthouse at the Northeast Head. Thus today the only life on the island is at the two lighthouses at opposite tips of the island.

Internal accessibility on St. Pauls is as difficult as landing on the island. The only road connects the southwest lighthouse with Atlantic Cove. This road is kept open by the lighthouse keeper whose supplies must be hauled by tractor from Atlantic Cove, where the supplies are landed. Various trails and roads cut by previous groups on the island have not been maintained and are practically obliterated by fresh growth. Walking the coastline is possible for much of the island's perimeter but nearly 20% of the coast consists of shear or overhanging cliffs which make passage impossible. The lighthouse keepers use small boats with outboard motors for transportation to various parts of the island; and it does not take long for a visitor to find that a boat is certainly the easiest and quickest means of transport available.

To reach the Money Point area at the tip of Cape Breton one must take the auto route known as the Cabot Trail to the village of Cape North and from there a twisting gravel road to the village of Bay St. Lawrence. From Bay St. Lawrence a private road owned by the Canadian National Railroad winds to the top of the mountain where a CNR radio relay station is located. A key to the gate which blocks this private road must be obtained in the village of Bay St. Lawrence. From the radio station one can go down the precipitous road to the lighthouse at Money Point. The road to the lighthouse is accessible only to jeeps or tractors. Cars or trucks should be left at the top of the hill. The main occupation of the inhabitants of Bay St. Lawrence is fishing. Farming is nearly impossible on the steep slopes; and no industry is closer than 75 miles.

B. Topography

Perhaps the most notable feature on St. Paul Island is the rugged rocky coastline. Cliffs ranging from 10 to 100 or more feet in height form the entire perimeter of the island. Terraces are present at a few locations, otherwise the cliffs merge with grassy or evergreen slopes of varying steepness, and culminate in relatively flat summits with altitudes of about 450 feet. The summit of Groggan's Mountain, at 475 feet, is the highest point on the island.

At the northern tip of the island a small 50 feet wide strait known as the Tittle separates the Northeast Head into a small sub-island. This small segment of land is approximately 900 by 600 feet. The rock cliffs on its west side are about 10 feet high. A rocky slope rises gradually to the east to an altitude of 50 feet just past the center of the Head. This elevation remains nearly the same all the way to the eastern cliffs which drop straight down forty to fifty feet to the water. The entire Head appears to be a large roche moutonnee.

Over the entire length of the island the eastern slopes are much steeper and higher than the western slopes. The eastern slopes of Norwegian Mountain are probably the steepest slopes on the island; some of them being greater than 45° . The west slope of this mountain is gradual and ends in an ill-defined north-south valley extending from Atlantic Cove to Martin Powers West Cove. Between Groggan Mountain and the West Coast, and in the west central part of the island the topography is quite flat with altitudes ranging upwards from 300 feet.

Money Point

The unusually steep slopes at Money Point on Cape Breton rise to altitudes greater than 1000 feet within less than a quarter of a mile from the shoreline. At the base of these steep slopes is a terrace 10 to 15 feet above sea level. The terrace broadens to the north along the eastern

shoreline of Money Point until it is approximately 200 to 300 feet wide near the lighthouse. Flat pebbles with rounded edges show shingled structure on this terrace. Deep V-shaped valleys have been cut by the streams flowing from the upland areas. Approximately one mile up the stream near the Money Point lighthouse a recent rockslide has left a broad scar in the valley wall. The upland areas form part of the large Northern Tableland of Cape Breton Island. The 1400 foot high plain is quite striking from the top of the uplands.

C. Drainage

There are two fresh water lakes on St. Paul island. The northern one has two small outlet streams but no visible streams feed the lake. The southern lake has only one outlet and again no visible feeders. It is assumed that the lakes are spring fed as the bottom water is quite cold, even in the shallow areas where the depth is only two to three feet. In all of the relatively flat upland areas one finds bogs. Petrie's Pond, at an altitude of 225 feet, is a small body of water, about 200 by 100 feet, completely surrounded by peat moss. However, in most cases no water is visible until one steps on the moss and sinks into a few inches of it. There are a few small streams draining the bogs but the drainage is slow and there is little water in most of the streams. A few of these streams were dammed for water reservoirs by previous residents of the island. The

water is a rather unappetizing shade of brown and usually contains small particles of roots, stems, and other debris from the bogs. Nevertheless, it is not contaminated.

Money Point

Within the investigated area at Money Point two streams drain the uplands; one flows northward to Money Point, the other southward to dissect the Aspy Fault Scarp. Both streams originate in damp swampy areas of the uplands. However, they carry much more water than the streams of St. Pauls, and have cut deeply into the uplands to form V-shaped valleys.

D. Vegetation and Animal Life

St. Paul Island

Vegetation consists predominantly of thick growths of evergreens which offer a great amount of resistance to anyone tramping the island. The following quote from a paper by a botanist aptly describes the forested areas of the island. (Erskine, 1955)

"The Atlantic side of the island gives the impression of being heavily wooded, except that the trees grow in peculiar steps up the hillsides. Apart from a few white spruce near Coggin's Cove, the forest consists of undersized firs. The soil is damp and has little cohesion, so that when the trees reach about twenty-five feet in height they are blown over and lean against their neighbors uphill. These now have to support both the weight of the dead trees and an increased pressure from the wind and consequently topple in turn. So a slow wave of collapse works up the hillside. Meanwhile, where the trees have recently fallen there springs up a thick growth of annuals and shrubs and the reproduction of the firs. In a few years the firs

have smothered all competition and are choking each other. They are protected from the worst of the wind by the slightly older and taller trees below them, but at last these reach their critical height and topple upon them."

While ascending the slopes above the sea cliffs one notices a definite sequence of vegetation. First grasses appear, short at first but gradually becoming taller; second stunted firs, three to six feet in height, appear; then the fir forests of the previous paragraph complete the sequence. The zone of stunted growth appears as a hedge of horizontal branches through which it is impossible to walk. After a bit of experience one can actually walk on top of these stunted fir trees. At the heads of the coves there usually is no grass and the stunted firs grow to the edge of the cliff.

Various mosses, grasses, ferns, and other plants grow plentifully in the bogs. Botanists who have studied the plant life of these bogs have discovered new species and many new varieties of familiar plants. (Erskine, 1955 and Perry, 1931) The abundance of wildflowers over the entire island is quite striking even to non-botanists.

Owing to the isolated nature of the island there is practically no wildlife, other than birds, on the island. There are no fish in the lakes. Trout were once introduced into the northern lake but they failed to spawn and soon became extinct. Frogs and salamanders are also absent. Although Erskine (1955) states that bats have not been observed, we saw two bats during our stay on the island.

Rabbits were introduced to the island by the southwest light keeper in 1945. Some have managed to survive but are observed only on the southern part of the island. Seabirds, shorebirds, and landbirds are plentiful.

Money Point

The vegetation in the area around Money Point consists of grass and wildflowers on the terrace and heavy forests on the slopes and uplands. Both deciduous and coniferous trees make up the forested areas. There are none of the stunted zones or windfall terraces which are so prevalent on St. Pauls. Animal life was abundant, in fact the bears were too abundant, according to the sheep owners. While we were working in this area one of the inhabitants brought in a 280 pound black bear which he had killed.

E. Geomorphic Features

St. Paul Island

The steepest and highest sea cliffs are on the eastern side of St. Pauls. This is partially a result of the nearly vertical foliation in the schists and the vertical contacts between interbedded schists and amphibolites. Both the foliation and the contacts follow the northerly strike of the cliffs. On the western side of the island the predominant gneiss and pegmatite produce a more irregular shoreline.

All of the major coves on St. Paul are expressions of fault zones. An east-west fault zone easily explains the occurrence of Martin Powers East and West Coves, and the narrow neck between them. This neck is being destroyed by wave and ice action, and three separate islands will remain. The Tittle is the result of a similar sequence of events. Two faults intersect at Trinity Cove. A north-south fault zone extends from Atlantic Cove to Martin Powers West.

At a few locations along the east coast caves have developed. The largest of these occurs approximately 2000 feet north of Moon Point in what the writer has named Sea Cave Cove. The cave is 10 feet wide and extends into the rock a distance of 15 feet. The back wall of the cave is a brecciated shear-zone. This cave and other smaller ones are interpreted as the result of relatively rapid erosion of narrow shear zones which strike parallel to the foliation.

Two terrace levels are apparent on St. Pauls. On the west coast at Petrie's Point, Goat Rock, and the point north of Goat Rock broad flat surfaces are present at an altitude of 20 feet. At Jessie Cove there is a flat terrace-like surface about 35 feet above sea level. None of these west coast surfaces show evidence of deposition. Only a thin veneer of grass-covered humus is present. On the east coast the 20 foot terrace can be traced from Moon Point to the north for perhaps 2500 feet. At various points

on this terrace there are evidences of wave action. Approximately 200 feet south of the previously described sea cave are pot holes, a few feet from the sea cave are flat, rounded boulders enclosed in a sandy matrix, and approximately 1000 feet north of Moon Point there are flat, shingled pebbles with rounded edges. These features on a surface 20 feet above sea level indicate a wave cut terrace. Perhaps the higher surface seen only at Jessie Cove represents another level of wave cutting action, but there is no evidence to support this hypothesis.

The accordance of summit levels on St. Pauls remains unexplained. On the aerial photos and topographic maps of St. Pauls one notices that the four highest elevations on the island are relatively flat-topped hills having altitudes between 450 and 475 feet. Whether these summits are related to the 1400 feet high plain of northern Cape Breton is not known.

Money Point

At Money Point three significant geomorphic features are apparent: (1) the unusually steep eastern slope of the highland. This results from an extension of the Aspy fault scarp which extends southeastward across Cape Breton Island. (2) the uplifted peneplain which is particularly striking from a boat several miles away in the Cabot Strait. In this area the average altitude of the plain is 1400 feet. It is part of a large dissected peneplain which slopes to the south

and can be traced to southern Nova Scotia where it is only 400 to 500 feet above sea level (Goldthwait, 1924). (3), the terrace around Money Point. This terrace is 10 to 15 feet above sea level and extends for several miles along the eastern shoreline. From a boat several hundred yards from shore the terrace is easily traced along the coast.

F. Erosion and Soils

St. Paul Island

Rocks within the range of wave action are subjected primarily to mechanical weathering but the rocks subjected to subaerial or subsoil erosion are decomposed in various ways. Schists become soft and "rotten" especially beneath the dark humus soil. Where winds have continually blown away the decomposing grains of the schists, resistant staurolite and garnet crystals stand out in relief.

Where the amphibolite near the Tittle has been exposed to the wind and salt spray it forms a pattern of small ridges and valleys parallel to the foliation and bedding. Slight changes in composition between bedding lamellae with consequent variation in weathering resistance cause the formation of ridges $\frac{1}{2}$ to 1 cm. wide and 2 to 5 cm. high. In some cases bridges, or holes, form in the ridges resulting in a rather intricate erosional pattern.

The granite gneisses weather to a residual, white, arkosic gravel containing fragments up to 1 or 2 cm. across. Thickness of the gravel ranges from a thin veneer up to 10 cm.

The schistose layers which occur in the gneisses consist mainly of quartz and biotite; and weather to a dark sandy residual soil.

The soil usually consists of a layer of humus which covers either decomposing schist or residual gravel from the gneiss. The total thickness of these soils seldom exceeds 2 feet and the humus generally comprises more than half of this. Soil development along the western shore is often limited to only the residual gravel. The wind and salt spray make it impossible for plant life to exist. In fact there is evidence that plant life is today receding even further from the western shoreline. Most of the stunted fir trees at the edge of the zone of plant life are dead and the humus around their roots is gradually blowing away. At several places there is a wall of humus nearly one foot high, and parallel to the coast 200 to 300 feet from the water. From these ridges to the cliff edges there is only arkosic gravel except for a few outliers of humus where the roots of dead fir trees still hold it in place.

G. Glacial Features

J. S. Erskine, in his paper on St. Paul Island states,

"The boulders on the island seem all to be detached from the local rock and never to be erratics or to show signs of ice-action. There are no moraines, no scoured or scratched faces of rock."

He further states that,

"There is no positive evidence that it was glaciated at all."

Neale, in his descriptive notes accompanying preliminary map 55-23 states,

"A thin veneer of glacial till covers parts of the Cape Breton Highlands, and stratified drift, up to 40 feet thick, covers parts of the St. Lawrence Bay lowland. These are the only evidences of Pleistocene glaciation noted within the map-area."

In spite of these comments many glacial features are present on St. Pauls. Striae are abundant on the Northwest Head and on the rocks immediately south of the Tittle. Other striae were found on the neck between Martin Powers Coves. Strikes of the striae vary between $N55^{\circ}W$ and $N 85^{\circ}W$. In the vicinity of the Tittle there are several semi-ellipsoidal mounds which resemble whales' backs. These "whale-backs" are generally from 3 to 4 feet wide and from 10 to 15 feet long; and the long axes are always oriented towards the east. A few of these are cut off sharply on their eastern ends, thus appearing as roche moutonnee. Glacial grooves and gouges are found on most of these structures. Near the southwest lighthouse there is a highly polished rock surface that is probably the result of glacial action.

In several places along the road on the east side of Groggan Mountain the slope is littered with large unsorted boulders. A stream bed in this same area exposes more of these large unsorted boulders. In all of the places where these boulders are uncovered it can be seen that the vegetation is growing on top of the boulders. Perhaps all of the slopes on the eastern side of the island are strewn with boulders

which are hidden by the vegetation. All of the boulders consist of the gneissic rocks that are predominant on the west side of the island. No obvious erratics were noted, except for three small boulders of granite gneiss found approximately 600 feet north of Moon Point. All of the underlying rock is amphibolite. It is logical to assume that these rocks were transported from the western part of the island by a glacier.

The evidence mentioned above indicates conclusively that the island was glaciated and that the ice moved from west to east. The overall shape of the island with its rather gentle western slopes and its steep eastern slopes strewn with boulders of the western rock type coincides with the conclusions drawn from observation of the minor features. The absence of erratic rock types on St. Paul Island is accounted for by the fact that any glacier coming from the west would travel over 250 miles of water which is presently several hundred feet deep.

H. Stratigraphy and Petrography

St. Paul Island

The only previous geologic work on St. Paul Island was done by a field party of the Geological Survey of Canada in 1954. A preliminary map with marginal notes was later published (Neale, 1956). Names were not assigned to the rock units which consist of schist, gneiss, amphibolite, and

pegmatite. Owing to the fact that the coastline forms one continuous outcrop with not one break in the exposure, the geology is relatively easy to study. From Martin Powers Coves to the north, outcrops are scattered about the inland area, whereas to the south, vegetation and bogs cover the entire land area.

All of the island's rock units are metamorphic and will be discussed in the order of their geographic occurrence from west to east. Most of the work was concentrated on the schists of the northeastern section of the island. Consequently, the descriptions are more complete for these rocks than for those of the western section.

The western $2/3$ of St. Paul Island is mapped as one unit, gneiss, schist, and pegmatite. In general the proportion of schist increases to the east; and that of pegmatite to the west. However, the predominant rock type is gneiss. The interbedded schists and gneisses have strikes from N to $N20^{\circ}W$ and dips from $75^{\circ}W$ to $80^{\circ}E$. Although some of the pegmatites are parallel to the gneisses and schists, most of them cut across the structure as dikes.

The gneisses vary in color from pink to dark gray depending upon the amount of biotite present. Quartz and feldspar are always present as major constituents, biotite is present in widely varying amounts, and muscovite is common as a minor constituent. Grain size in the gneisses varies from less than a millimeter to several millimeters.

In the only thin section made of the gneiss the feldspar is microcline, biotite occurs only in a few layers, muscovite and biotite are well oriented, quartz is crushed and shows undulatory extinction, and apatite is present as an accessory.

Schists interlayered with the gneiss vary in thickness from one foot to tens of feet. Muscovite, quartz, biotite, and usually garnet are present as major constituents. The garnets often occur as clusters. A thin section from one of the large schist horizons at Lookout Point shows kyanite and staurolite in addition to muscovite, quartz, biotite and garnet. Mixed with the quartz are grains of oligoclase, but the absence of twinning makes it difficult to estimate the amount. Ilmenite, magnetite, apatite, tourmaline, and rutile, as an alteration of ilmenite, are present as accessories. Staurolite is found no further west than Lookout Point, but kyanite is found at several locations around the Southwest Head and further to the west. A rather spectacular development of kyanite was discovered at Petrie Point where a schist contains one narrow band consisting of nearly 50% kyanite as bladed crystals one inch long. A thin section of one of the more usual kyanite schists in this locality shows the assemblage to be quartz, muscovite, biotite, garnet, kyanite, and a few grains of oligoclase. Magnetite, ilmenite, and apatite occur as accessories.

A few beds of amphibolite occur among the schists and gneisses. Most of these are approximately one to two feet thick; but one bed several feet thick appears near the point north of Goat Rock. A thin section from one of the thinner beds contains hornblende, biotite, pligoclase, clinozoisite, sphene around rutile centers, and apatite. The large amphibolite bed is highly altered. Thin sections show amphibole considerably altered to chlorite, large flakes of chlorite which were originally biotite, altered feldspar, white micas with numerous parallel streaks, and much iron staining. Some of the chlorites display the same type of parallel streaking as the white micas. A less altered sample from the same amphibolite contains biotite in all stages of alteration to chlorite.

Most of the pegmatites are pink and contain quartz and feldspar in grains up to two centimeters across. Smaller muscovite grains are often present. The width of the pegmatite dikes varies from an inch to tens of feet. Certain of the dikes have internal banding of quartz and feldspar. Some small dikes contain quartz centers with feldspar borders, but others contain feldspar centers with quartz borders. A more striking pegmatite crops out on the point to the west, and south, of Martin Powers Cove. This intrusion occurs as a large mass rather than a tabular dike like the other pegmatites. Crystals of orthoclase and books of muscovite, both several inches across, make up the majority of the pegmatite.

Smaller quartz grains of irregular outline are also present.

The northeastern portion of the island was mapped in more detail and has been divided into the following units whose areal distribution are shown on the accompanying map.

	Rock Type	Thick-ness	Mapped Unit
west	Interbedded schist and quartzite	525'	525'
	Amphibolite	880'	930'
	Interbedded amphibolite and quartzite	50'	
	Interbedded schist and quartzite	240'	510'
	Interbedded schist and amphibolite	270'	
	Epidote-rich amphibolite	275'	275'
east	Staurolite schist	900+'	900'

The vertical thicknesses of these units are based on steel tape measurements and vertical dips. The measured dips vary between 75°W and vertical, and would probably average nearly vertical. Thus the figures are probably within a few feet of the actual thickness.

The westernmost of these units is separated from the gneiss unit by a sheared zone. The gneiss is badly brecciated but resutured; appearing as a metamorphosed conglomerate. On the schist side of the zone there is a drag fold whose axis plunges 45° at N20°E. The movement indicated is left-handed.

Quartzites and schists in which the bedding and foliation are parallel are the predominant rock types in the 525 foot unit. The schists contain quartz, muscovite, biotite, garnet, and staurolite as major constituents, oligoclase as a minor constituent, and magnetite, ilmenite, apatite, and tourmaline as accessories. The grain size and ratio of the minerals varies considerably. On a cliff face in Martin Powers West Cove large garnets, $7\frac{1}{2}$ inches in diameter, form prominent bumps on the weathering schist. Two or three inch quartzite lenses are not infrequent in the schist. Interbedded with the schists are many quartzite beds from a few inches to four feet thick. Most of these are light pink and contain pink garnets a millimeter or less in diameter. Several of the quartzite beds show boudinage structure. To the east, schist becomes more predominant; but the last bed of quartzite is much larger than any of the quartzite beds to the west. It measures 24 feet thick. A few beds of amphibolite from two to three feet in thickness are scattered throughout this unit. These contain hornblende, oligoclase, and biotite as major constituents, and magnetite, ilmenite altering to sphene, and apatite as accessories.

Between the above map unit and the amphibolite unit there is another sheared zone which strikes approximately north. Many small drag folds are in the schist. The amphibolite strikes North and dips between 75° W and vertical. The beds vary in thickness from thin lamellae to several

feet, and in color from very light green, almost white, to ¹¹⁷ dark green. Thin sections were made of the various types of amphibolite. Some of the light colored bands can hardly be called amphibolite. They consist of oligoclase, calcite, and sphene. However, most of the sections contain differing proportions of hornblende, oligoclase, clinozoisite, and sphene. Stringers of calcite and chlorite are numerous, and the accessory mineral, apatite, is always present. Most of the opaques, presumably ilmenite, have been altered completely to sphene. A few grains of quartz appear in small clusters in a few sections, and biotite occurs in layers in some sections.

Within the amphibolite are zones of quartzitic material. One such zone is 38 feet thick and consists of thin bands, from $\frac{1}{2}$ to 1 inch thick. Another of these zones of finely banded quartzitic material measures 16 feet thick. The color of the bands varies between light grey and light pink. Sparse grains of oriented biotite occur in some bands. The quartzite horizons become more numerous to the east. The last 50 feet before the sea cave at Sea Cave Cove consists of several alternations between quartzite and amphibolite, and ends with an 11-foot zone of light pink and gray bands each approximately one inch thick. This entire map unit contains many pink granitic dikes varying in thickness from a few millimeters to 10 feet. Several of the smallest of these dikes are ptygmatically folded into rather fantastic shapes. A few 4 to 6 inch

calcite layers, recrystallized to marble have been stretched into discontinuous lenses.

Between the last quartzite of the amphibolite unit and the schist to the east there is another north-striking sheared zone expressed as a sea cave. The schist in, and next to, the sheared zone shows replacement of garnets by chlorite and considerable development of pyrite. Textures of the schists in this unit vary from schistose, or flaky, to granular. This variation is caused by differences in the ratio of quartz to mica, which, in turn, would be caused by differences in the original content of SiO_2 , K_2O , and Al_2O_3 . Thin sections of the schists show the usual mineral assemblage to the quartz, muscovite, biotite, staurolite, and garnet as major constituents, oligoclase as a minor constituent, and magnetite, ilmenite, apatite, and tourmaline as accessories. The amount of each major constituent varies considerably from section to section. In some cases there is almost no staurolite, while in others there is abundant staurolite. The same holds true for garnet and muscovite. Interbedded with the schists are zones of quartzitic material which is similar to that described with the amphibolites. These zones range from 10 to 30 feet in thickness and consist of one-inch bands of light pink to light gray, fine-grained quartzite. Four thin beds of amphibolite also occur in this 240 foot zone. A thin section of the amphibolite shows no feldspar but more quartz than usual. Hornblende, clinozoisite, sphene, and

accessory pyrite and apatite complete the assemblage.

In this section pyrite is unusually abundant.

For the next 270 feet to the east schists are interbedded with amphibolites. Most of the beds range from one to five feet thick but a few beds of schist attain thicknesses from 20 to 30 feet, and one amphibolite attains a thickness of 21 feet. The proportion of amphibolite beds in this unit increases towards the east. The schists of this zone fit the same description as those given in the previous paragraph. In some beds garnets two centimeters in diameter are found. One interesting sequence of graded beds, each from five to six inches thick, extends for 33 feet. Each of these shows quartzite grading into schist, or vice versa. Sharp contacts between quartzite and schist are practically non-existent. Assuming that a sharp contact between a schist and a quartzite would indicate the bottom of the quartzite there are a few indications that the top of the section lies to the west; but the evidence is far from conclusive. A thin section of the amphibolite shows only a trace of feldspar but much more quartz than usual. Hornblende and sphene are again present but no clinozoisite. Several pink to red pegmatite dikes are present in the unit. In one of the dikes a block of schist was found that had been rotated so that the foliation is oriented in a different direction to that of the surrounding schist.

East of the above-described unit is a 275-foot

section composed almost completely of amphibolite. Lenses and layers of an epidote-rich variety make a rather interesting pattern throughout the unit. Several of these epidote-rich layers show boudinage structure. Massive chlorite and crystals of epidote fill the spaces between the boudins. Although several faults displace the amphibolite beds, epidote layers can be used satisfactorily as marker horizons. Throughout the unit the bedding strikes N10°E and dips from 75°W to vertical. Near the eastern edge of the amphibolite is a zone of schist 13 feet thick. Beyond this is another 10 feet of amphibolite, followed by the next schist unit.

The easternmost map unit on the island is a coarse-grained schist with prominent staurolite crystals, some of which are several centimeters long. Most of the staurolite is not twinned. Within the first 100 feet of this schist there are four more amphibolite beds, each approximately one foot thick. These are the only amphibolite beds found in this unit. There are all gradations between mica-rich schists and schistose quartzite. Many of the coarse-grained schists contain quartz in lenses up to 2 inches across and 6 inches long, or in narrow crenulated stringers 2 millimeters thick. Several thin sections of this schist show quartz, muscovite, biotite, staurolite, and garnet as major constituents, oligoclase as a minor constituent, and magnetite, ilmenite, apatite, and tourmaline as accessories. Several zones of

retrograde reactions were noted and thin sections were made of several of the retrograde assemblages. In some cases staurolite has been completely replaced by clots of sericite. One section showed a center of sericite surrounded by fairly coarse white mica. The mica in these replacement reactions is randomly oriented in contrast to the well-oriented mica of the schist. An interesting feature which occurred in several partially replaced staurolites was the appearance of zoning around the remnants of the original grain. The zone next to the staurolite is sericite, the next outer zone is opaques, and the outermost zone is chlorite. Garnets appear in all stages of replacement by chlorite. Some garnets are almost completely replaced, others have only outer rims of chlorite, and others are riddled with tiny chlorite veinlets which fill fractures.

Rather than describe the features of each thin section it is more convenient to describe, in general, some of the details which are consistently common. All quartz grains are highly fractured and show undulatory extinction. Quartz grains in many of the schists contain liquid inclusions. The tiny liquid-filled planar cavities are randomly oriented. In some of the larger cavities, approximately 5 microns in diameter, a minute bubble can be seen floating on the liquid. All micas show good orientation except in replacement textures. Biotite is pleochroic in shades from orange-brown through brownish green to green, and pleochroic haloes are

common. All staurolite shows sieve texture, with quartz and platelets of ilmenite as inclusions. In some staurolite grains the inclusions form in concentric zones parallel to the crystal outline. The staurolite is always pleochroic in light orange. Garnets always show quartz inclusions, often in the familiar snowball pattern. In the schists ilmenite always occurs as platelets; but in the amphibolites it occurs only as centers of sphene grains. Magnetite is always in the form of irregularly shaped grains. Euhedral tourmaline in the schists is pleochroic in blue-gray or green-gray. The feldspars are always altered along cleavage planes.

Plagioclase compositions in the schists were identified by index of refraction measurements in oil mounts; and in the amphibolites by extinction angles of combined albite-carlsbad twins or by comparison of their index with the thin section cement. Clinozoisite was identified on the basis of abnormal blue and yellow interference colors and inclined extinction. The hornblende has pleochroism of X=light greenish-yellow, Y=light brownish-green, and Z=bluish-green where $X < Y < Z$. The extinction angle is $Z \wedge c$ $15-20^\circ$, $2V \approx 90^\circ$, and the interference colors are second order. Sphene always occurs as a replacement of rutile or ilmenite.

In order to make certain that the white mica was muscovite, and not paragonite, all of the white micas were scanned on the X-ray diffractometer over the first three

basal reflections. In all cases only the single peak of muscovite was present.

Money Point

Previous geologic work at Money Point is limited to a reconnaissance report in 1875 (Fletcher, 1875-76), a preliminary map with marginal notes, and some exploration activities by McPhar Geophysics. In general the rocks consist of low to medium grade metamorphics which were originally sediments and volcanics. It is interesting to note that these rocks strike towards St. Paul Island, 15 miles to the northeast.

The accompanying geologic map of the Money Point area was traced from aerial photos and is probably not entirely to scale because of the distortion in the photos. Geology was mapped by the compass and pace method. Traverses were made along the coast, up the stream west of the Money Point lighthouse, and down the stream to the south of the road to the radio relay station.

The coastal traverse started in the pink granite of the southern part of the map. In thin section the granite consists of quartz, perthite, and orthoclase as major constituents, and biotite partly altered to chlorite, apatite, and relatively few opaques as minor and accessory minerals. The quartz is crushed and shows undulatory extinction, orthoclase occurs in many cases as carlsbad twins, and all of the feldspars are considerably altered, except for a thin rim

around each grain.

The granite has an intrusive relation with the interbedded volcanics and sediments to the north. The latter rocks appear as dirty quartzites, phyllites, and volcanics with phenocrysts. Strikes of the beds vary between N25°E and N42°E while the dips remain nearly constant at 80°W. Lenses, cross bedding, and penecontemporaneous deformation features are preserved in a few of the quartzite and phyllite beds. One set of reasonably good cross laminations indicates top to the east. A calcareous bed among the quartzites is squeezed out into lenses. Some of the darker layers in the sequence contain thin epidote-rich lamellae which have boudinage structure. Quartz stringers occur in many orientations throughout most of the sequence. Thin sections of the various rock types were examined. The porphyritic type shows subhedral phenocrysts of orthoclase and albite in a matrix of quartz and feldspar. The matrix is not as fine grained as that of most porphyries. Except for thin clear rims the feldspars are highly altered. Tiny grains of biotite in oriented layers give an augen-like appearance to the phenocrysts. In another thin section small porphyroblasts of biotite and hornblende ($Z \wedge c, 20^\circ$) have formed in a matrix of fine-grained quartz, feldspar, muscovite, and biotite. The biotite of the matrix is concentrated in parallel planes. There are practically no opaques in the slide. A small zone of calcite; and thin zircon-rich lamellae are also observed.

A third section contains fine-grained biotite, muscovite, and quartz surrounding porphyroblasts of quartz-filled biotite. Several altered feldspars are also present. The rock might be named spotted phyllite.

A fault separates the above-described sequence from dark gray to black volcanics to the north. In some of the volcanic layers columnar jointing is present. Much epidote and a small amount of calcite occur as stringers, boudinaged lenses, and small pockets. There are several zones of finely banded pink and gray quartzitic material. The entire sequence strikes approximately $N30^{\circ}E$ and dips $80^{\circ}W$. A thin section shows hornblende as both small needle-like crystals which can be resolved only with a high power objective, and small fibrous bundles. The extinction angle and habit identify these as hornblende. Plagioclase, possibly oligoclase, epidote, and a few quartz grains make up about 15% of the section. Numerous opaque masses complete the assemblage. In summary this rock appears to be an intermediate to basic volcanic which has been metamorphosed just enough to cause the formation of hornblende.

To the northwest of the volcanics and in conformable contact with them is a sequence of quartzites and phyllites in which bedding and foliation are parallel at $N40^{\circ}E$, vertical. Several right-handed drag folds strike in the same direction as the foliation. An east-striking basaltic dike occurs at the base of the road from the top of the highland.

A thin section of one of the phyllites is composed predominantly of muscovite and quartz. A few grains of biotite, a stringer of calcite, and minor opaques complete the section. The mica flakes show only fair orientation.

The next unit to the northwest is a conformable sequence of andesites and rhyolites in the form of flows and tuffs. Colors of these beds vary from dark gray to greenish gray and from light pink to pinkish orange. Much fracturing and minor faulting are present throughout the sequence. A drag fold too tight for the competency of the beds causes the formation of folded layers of breccia. On the basis of the intrusion of a flow of andesite into the rhyolite below it the top of this sequence is to the east. Conformably to the northwest is a section of rock containing amphibole from one to two inches long in a coarse white feldspar matrix. The amphibole becomes continually coarser to the northwest. All of these beds strike between N 20 and 30°E and dip 80°W.

About 200 feet southwest of the Money Point lighthouse phyllite beds again form the section. In these beds are found the first garnet ~~to be found~~ along the coast. A thin section shows the rock to consist of garnet and biotite porphyroblasts in a fine-grained matrix of chlorite, muscovite, and quartz. Apatite, magnetite, and platelets of ilmenite complete the assemblage. The biotite porphyroblasts contain abundant inclusions of quartz. A thin section from a bed approximately 100 feet northwest of the lighthouse

contains plagioclase phenocrysts in a fine-grained matrix of feldspar and a small amount of quartz. Other minerals include hornblende, garnet, chlorite, epidote, tiny biotite flakes, and magnetite. This seems to indicate that a few volcanic horizons occur in this part of the section.

On the point in front of the lighthouse a complex system of folding and faulting is present. Within this area a few light green phyllitic beds contain elongate inclusions which may be either stretched pebbles or stretched feldspar phenocrysts. The stretched material is white and crumbly, and can be scraped out with a knife. The largest of these features are approximately 4 millimeters in diameter and 5 centimeters long. They are all oriented in the same direction with a plunge of 5° in a direction $N 35^{\circ}E$ which is the same strike as the foliation.

Many outcrops are present in the bed of the stream which empties into the ocean to the west of the lighthouse. The exposures become scarce a few thousand feet upstream but outcrops can be found up to a mile or more. Most of the outcrops are green to gray-green schists which have parallel bedding and foliation striking $N 20-30^{\circ}E$ and dipping about $80^{\circ}W$. Thin sections show that many of these rocks consist of small garnet and biotite porphyroblasts in a matte-like matrix of fine-grained muscovite, chlorite, and quartz. Magnetite and platelets of ilmenite are the opaques. Some of the thin sections have no biotite and only a small amount of chlorite

and muscovite. These more quartzitic zones are sometimes present as lamellae in the more schistose thin sections. In fact, slices made perpendicular to the bedding in most of these rocks show the schistose and quartzitic layers to be finely laminated, often only a few millimeters thick.

In the stream to the south of the road to the radio relay station there are no outcrops for nearly 4000 feet downstream. But beyond this there are almost continuous exposures of schist, amphibolite, and, after a sharp westerly bend in the stream, banded gneiss. Bedding and foliation are parallel at N 30-40°W and the dip varies from 45 to 70°E. This is a marked change from the west dip of the previously described sequences. The first outcrop downstream consists of schist with tiny garnets less than a millimeter across. However, the schists further downstream are considerably coarser-grained and contain macroscopic quartz, muscovite, biotite, garnet, and staurolite. Thin sections have apatite, tourmaline, oligoclase, magnetite, and platelets of ilmenite as minor or accessory minerals. Hand specimens contain thin layers of quartz (less than one inch thick) which pinch and swell along the foliation planes. Several of the beds in this sequence are more quartzitic than others. One thin section shows very little muscovite, and only a grain or two of garnet and staurolite. A thin section of a retrograde assemblage has biotite almost completely altered to chlorite, and staurolite with rims of sericitic material.

A few interbedded amphibolites were observed. A thin section of one of these contains well-oriented hornblende, quartz, and oligoclase as major constituents, and apatite, magnetite, and platelets of ilmenite as accessories. The amphibole has pleochroism: X = greenish-yellow, Y = green, Z = greenish-blue; and $Z \wedge c$, 20-25°. After the sharp turn to the west made by the stream the outcrop consists of banded gneiss whose bands are parallel to the bedding and foliation of the schist.

I. Structural Geology

St. Paul Island

On St. Paul Island the bedding and foliation are parallel, striking from N10°E to N20°E and dipping nearly vertical. On the geologic map the beds appear to strike slightly west of north, owing to numerous left-hand faults which strike perpendicular to the bedding. Several sheared zones 10 to 40 feet wide parallel the foliation. Drag folds and retrograde reactions are present in all of these zones. One of the zones forms a valley extending from Atlantic Cove to Martin Powers West Cove. Another forms the sea cave which was discussed in previous sections. Several of these zones occur at the contacts of schist with gneiss, amphibolite, or quartzite. The gneiss, quartzite, and amphibolite of these areas are highly fractured, whereas the schists are distorted into drag folds. At the contact between gneiss and schist in Atlantic Cove the gneiss has been fractured into a con-

glomeratic breccia consisting of rotated gneiss fragments. In the schist of this contact there is a drag fold whose axis plunges 40° in a direction $N20^\circ E$. A left-hand movement is indicated. A few other drag folds are found here, and at least one can be found at the outcropping of any sheared zone. Without exception the drag folds plunge from 30° to 40° in a direction which is slightly east of north. Nearly all of the drag folds indicate a left-hand movement.

The major fault on the island is the east striking one shown on the map at Martin Powers Coves. This is actually a fault zone in which three or four faults have a total strike slip of nearly 700 feet. On the west this fault zone intersects the sheared zone which extends northward from Atlantic Cove. The island has many east striking faults with dips between $60^\circ S$ and vertical. Within one 200 foot interval a series of ten left-hand faults with 1-20 foot displacements were found. The Tittle is another of these east striking faults. The dragging of beds south of the Tittle from $N5^\circ E$ to $N20^\circ W$ indicates a left-hand movement. A few of these east striking faults are right-handed but a large majority are left-handed. Two other directions of faulting were found. One consists of right-hand faults striking from $N 20$ to $25^\circ E$ and dipping vertically. The other consists of left-hand faults striking from $N 40$ to $45^\circ W$ and dipping from 60 to $70^\circ S$. Most of these faults have strike slips between one and 10 feet. Joints were found in all of the rocks but no study of them was made.

The pegmatite dikes do not appear to have caused any textural or mineralogical changes in the rocks which they intruded. This is not at all surprising. There is evidence that the pegmatites intruded late in the metamorphic history of the area. At such a time the mineral assemblages in the amphibolites and schists would be stable in the range of temperature associated with a pegmatite intrusion. Therefore, no reaction could take place. Two independent bits of evidence indicate that the pegmatites intruded late in the metamorphism. At one place the pegmatite intrusion pushes the foliation into a different orientation (Figure 5). In another case there is an inclusion of schist in the pegmatite. The orientation of the foliation in the inclusion is quite different from that of the surrounding schist. Another occurrence as shown in Figure 6 indicates that the pegmatite intruded after the formation of the east striking faults. Another interesting feature in a few of the three or four inch wide pegmatites is the occurrence of coarse-grained borders around fine-grained cores.

Ptygmatically folded veins of quartz or quartz-feldspar are very common in the schists and amphibolites. Near pegmatite intrusions these features seem to be especially plentiful. The largest of these veins are approximately four inches wide. It was noticed in many cases that the orientation of the folds in these veins is parallel to the schistosity (see Figure 7). In one instance the vein was fractured and

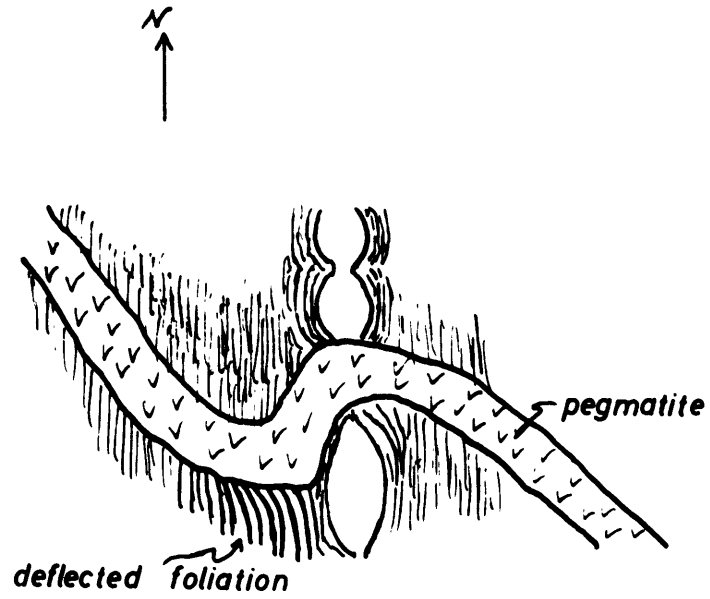


Figure 5. Deflection of foliation by pegmatite intrusion. scale xl/12

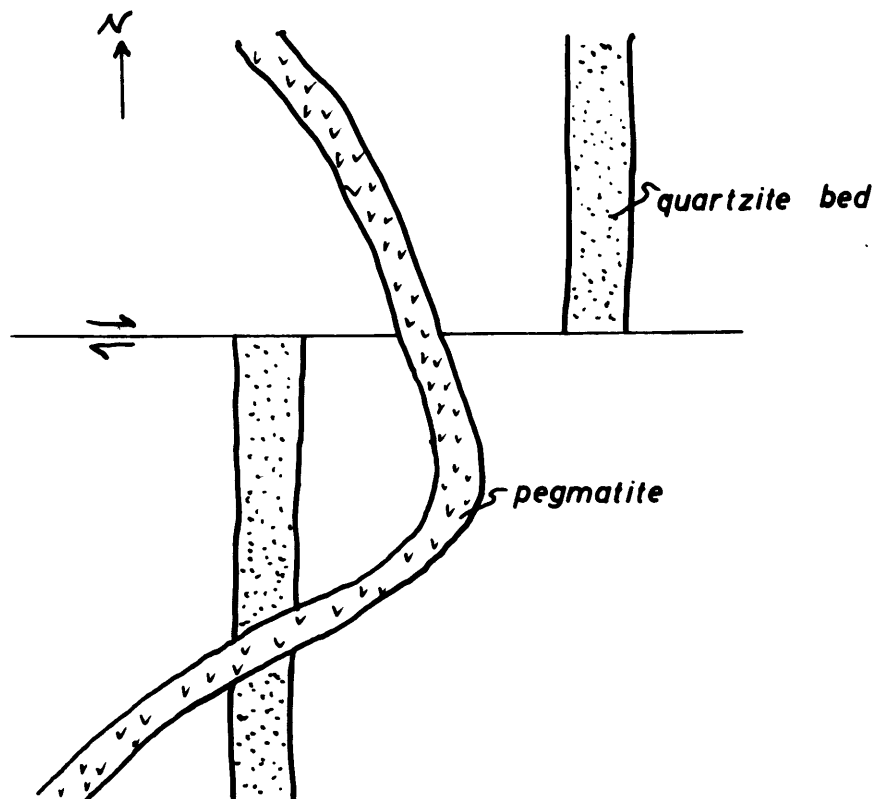


Figure 6. Relative age relationship of pegmatite intrusion and faulting. scale: xl/5

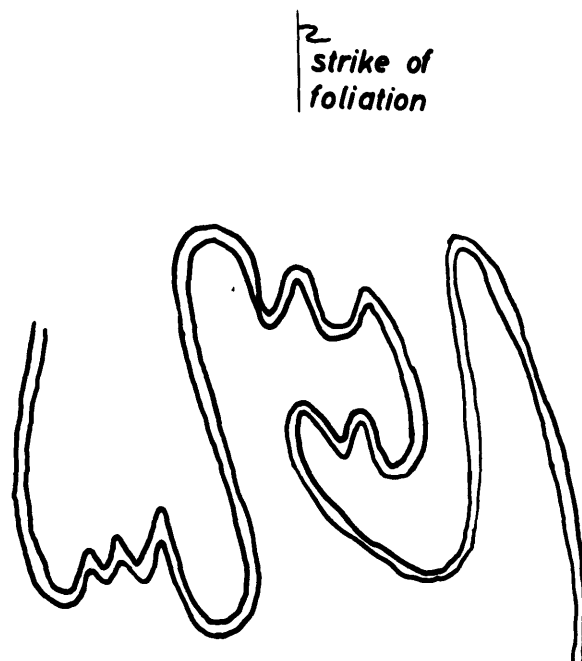


Figure 7. Plan view of ptygmatic folding. Axial planes of folds are parallel to foliation. scale: $\times 1/10$

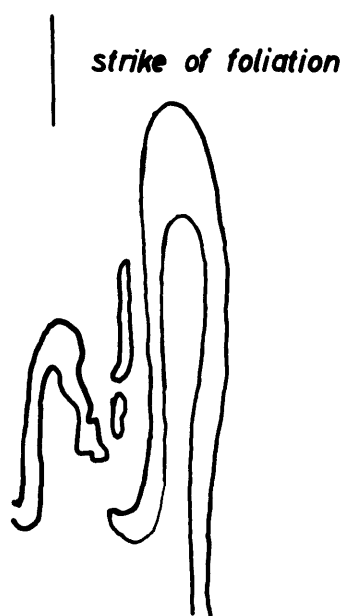


Figure 8. Plan view of faulted ptygmatic fold. Axial planes of folds and displacement of fault are parallel to foliation. scale: $\times 1/8$

displaced along the foliation (see Figure 8). From this evidence it would appear that many of the ptygmatically folded veins are a result of plastic flow caused by a shearing couple along the foliation plane.

Boudinaged beds of quartzite and epidote-rich amphibolite are common in the schist and amphibolite, respectively. Some of the quartzite boudins are two or three feet long and one foot wide. Between the boudins pockets of recrystallized quartz and chlorite, epidote and chlorite, or quartz and epidote occur. Perhaps the most unusual boudinage structure was found at Money Point, where an epidote-rich layer was boudinaged in a less epidote-rich layer which was also boudinaged. The surrounding rock is schist (see Figure 9).

Crenulations on the foliation planes were noted in many of the schists. The intersection of the crenulations and the foliation plane plunges 50° in a direction S 5° W (see Figure 10). Stretched layers of marble occur in many of the amphibolites. Near the southwest lighthouse a section of quartzites, or possibly salic volcanics, is highly contorted into very tight folds. These contortions have produced no fracturing. At no other location on the island were quartzitic beds distorted to this extent without fracturing.

Money Point

At Money Point the relief and scarcity of inland outcrops make the structural relationships less certain than on

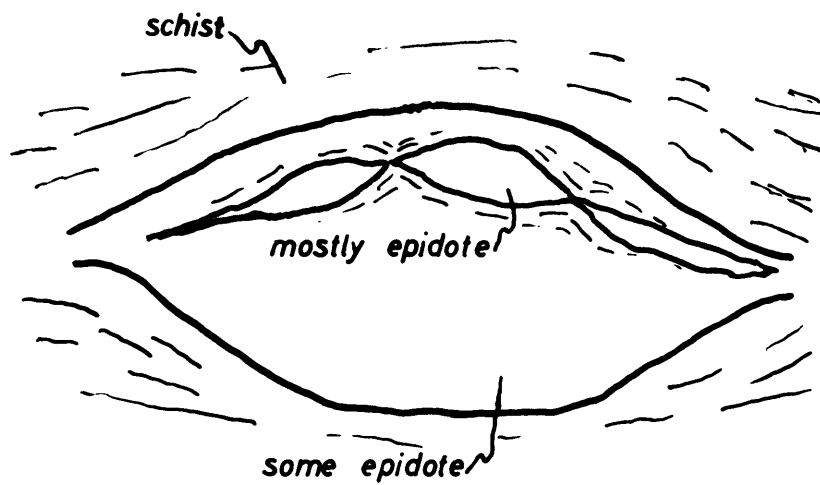


Figure 9. Boudinaged epidote layer within a boudin. scale: x1/3

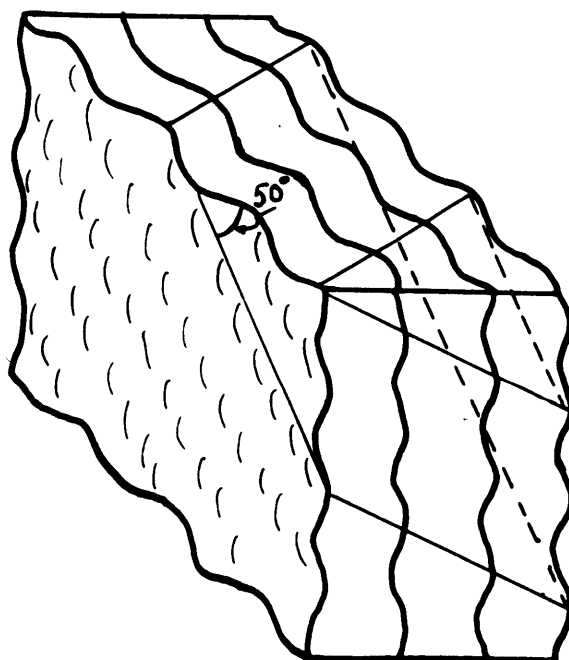


Figure 10. Crenulation on the foliation. Intersection of axial planes of crenulation and foliation plunges 50° . scale: x10

St. Paul Island. The change in dip from west to east between the stream north of the road and the stream south of the road is probably a result of folding. The bedding in the stream to the north has an average strike of $N24^{\circ}E$ and dips between 70 and $80^{\circ}W$. A close examination of the foliation shows it to dip a few degrees steeper, and essentially vertical. The outcrops in the stream to the south again show the foliation to dip a few degrees steeper than the bedding, but all of these dips are to the east. These features seem to indicate a north plunging syncline. A tight fold at the Money Point Lighthouse can easily be interpreted as a relatively large drag fold on the limb of a larger fold. If this is the case the couple associated with the drag fold indicates the eastern limb of a syncline. This would agree with the synclinal structure mentioned above.

Two directions of faulting were common throughout the Money Point area: a left-hand set at $N35^{\circ}E$, $80^{\circ}E$ and a right-hand set at $N65^{\circ}W$, vertical. The displacements on most of these are on the order of a few feet; but one of the left-hand faults on the east coast has a strike slip of a few hundred feet. Several small drag folds in the plane of foliation occur along the east coast. All of the drag folds plunge gently to the northeast; and most of them indicate right-hand couples. In one of the salic volcanic sequences a drag fold is too tight for the competency of the beds, and a series of breccia beds has formed.

J. Summary

Many of the facts associated with the geology of St. Paul Island and Money Point indicate a similar geologic history for both areas. The lithology of both areas indicates an original sequence of interbedded volcanics and sediments. The strikes of the bedding and foliation coincide within a few degrees. The metamorphic grade increases from east to west at both locations. On Money Point the change is from phyllites to staurolite schists; on St. Pauls from staurolite to kyanite schists. The approximate location of the kyanite isograd is shown on the geologic map of St. Paul Island.

Over the entire highland area of northern Cape Breton patches of schist and amphibolite are numerous in a "sea" of gneiss and granite. (MacLaren, 1956a,b; Neale, 1955, 1956a, b,c) It is possible that this entire area including much of the Cabot Strait was once covered with interbedded volcanics and sediments. In fact, one might even go so far as to suggest a geosyncline extending from Cape Breton through western Newfoundland where similar metamorphic rocks are found in the Long Range.

A potassium-argon age determination was made on one of the biotites from a staurolite schist which outcrops on the Northeast Head of St. Paul Island. The A/K ratio is 0.023 which corresponds with an age of 360 million years if the constants $\lambda_e = 0.585 \times 10^{-10}$ and $\lambda = 5.3 \times 10^{-10}$ are used. The

air correction in the argon run was less than 1%. From previous age work on Nova Scotian granites which intrude lower Devonian sediments the age of 360 million years is known to represent a significant event in the geologic history of the region. (Fairbairn et al, in press). The crystallization of the micas in the granites took place at approximately the same time as the recrystallization of the biotite from St. Pauls. It seems safe, then, to assume that the metamorphism which formed the schists of Cape Breton and St. Paul Island accompanied the intrusion of granite on the mainland of Nova Scotia. This event is often referred to as the Acadian Revolution.

The geologic history, in brief, would start with an extensive area of interbedded volcanics and sediments of early paleozoic or pre-cambrian age. The sediments and volcanics were metamorphosed to phyllites, schists, and amphibolites during the Acadian orogeny which seems to have taken place approximately 360 million years ago. During the late stages of metamorphism faulting and pegmatite intrusions took place. The only other traces of geologic history are those of glaciation. Ice movement during glaciation was towards the east.

III SAMPLING AND MINERAL SEPARATION

A. Theory

Two objectives were kept in mind during the sampling. First, samples of the various rock types were to be taken for thin section analysis; and second, samples of schist were to be taken for phase equilibrium studies. Although the former objective presents no particular difficulties, the latter requires specific types of samples. Of basic importance to any phase equilibrium study is a knowledge of phase diagrams which have their theoretical foundation in the science of thermodynamics. For the geologist who is interested in phase studies one of the simplest and most useful concepts from thermodynamics is that of the phase rule, first formulated by Gibbs (Gibbs, 1928). A brief review of the phase rule and its use in sampling is contained in the next few paragraphs.

Derivation of the phase rule is included in nearly every thermodynamics text (see Gibbs, 1928; Guggenheim, 1950). Mathematically it may be stated as follows:

$$f = c + 2 - \phi$$

where: f represents the degrees of freedom, that is, the number of intensive variables which may be varied without changing the mineral assemblage,

c is the number of components,

and ϕ is the number of phases.

For the first part of the following discussion let us assume that the system is closed, that is, there are no

mobile components. From the above equation it is apparent that the ideal sample would be one containing $c+2$ phases, thus reducing the degrees of freedom to 0. Such a mineral assemblage would be represented as an invariant point on a plot of temperature vs. pressure; and could exist, therefore, at only one condition of temperature and pressure. Because of the limitation produced by only one combination of temperature and pressure such an assemblage, although not unknown (Hietanen, 1956), would be extremely rare in nature.

If there are $c+1$ phases, the degree of freedom is one. In other words, for the assemblage to remain unchanged the temperature would have to vary as a function of pressure. On a plot of temperature vs. pressure this would be represented by a reaction curve. Again, because of the restricted conditions of temperature and pressure, such an occurrence would be rare.

The most likely assemblage would be that with c phases, or two degrees of freedom. Both temperature and pressure can vary randomly without changing the assemblage. In any closed system this would be the minimum number, and the most likely number, of phases to occur.

For an open system the formulation of the phase rule remains unchanged, but there are now more intensive variables in the system. Not only temperature and pressure but also the chemical potential of each mobile component may vary. In order to represent graphically a system with one mobile

component the three dimensions of temperature, pressure, and the chemical potential of the mobile component must be combined. In this three dimensional diagram $c+2$ phases would be represented by a point, $c+1$ phases by a line, c phases by a plane, and $c-1$ phases by a volume. The least likely of these assemblages would be the $c+2$ which can occur at only one combination of temperature, pressure, and chemical potential. The most likely of these assemblages would be the $c-1$ in which the temperature, pressure, and chemical potential can vary independently without changing the assemblage. If additional mobile components are present, additional intensive variables must be considered. Graphical representation becomes possible only by means of projections; and the mathematics becomes that of multi-dimensional vector space. However, the phase rule remains the same.

From the preceding discussion it is apparent that the more phases in a rock of a given number of components, the more one can deduce about the conditions of its formation.

In order to sample the field occurrences adequately one must first define the components which make up the system to be studied. Then one must find field occurrences which contain grains coarse enough to identify in hand specimens. By comparing the number and composition of the phases with the system to be studied one may then decide either to discard or collect the specimen.

For the problem under study--high grade metamorphism of pelitic sediments--the system was defined by SiO_2 , Al_2O_3 , K_2O , MgO , FeO , and H_2O . It was realized that other components such as Na_2O , MnO , and CaO would be present; but it was hoped that these would make up only a minor part of the total composition. If these components are present in only small quantities the phase relations will be little changed. In the six component system defined above it is reasonable to assume that H_2O might well be a mobile component. Therefore, a rock with five (c-1), or more, phases containing these components would be a suitable sample. For example, a typical staurolite zone specimen composed of quartz, muscovite, garnet, biotite, and staurolite would contain SiO_2 , K_2O , Al_2O_3 , FeO , MgO , and H_2O (assuming the garnet to be a member of the almandine-pyrope series). Such a specimen would be adequate. More desirable would be a specimen from the kyanite isograd, composed of quartz, muscovite, biotite, garnet, staurolite, and kyanite. This has the same components but an extra phase has been added. A specimen containing only quartz, muscovite, biotite, and garnet would be discarded.

For the phase rule to be validly applied equilibrium must have been maintained. Therefore, evidence of retrograde or replacement reactions should be carefully watched for and specimens of this nature should be avoided. However, a sample for descriptive thin section information might be well worth while. Weathered specimens should also be avoided. Leaching

of certain elements during weathering might produce erratic mineral compositions which would result in misleading phase diagrams. On St. Pauls it was found that the rocks which had been continually battered by waves and ice produced fresh surfaces. In other locations the schists were weathered to a soft crumbly mass, often to a depth of several inches.

As far as possible correct identification must be made in the field. This is insufficient if a garnet contains a large amount of MnO or CaO, or if a biotite contains 5% TiO₂. These are problems which have their final solution only in the laboratory. By collecting several samples which, at least, appear suitable there is a good chance that a few will meet the requirements. Another problem which cannot always be avoided in the field is the collection of specimens which have undergone retrograde or replacement reactions. In many samples these features are obvious only under a microscope. Again it can only be recommended that a large number of samples be taken in the hope that a few will meet the requirements.

B. Choice of Final Samples

From 45 specimens which appeared unaltered and homogeneous, after slicing, thin sections were prepared for a final check on the suitability of the samples. Examination of the thin sections further limited the number of samples to 24.

Nearly all of the thin sections showed small amounts of chlorite and sericite replacing various minerals. On all but one slide biotite showed some degree of alteration to chlorite. Tiny veinlets of chlorite fill the fractures which occur in many garnets. Several slides show thin rims of chlorite around garnets which have undergone some retrogression. Zoned alteration rims occur around several staurolite grains. Next to the staurolite is a zone of sericite, outside the sericite is a zone of opaques, and outside the opaques is a zone of chlorite. In the fracture fillings in staurolite grains a core of chlorite plus opaques is surrounded by sericite. The small amount of oligoclase which is present in all of the slides showed cloudy alteration along its cleavage planes.

After the elimination of all but the slightly or not altered specimens the problem of inclusions was examined. Several staurolite grains contained thousands of tiny opaque grains only one or two microns in diameter. These grains are magnetic and are distinct from the larger ilmenite platelets which also form inclusions in the staurolite. It is assumed that these tiny grains are magnetite. All of the staurolite grains contain inclusions of quartz but these are usually larger than 50 microns and can be mechanically separated. All but a few of the garnet grains are literally filled with quartz inclusions. When a large percentage of these inclusions are smaller than 30 microns it becomes

extremely difficult to separate the quartz and garnet.

A final elimination was based upon the amount and size of the inclusions. After this elimination 24 samples remained for separation into constituent phases.

C. Separations

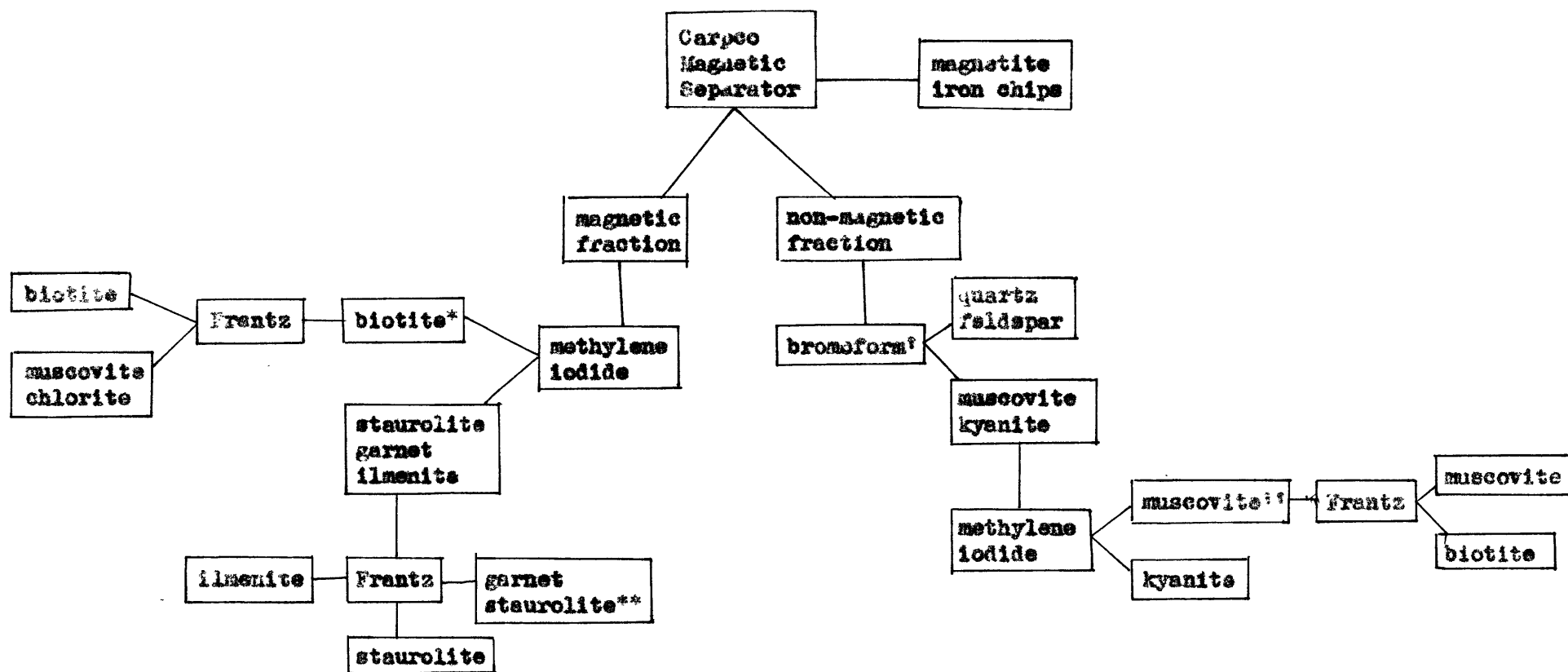
In order to separate the constituent minerals the hand specimens were first pulverized with a jaw crusher and disc grinder. The screened fractions -80, +100 and -100, +200 were then run through the procedure shown in the flow chart of Figure 11.

Because the staurolite fraction and the garnet with staurolite fraction show many inclusions further processing is necessary. The following steps were adequate for the liberation of and separation of most inclusions.

1. Grind in agate mortar
2. Screen, collecting -200 +325; -325 +400; and -400 fractions
3. Using liquid close to the index of refraction of the mineral being separated check each size fraction for liberation of inclusions.
4. If -400 fraction must be used place small portions of it in a 100ml beaker and with a wash bottle squirt acetone into the beaker until the sample is well-stirred. After five seconds decant the acetone. Continue this procedure until the acetone remains clear after five seconds. The remaining grains are coarse enough to pass through the Frantz.
5. Pass the coarsest fraction in which the inclusions are liberated through the Frantz. After several passes the samples are quite pure.

These procedures produce staurolite which is 98%+ pure. It is impossible to remove all of the quartz

Figure 11. Flow Chart for Mineral Separations



* small amounts of chlorite and muscovite may be present

**because of varying combinations of inclusions garnet cannot be obtained free of staurolite

† may require slight dilution

‡ a small amount of biotite may be present

inclusions from most garnets. There are always a few inclusions in the 5-10 micron size range. These make up a very small percentage of the total sample and can be neglected. All of the separated mineral samples were checked under the petrographic microscope in a liquid having an index of refraction close to that of the mineral. Grain counts were made and samples which were not at least 98% pure were rerun through appropriate steps of the separation procedure until the desired purity was attained. Because of very fine quartz inclusions in the garnets some of the garnets may contain more than 2% quartz.

IV CHEMICAL ANALYSES

A. Problems and Techniques

The analyses were made by instrumental, or so-called, "rapid silicate" techniques. In brief, the SiO_2 , TiO_2 , Al_2O_3 , total iron as Fe_2O_3 , and MnO are determined spectrophotometrically with the following indicators; molybdenum blue, tiron, alizarin red-S, orthophenanthroline, and permanganate, respectively. The CaO and MgO are titrated with versene using murexide and eriochrome black-T, respectively, as indicators. FeO is titrated with dichromate; and K_2O and Na_2O are determined with a Perkin-Elmer flame photometer using Li as an internal standard.

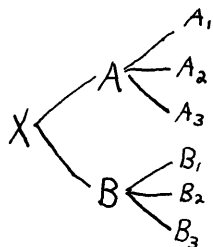
Although several of the procedures were modified, the outline of Shapiro and Brannock (1956) was used. The major departure from the original outline is in the CaO and MgO determinations. This change was adopted by Shapiro and Brannock in 1958 (personal communication). The change involves complexing the R_2O_3 group with a solution of triethanolamine and sodium cyanide before titrating with versene. This is considerably easier, and perhaps more accurate, than the previous method of precipitation and filtration of the R_2O_3 group at a carefully controlled pH. Other changes were minor, involving concentration changes which must be varied considerably more with mineral analyses than with rock analyses. The details of the procedures used are available

in the spectrophotometer laboratory of the Department of Geology and Geophysics at M.I.T.

B. Precision

Perhaps the greatest advantage offered by instrumental techniques is the ease with which replicate analyses can be made, with resultant high precision. The final value for an element from any single weighing can usually be shown to have a reasonably small standard error.

Nearly all of the minerals were analyzed in duplicate. In a few cases enough sample for duplicate weighings was not available. From each of the duplicate weighings a solution was made. From each solution pairs of aliquots were taken for determinations. Thus most of the final results are a combined average of pairs of solutions from each of duplicate weighings. The diagram below may better illustrate this procedure. The original sample, x , is weighed in duplicate and made into duplicate solutions, A and B. From each of solutions A and B pairs of aliquots are taken, A_1 and A_2 from A; and B_1 and B_2 from B.



In the determinations of CaO and MgO a third aliquot was frequently taken from solutions A and B. These are shown as A_3

and B_3 in the diagram. ~~In the next few paragraphs the precision of each element will be discussed.~~

In order to illustrate the reproducibility of the analyses the best and worst results of pairs, such as A_1 and A_2 , and of duplicate weighings, such as A and B, are shown in Table 3. The standard deviations, standard errors, and relative errors for the worst pairs and the worst duplicates are also included in Table 3. Definitions of these terms are:

$$\text{standard deviation, } s = \sqrt{\frac{\sum d^2}{n-1}}$$

where d is the deviation from the arithmetic mean of a single measurement.

and n is the number of measurements.

$$\text{standard error (of the mean), } s_x = \frac{s}{\sqrt{n}}$$

$$\text{relative error, } E = \frac{s_x}{\bar{x}}$$

where \bar{x} is the arithmetic mean.

C. Accuracy

There are two primary causes of inaccuracy in analyses made by spectrophotometry, flame photometry, and titrations. Either the standard solutions may be inaccurate or various other elements may cause interference with the colors produced by the element being investigated. The former of these problems can usually be overcome by making up new solutions, using purer standards, or weighing and diluting more accurately.

The latter will depend upon the composition of the sample. Thus, the nature and intensity of any interference will vary from sample to sample. To overcome a problem of this nature the elements which cause interference must be determined and by means of correction factors or further addition of reagents the interference must be eliminated.

In the procedures used by this study interference by major elements has been taken into consideration but that of minor elements has not. It is assumed that the effect of minor elements will be only a small part of the total and, therefore, negligible. However, this might not be valid in the TiO_2 determinations of garnet. The indicator used is known to be sensitive to the element chromium which concentrates in garnet. At the low concentrations of TiO_2 encountered it is entirely possible that in some garnets a significant portion of the reported TiO_2 is actually Cr.

In order to test the accuracy of the procedures one can analyze standards which have compositions similar to that of the analyzed samples. Available standards which approximate the compositions of almandite garnet and the biotites of this study do not exist. The closest approximation is the diabase W-1 which has been analyzed by 35 laboratories (Fairbairn et al, 1953). In Table 4 a comparison of the values obtained for W-1 in the present study and the average of 35 laboratories is made. Values obtained for G-1 and Haplogranite are also compared with the averages from other laboratories.

G-1 and Haplogranite have compositions which are considerably different from the analyzed garnets and biotites and should not be considered in a rigorous comparison of accuracy.

Further tests of accuracy can be made with the garnet analyses. First, the totals of the analyses should be close to 100%; and second, the molecular ratios should balance according to the idealized formula $(RO)_3 \cdot (R_2O_3)_2 \cdot (SiO_2)_3$. It may be seen from Table 5 that all of the garnet analyses are close to 100% total. From Table 6 it may be seen that the molecular ratios are high for SiO_2 and low for RO and R_2O_3 . It was stated previously in the section on mineral separations that garnet could not be obtained free from tiny quartz inclusions. The excess SiO_2 is usually about 3% which is approximately the amount one would estimate from oil mounts of the garnet grains. A correction for the excess quartz can be made and the results after correction are shown in Table 7. It is seen that most of the analyses now show a small excess of R_2O_3 and a comparable deficit of RO . The first explanation which comes to mind is an error in the ferrous iron determination. It is possible that some of the ferrous iron became oxidized during the decomposition of the garnet. In fact the one garnet with less than 1% Fe_2O_3 , SP107, does not show this excess of the R_2O_3 molecule. With this possibility in mind several of the garnets were rerun by various methods which would reduce the possibility of oxidation to a minimum. The FeO determinations remained essentially the

same. As a final check on the possibility of oxidation one of the garnets was analyzed by Dr. J. Ito of the Harvard Mineralogy Department. His results are essentially the same. An error in the ferrous iron determination does not appear to be the reason for the discrepant molecular ratios. Dr. Ito mentioned that some of the garnets which he had analyzed had more Fe_2O_3 than could be accounted for by the molecular ratios. These garnets, he stated, were of a deeper red color than most. Upon showing Dr. Ito one of the uncrushed garnet samples of this study he agreed that these seemed to be of a deep red color similar to some in which he had found high Fe_2O_3 , but without a reduction in the Al_2O_3 content. One of the best examples of this type of garnet was used in an infra red absorption study (Clarke, 1957) where intense lines, believed to be caused by ferric iron, were found. The molecular ratios for this garnet are included in Table 6. It can be easily seen that there is a large excess in the R_2O_3 position. The only explanation of this type of composition is that some of the ferric iron is in the structural site of ferrous iron. According to texts on crystal chemistry this is a definite possibility (Evans, 1948). It is possible that this is the explanation of the high R_2O_3 ratio in the garnets of this study.

BIBLIOGRAPHY

- Alderman, A.R. (1935), Almandine from Botallack, Cornwall: *Min. Mag.*, 24, 42-48.
- _____ (1936), Eclogites in the neighborhood of Glanelg, Invernessshire: *Quart. Jour. Geo. Soc.*, 92, 488-530.
- Barth, Tom (1936), Structural and petrologic studies in Dutchess Co., N.Y., Part II: *Geol. Soc. Amer. Bull.*, 47, 775-850.
- Buddington, A.F. (1952), Chemical petrology of some metamorphosed Adirondack gabbroic, syenitic, and quartz syenitic rocks: *Am. Jour. Sci.*, Bowen Volume, 37-84.
- Chinner, G. (1958), Ph.D. Thesis at Cambridge, England.
- Clark, S.P. (1957), Absorption spectra of some silicates in the visible and near infrared: *Am. Mineral.*, 42, 732-742.
- Clark, Robertson, and Birch (1957), Experimental determinations of kyanite-sillimanite equilibrium relations at high temperature and pressure: *Am. Jour. Sci.*, 255, 628-640.
- Conant, L.C. (1935), New Hampshire garnet deposits: *Econ. Geol.*, 30, 387-399.
- Duparc, Wunder, and Sabot (1914), Contribution a l'etude des mineraux des pegmatite de Madagascar: *Soc. Franc. Mineralogie Bull.*, 36, 19-30.
- Du Rietz, T. (1935), Peridotites, serpentines, and soapstones of northern Sweden: *Geol. foren. Stockholm Forh.*, 57, 133-260.
- Erskine, J.S. (1955), St. Paul Island: *Jour. of Education*, Dept. of Education, Halifax, Nova Scotia; June, 1955, 3-13.
- Eskola, P. (1921), *Vidensk Skr. I mat-natur*, 8, 28-44.
- _____ (1952), On the granulites of Lapland: *Amer. Jour. Sci.*, Bowen Volume, 133-171.
- Eugster, H. (1957), Stability of annite: *Geophys. Lab. Ann. Rpt.* 1956-57, 161.
- Evans, R.C. (1948), *An Introduction to Crystal Chemistry*: Cambridge University Press.

- Fairbairn, H.W. et al. (1953), Precision and accuracy of chemical analysis of silicate rocks: *Geochimica et Cosmochimica Acta*, 4, 143-156.
- _____ et al. (in press), Age of the granitic rocks of Nova Scotia: *Geol. Soc. Amer. Bull.*
- Fleischer, M. (1937), Relation between chemical composition and physical properties in the garnet group: *Amer. Mineral.*, 22, 751-759.
- Fletcher, H. (1875-76), Report on explorations and surveys in Cape Breton, Nova Scotia: *Geol. Surv. Canada Rpt. of Progress*, 1875-76.
- Folinsbee, R.E. (1941), The chemical composition of garnet associated with cordierite: *Amer. Mineral.*, 26, 50-53.
- Ford, W.E. (1915), A study of the relations existing between the chemical, optical, and other physical properties of the members of the garnet group: *Amer. Jour. Sci.*, 40, 33-49.
- Fyfe, Turner, and Verhoogen (1958), Metamorphic reactions and metamorphic facies: *Geol. Soc. Amer. Mem.* 73.
- Gibbs, J. Willard (1928), *The Collected Works of J. Willard Gibbs*, vol. I: Longmans, New York.
- Goldthwait, J.W. (1924), *Physiography of Nova Scotia*: *Geol. Surv. Canada Mem.* 140.
- Groves, A.W. (1935), Charnockite series of Uganda, British East Africa: *Quart. Jour. Geol. Soc.*, 91, 150-207.
- _____ (1951), *Silicate Analysis*, 2d Ed.: London, Allen and Unwin.
- Gossner, B. (1931), *Über die chemische Zusammensetzung in der Granatgruppe*: *Neues Jahrb.*, Beilage-Band 64A, 225-233.
- Guggenheim, E.A. (1950), *Thermodynamics*, 2d Ed.: Interscience, New York.
- Guppy, Eileen M. (1956), Chemical analyses of igneous rocks, metamorphic rocks and minerals 1931-1954, with petrographical descriptions: *Geol. Surv. Great Britain Mem.*, 1956.
- Halferdahl, L.B. (1957), Chloritoid: *Geophys. Lab. Ann. Rpt.* 1956-57, 225-228.

- Hall, A.J. (1941a), Relation between chemical composition and refractive index in the biotites: *Amer. Mineral.*, 26, 34-41.
- _____ (1941b), Relationship between colors and chemical composition in biotites: *Amer. Mineral.*, 26, 29-33.
- Harker, A. (1893), On the migration of material during the metamorphism of rock masses: *Jour. Geol.*, 1, 574-578.
- _____ (1939), *Metamorphism*: Methuen and Co., Ltd., London.
- Heinrich, E.W. (1946), Studies in the mica group; the biotite-phlogopite series: *Amer. Jour. Sci.*, 244, 836-848.
- Henriques, A. (1957), The alkali content of kyanite: *Arkiv Min. Geol.*, 2, 271-274.
- Hietanen, A. (1936), Uber den Rhodonit and andere Manganminerale von Simso, Pohjanmaa: *Comm. Geol. Finlande Bull.*, 115, 387-400.
- _____ (1956), Kyanite, andalusite, and sillimanite in the schist in Boehls Butte quadrangle, Idaho: *Amer. Mineral.*, 41, 1-27.
- Howie and Subramaniam (1957), The paragenesis of garnet in charnockite, enderbite, and related granulites: *Min. Mag.*, 31, 565-585.
- Junner, N.R. (1927), Notes on the petrology of certain associated Mn silicate bearing rocks: *Am. Inst. Min. Met. Eng. Trans.*, 75, 385-395.
- Juurinen, Aarno (1956), Composition and properties of staurolite: *Suom. Tiedeak. Toimit. Ann. Acad. Sci. Fenn.*, ser. A. III, 47, 1-53.
- Klemm, G. (1922), Der Granatfels von Gadernheim in Odenwalde und seine Nebengesteine: *Neues Jahrb. Referate*, 2, 39-41.
- Lacroix, A. (1914), Les granats des groupes almandin-spessartite-pyrope a Madagascar: *Soc. Franc. Mineralogie Bull.*, 37, 108-112.
- Lee, Don (1958), A chlorine rich biotite from Lemhi County, Idaho: *Amer. Mineral.*, 43, 107-111.
- MacLaren, A.S. (1956a), Cheticamp River, Inverness and Victoria Counties, Nova Scotia: *Geol. Surv. Canada Paper* 55-36.
- _____ (1956b), Ingonish, Victoria County, Nova Scotia: *Geol. Surv. Canada Paper* 55-35.

- McIntire, W.L. (1958), A thermodynamic treatment of trace element distribution in geologic systems with applications to geologic thermometry: Ph.D. Thesis in Dept. of Geol. and Geophys. at M.I.T.
- Miyashiro, A. (1949), Stability of kyanite-sillimanite-andalusite and the physical condition of metamorphic process: Geol. Soc. Japan Journ., 55, 218-223.
- _____ (1953), Ca-poor garnet in relation to metamorphism: Geochim. et Cosmochim. Acta, 4, 179-208.
- _____ (1956), Data on garnet biotite equilibrium in some metamorphic rocks of the Ryoke zone: Geol. Soc. Japan Jour., 62, 700-702.
- Modell, David (1936), Ring dike complex of the Belknap Mountains, New Hampshire: Geol. Soc. Amer. Bull., 47, 1885-1932.
- Naidu, P.R.J. (1954), Minerals of charnockites from India: Schweiz Min. Petr. Mitt., 34, 204-279.
- Neale, E.R.W. (1955), Dingwall, Victoria County, Cape Breton Island, Nova Scotia: Geol. Surv. Canada Paper 55-13.
- _____ (1956a), Cape St. Lawrence, Inverness and Victoria Counties, Nova Scotia: Geol. Surv. Canada Paper 55-22.
- _____ (1956b), Cape North, Victoria County, Nova Scotia: Geol. Surv. Canada Paper 55-23.
- _____ (1956c), Pleasant Bay, Inverness and Victoria Counties, Nova Scotia: Geol. Surv. Canada Paper 55-24.
- Pabst, A. (1931), Garnets in the glaucophane schists of California: Amer. Mineral., 16, 327-333.
- Perry (1931), Rhodora, May, 1931 (Journal of the New England Botanical Society).
- Phillips, F. Coles (1930), Mineralogical and chemical changes induced by progressive metamorphism in the Green Bed group of the Scottish Dalradian: Min. Mag., 22, 239-256.
- Pitcher and Sinha (1958), The petrochemistry of the Ardara Aureole: Quart. Jour. Geol. Soc. of London, 113, 393-408.
- Preclik, K. (1924), Uber einen Almandin-Cordierithornfels unbekannter Herkunft: Centralbl. Mineralogie, 1924, 652.
- Quensel, P. (1951), The charnockite series of the Varberg district on the southwest coast of Sweden: Arkiv. Min. Geol., 1, 227-332.

- Roy, R. (1949), Decomposition and resynthesis of the micas: Amer. Ceram. Soc. Journ., 32, 202-209.
- Schairer and Yagi (1952a), System $\text{FeO-Al}_2\text{O}_3\text{-SiO}_2$: Amer. Jour. Sci., Bowen Volume, 471-512.
- _____ (1952b), The stability relations of Fe cordierite and almandite garnet: Amer. Geophys. Union Trans., 33, 328.
- Schumann, H. (1930), Uber moldanubische Paraschiefer aus dem niederosterreichischen Waldviertel zwischen Gfohler Gneis und Bittesher Gneis: Tscherm. Min. Petr. Mitt., 40, 73-187.
- Seidel, P. (1923), Zeitschr. Krist., 57, 416.
- Shapiro and Brannock (1956), Rapid analysis of silicate rocks: U.S.G.S. Bull. 1036-C.
- Smith, J.V. and Yoder, H. (1956), Experimental and theoretical studies of the mica polymorphs: Min. Mag., 31, 209-235.
- Snelling, N.J. (1957), A note on the composition of a staurolite from the Caenlochan schists: Min. Mag., 31, 603.
- Sollas, W.J. (1891), Roy. Dublin Soc. Sci. Proc., new series, 7, 49.
- Stewart, F.H. (1942), Chemical data on a Si-poor argillaceous hornfels and its constituent minerals: Min. Mag., 26, 260-266.
- _____ (1950), Note on garnet crystals from Cairnie, Aberdeenshire: Min. Mag., 29, 252-253.
- Subramaniam, A.P. (1956), Mineralogy and petrology of the Sittampundi Complex, Salem District, Madras State, India: Geol. Soc. Am. Bull., 67, 317-390.
- Thompson, J.B. (1955), Thermodynamic basis for the mineral facies concept: Amer. Jour. Sci., 253, 65-103.
- _____ (1957), The graphical analysis of mineral assemblages in pelitic schists: Amer. Mineral., 42, 842-858.
- Tilley, C.E. (1926), On garnet in pelitic contact zones: Min. Mag., 21, 47-50.
- _____ (1936), Paragenesis of kyanite eclogites: Min. Mag., 24, 422-432.
- von Eckermann, H. (1922), The rocks and minerals of the Mansjo Mountain: Geol. foren. Stockholm Forh., 44, 203-409.

- Winchell (1927), Elements of Optical Mineralogy, Part 2:
Wiley and Sons, New York.
- Winchell, H. (1958), Composition and physical properties of
garnet: Amer. Mineral., 43, 595-599.
- Wiseman, J.D.H. (1934), The central and southwest highland
peridotites: A study in progressive metamorphism: Quart.
Jour. Geol. Soc. London, 90, 354-417.
- Wones, D.R. (1958a), The phlogopite-annite join: Geophys. Lab.
Ann. Rpt. 1957-58, 194.
- _____ (1958b), Phase relations of the biotites on the join
phlogopite-annite: Geol. Soc. Amer., Abstr. Ann. Mtg. 1958.
- Yoder and Eugster (1954), Phlogopite synthesis and stability
range: Geochim. et Cosmochim. Acta, 6, 157-185.
- _____ (1955), Micas: Geophys. Lab. Ann. Rpt., 1954-55,
124-129.
- Yoder (1955), Almandite stability: Geophys. Lab. Ann. Rpt.,
1954-55, 97.
- Youden, W.J. (1951), Statistical Methods for Chemists: Wiley
and Sons, New York.

Biographical Sketch

The author was born in South Portland, Maine, on November 16, 1930. He was educated in the public school system of South Portland through the fourth grade and in the public school system of Berlin, New Hampshire from the fourth grade through high school. He graduated from high school in 1949 with a scholarship awarded annually by Brown Company, of Berlin, New Hampshire. This scholarship is based on competitive examinations given to students in the northern New Hampshire area. Simultaneously he was awarded an M.I.T. alumni scholarship for the freshman year at M.I.T.

Undergraduate training leading to the S.B. degree was received at M.I.T. between September 1949 and June, 1953. After graduating from M.I.T. the author entered active duty with the U.S. Army Corps of Engineers as a 2d Lt. Most of the army duty was spent with an intelligence detachment in Heidelberg, Germany. Following honorable discharge from the army as a 1st Lt. he re-entered M.I.T. in 1955 and received the M.S. degree in June, 1956.

The summers of 1955, '56, and '57 were spent as an assistant instructor at the M.I.T. Geology Summer Camp in Nova Scotia. The school years 1955-56 and 1956-57 were spent as a Teaching Assistant in the Department of Geology and Geophysics at M.I.T. and the school years 1957-58 and 1958-59 as a Research Assistant in the same department.

The summer of 1958 was spent conducting high temperature and pressure phase equilibrium studies with the U.S. Geological Survey.

The author was nominated to associate membership of Sigma Xi in 1956 and was promoted to full membership in 1959. He is also a member of the Mineralogical Society of America and of the American Geophysical Union.

He was married in 1953 to Colleen Murphy in Berlin, New Hampshire. At present he has two sons; Glenn Curtis, born 1955, and Duane Cullen, born 1956.